Optimizing hybrid-electric aircraft design and airline planning for efficient energy management and profitability through multidisciplinary coupling

Sofia Coelho Antunes

Technische Universiteit Delft

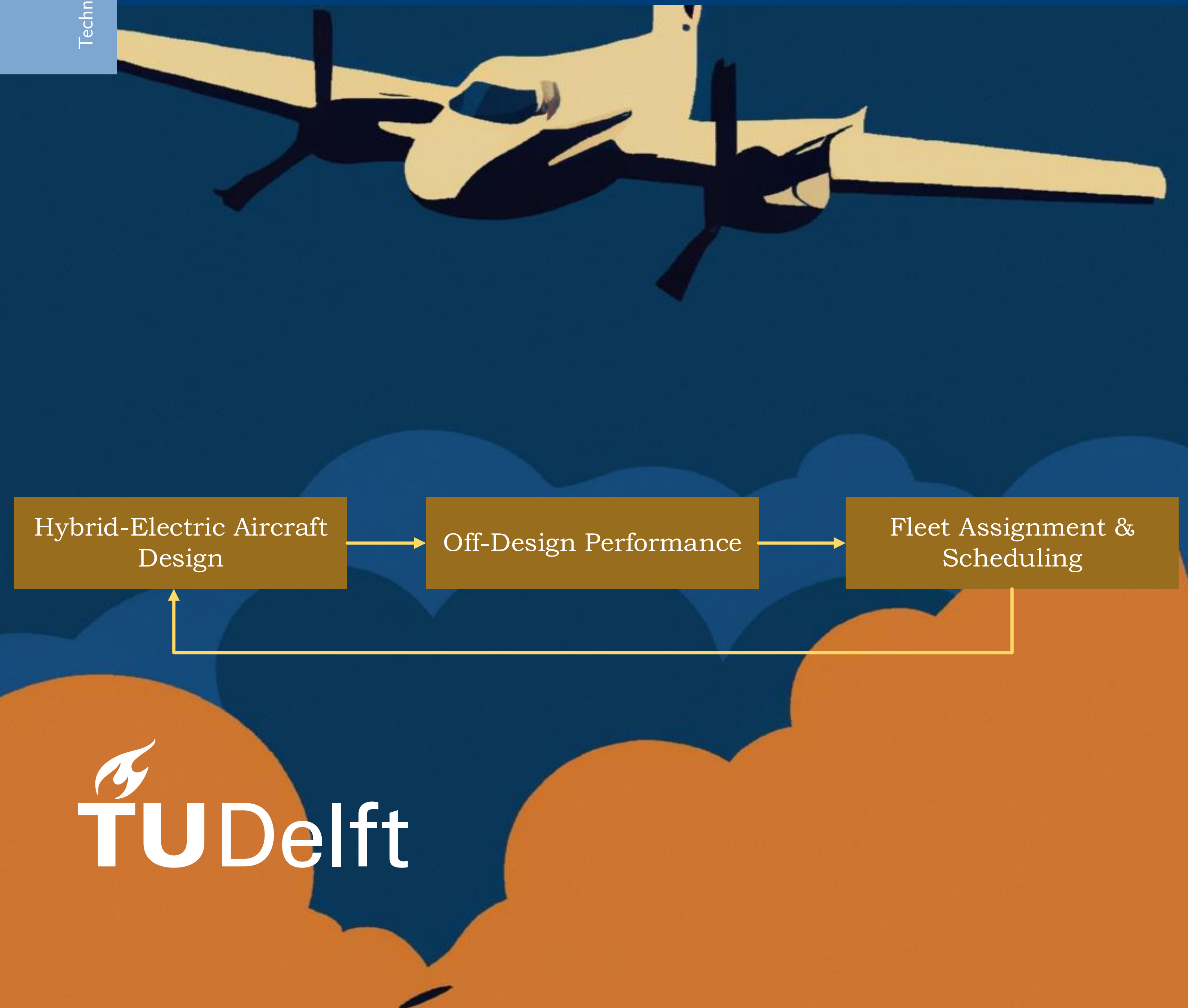

TU Delft

Optimizing hybrid-electric aircraft design and airline planning for efficient energy management and profitability through multidisciplinary coupling

by

Sofia Coelho Antunes

to obtain the degree of

Master of Science
in Aerospace Engineering

at the Delft University of Technology,
to be defended publicly on Friday March 15, 2024 at 10:00 AM.

Supervisor:	Dr. ir. M. Hoogreef	
	Ir. P. Proesmans	
	Dr. ir. B. L. dos Santos	
Thesis committee:	Dr. ir. M. Hoogreef ,	TU Delft, Supervisor
	Ir. P. Proesmans,	TU Delft, Supervisor
	Dr. ir. B. L. dos Santos,	TU Delft, Examiner
	Dr. ir. F. Oliviero,	TU Delft, Chair

An electronic version of this thesis is available at http://repository.tudelft.nl/.

Acknowledgements

The conclusion of my Thesis project on '*Optimizing hybrid-electric aircraft design and airline planning for efficient energy management and profitability through multidisciplinary coupling*' brings to an end my academic journey at TU Delft. The last five years have truly been an incredibly rich experience.

I would like to express my sincere gratitude to my supervisors Dr. ir. Maurice Hoogreef and Ir. Pieter-Jan Proesmans. Their support and guidance throughout this journey had a tremendous impact. I truly appreciate being given the freedom to align the project with my vision. Furthermore, I would like to thank Dr. ir. Bruno dos Santos for the valuable feedback and the big-picture suggestions during the development of this research.

Moreover, I would like to show my truest appreciation for my friends who have accompanied me in the last five years and brightened my life. You have played a great part in the person that I am today and often times you are not only a source of support but also inspiration.

Finally, I would like to thank my family for their support, continuous words of encouragement and love. I am immensely grateful for being given the opportunity to follow the path in which I am. Thank you for believing in me, even when I do not.

Sofia Coelho Antunes
Delft, March 2024

CONTENTS

List of Figures

List of Tables

Nomenclature

η_{BtT}	Total efficiency of chain: battery to thrust
μ	Ground friction coefficient
ρ	Air density
$BSFC$	Brake specific fuel consumption
DDP	Deep discharge protection
e_f	Specific energy of the battery
$E_{0,tot}$	Total energy at the beginning of the flight
e_{bat}	Specific energy of the battery
g	Gravitational acceleration
L/D	Lift-over-drag
NOD	Number of propulsion devices
P/W	Power-to-weight ratio
P_{ICE}	Power provided by the combustion engine
ROC	Rate of climb
s_G	Ground run distance
T/W	Thrust-to-weight ratio
tf	Trapped fuel fraction
W/S	Wing loading
W_{OE}	Operational empty weight
W_{PL}	Payload weight

INTRODUCTION

The aviation sector is continuously growing [1] [2]. The fast paced evolution clashes with the need to meet the ambitious climate goals set by the *United Nations*[3]. Thus, large efforts have been made within the research community to identify the most promising technologies which can help the industry move towards the aforementioned goals.

One of the technologies that has been identified to provide savings in terms of fuel is electrified powertrains [4]. Specifically, hybrid-electric powertrains. These powertrains have both a battery and kerosene as source of energy. This dual-energy characteristic provides designers with an additional degree of freedom: the supplied powersplit [5]. This variable controls the split between the power which is provided by the battery and the power which is provided by the fuel at every moment during the mission. Due to the addition of the battery, it has been shown by *Hoogreef et al.* [6] that hybrid-electric aircraft can suffer a large weight penalty at the design point and thus at on-design conditions are not beneficial from a fuel saving point of view. In spite of this, *Hoogreef & Bonnin* [7] have shown that at off-design conditions (lower payload and lower range) the fuel savings can be significant.

Often times aircraft operate at off-design conditions and thus the performance for which they are designed for not always matches the performance at which they are operated. This strong link between aircraft design and operational environment has already been identified in previous researches. For example, the fleet composition was optimised by *Scheers* [8], who connected a hybrid-electric conceptual design tool to a fleet-and-network allocation model (based on the model by *Zuijderwijk* [9]). The current research aims to build upon the work of *Scheers* and create a framework which links the design of hybrid-electric aircraft with an off-design performance analysis and an airline planning module. The latter should be able to select the fleet composition of an airline and construct its weekly schedule. All in all, the current research aims at answering the following two research questions:

1. *How does the off-design performance of a hybrid-electric aircraft change when it is operated at an off-design cruise Mach number or when it is redesigned for a different design range or design powersplit?*
2. *How is the performance of a network which integrates hybrid-electric aircraft affected by changes in the aircraft's off-design performance?*

Lastly, the thesis report is composed of three parts. Firstly, in **Part I**, a scientific paper is presented. In the former, the interdependencies between hybrid-electric design, their off-design performance and the network's performance are evaluated. This is achieved through the creation of a framework which links the aforementioned disciplines. By taking the network of the Air Nostrum airline as a reference, the framework is used to answer the previously outlined research questions. Furthermore, **Part II** includes the relevant Literature which supports the current research. This has already been graded under the TU Delft master course 'AE4020'. Lastly, **Part III** provides some additional work. It contains additional information regarding the creation of the *Fleet Assignment and Scheduling Module*, verification studies and additional results.

I

Scientific Article

Optimizing hybrid-electric aircraft design and airline planning for efficient energy management and profitability through multidisciplinary coupling

Sofia Coelho Antunes,*

Delft University of Technology, Delft, The Netherlands

Abstract

The aerospace market has seen a near-steady growth of around 4% in the last decades, and is forecasted to continue growing in the upcoming years. With the ambitious climate goals coming into play, especially in the European Union, it has become increasingly more important to find alternatives with reduced climate impact. Hybrid-electric powertrains have shown the potential to do so. If operated at a payload-range combination below their design values, the reduction in emissions could be significant. However, this relationship is not entirely understood. Furthermore, these powertrains would require airlines to adjust their operations. The interdependencies between the hybrid-electric design, their off-design performance and the network's performance are evaluated. The Air Nostrum network is used as a case study. The effect of modifying the design range and the design powersplit on the aircraft's off-design performance and network performance is evaluated. Several designs are constructed and several operational scenarios are generated. It is found that when the off-design performance of the hybrid-electric aircraft is considered in the fleet assignment and scheduling of an airline, CO_2 savings equal to 15% can be attained, while incurring a minimal loss in profit of 1.35%. This research highlights how modifying the design range of hybrid-electric aircraft has a larger impact on the applicability of the former in regional airline networks than the modification of the design powersplit.

Nomenclature

Acronyms

AR	Aspect Ratio [-]
$CASK$	Cost Available Seat Kilometer [€/km]
$ICAO$	International Civil Aviation Organization
LD	Landing Distance [m]
LF	Load Factor [-]
OD	Origin-Destination
OEI	One Engine Inoperative
$PMAD$	Power Management and Distribution
$RASK$	Revenue Available Seat Kilometer [€/km]
SOC	State of Charge [%]
TOL	Takeoff Length [m]

Constants

C_e	Cost per emission [€/ton]
g	Gravitational acceleration [m/s^2]

Greek Symbols

η	Efficiency [-]
γ	Flight path angle [deg]
ϕ	Supplied power ratio [-]
Π	Pressure ratio [-]
φ	Shaft power ratio [-]

Latin Symbols

$\dot{m}$	Mass Flow [kg/s]
bt	Block time [h]
C	Work Interaction coefficient [-]
C_D	Drag coefficient [-]
C_L	Lift coefficient [-]
C_{D0}	Zero-lift drag coefficient [-]
$c_{ownership}$	Aircraft ownership cost [€]
c_{pt}	Turbine's specific heat at constant pressure [J/kg K]
$CDemand$	Constrained demand [-]
D	Drag force [N]
E	Energy consumed [J]
e	Oswald efficiency factor [-]
e_f	Specific energy fuel [Wh/kg]
e_{bat}	Specific energy battery (pack) [Wh/kg]
e_l	CO_2 emissions on flight leg l [kg]
ep_{bat}	Specific power battery (pack) [Wh/kg]
h	Altitude [m]
hs	Specific enthalphy [J/kg]
L	Lift Force [N]

*Msc Student, Flight Performance and Propulsion, Faculty of Aerospace Engineering, Delft University of Technology

M	Mach number [-]
m	Mass [kg]
n	Propeller number [-]
P	Power [W]
P_p	Total powertrain power [W]
$P_{specific}$	Specific power [J/kg]
R	Range [m]
T	Thrust Produced [N]
$T_{specific}$	Specific thrust [Ns/kg]
$T_{t,4.5}$	Total temperature before the power turbine [K]
$T_{t,5}$	Total temperature after the power turbine [K]
tt_4	Turbine inlet temperature [K]
u	Direct passengers [-]
$UDemand$	Unconstrained demand [-]
UT_{max}	Maximum alloweble aircraft utilization [h]
V	Velocity [m/s]
W/P	Power loading [-]
W/S	Wing loading [-]
W	Weight [N]
w	Transfer passengers [-]
w_e	Emissions objective function weight [-]
W_l	Flight leg weight [€]
w_p	Profit objective function weight [-]
Sub & Superscripts	
0	Station zero
bat	Battery
$e1$	Electric motor 1
$e2$	Electric motor 2
f	Fuel/Kerosene
gb	Gearbox
gt	Gas turbine
$p1$	Propeller 1
$p2$	Propeller 2
$s1$	Primary powertrain
$s2$	Secondary powertrain
app	Approach phase
buffet	Buffet phenomena
cruise	Cruise phase
design	Design conditions
pay	Payload

1 Introduction

The growth of aviation in the last decades is difficult to ignore. Market forecasts from *Boeing* and *Airbus* estimate that this prosperity may mean a yearly growth of up to 3.8 % in the period between 2022 and 2041[1] [2]. Although this is received with a positive tone by the aviation industry, it also carries several challenges with it. In light of the recent ambitious climate goals set by the *United Nations*[3], one of the greatest challenges is maintaining the balance between profitability and sustainability.

Generally speaking, lowering the amount of fuel consumed directly correlates with lowering the amount of emissions produced. Given this fact, numerous attempts have been made across the aerospace industry to develop conceptual designs for aircraft powered by alternate fuels. One of these concepts revolves around the use of electrified powertrains [4]. However, one of the largest obstacles to electric flight is achieving a viable and safe specific energy density to cover enough profitable routes. Due to this limitation, electric aircraft would most likely be restricted to regional routes [5].

Hybrid-electric (HE) aircraft on the other hand, have as source of energy both a battery and kerosene and thus allow for the transport of more passengers for a longer distance [6]. In addition to providing more flexibility, the hybrid design provides designers with an additional degree of freedom and design variable: the supplied powersplit [7]. This variable controls the split between the power which is provided by the battery and the power which is provided by the fuel at every moment during the mission. The interplay between powersplit and fuel savings is not straightforward. *Hoogreef et al.* [8] concluded that on-design fuel savings highly depend on the combination of design range and design supplied powersplit. Large design ranges, imply a large battery and thus incur a weight penalty which is not compensated by the hybrid powertrain. Although it may be that at the design point, fuel savings don't occur, *Hoogreef & Bonnin* [9] have demonstrated that at off-design conditions (smaller mission length and smaller payload), the amount of fuel saved is significant. For an aircraft carrying 70 passengers with a design range around 900 km and a design cruise powersplit equal to 10%, when flying a mission with a length of around 500 km at maximum payload the fuel consumed decreases by up to 25%. The authors attribute this benefit to the ability to increase the supplied powersplit during cruise to values well above the design value.

Furthermore, the operational context in which aircraft are used has a significant impact on the block emissions. Moreover, deciding the type of missions a certain aircraft flies is part of airlines' strategic planning phase. This would also be the time to consider novel technologies, such as electrified powertrains, and the challenges they bring about (e.g. longer turnaround times). Moreover, the aircraft's performance and characteristics highly influence the choices an airline can make. More often than not the characteristics of the available aircraft do not exactly serve a certain network and thus the aircraft end up operating at a suboptimal level and thus have a larger environmental impact [10]. There is therefore a need to follow a systems-of-systems approach in which aircraft design and their operations are considered simultaneously. Several researchers have built frameworks which study the coupling and the interdependencies between aircraft design and an airline network. *Taylor & Weck* [11] were leaders in adopting this perspective on the aviation system. Shortly after, *Jansen & Perez* [12] created a framework which couples aircraft design optimization with their allocation to routes in an operator's network. Moreover, *Roy et. al* [13], developed a framework which couples aircraft design with fleet allocation while maximizing profit. Note that, the aforementioned researches share two common aspects: only consider profit as the driving factor in their optimizations and only consider conventional aircraft.

Recently, attention has turned to novel aircraft technologies. *Scheers* [14], connected a fleet-and-network allocation model (based on the model by *Zuijderwijk* [15]) to a hybrid-electric conceptual design tool and optimized the fleet composition based on the total airline profit. In addition to this, as a third separate step, the hybrid-electric aircraft were redesigned for minimum CO_2 emissions. This was accomplished by enabling adjustments to the cruise velocity, cruise altitude, and cruise supplied powersplit. Modifying these parameters led to a significant decrease in network CO_2 emissions without a significant penalty in terms of profit. This demonstrates the impact that these design variables have on the environmental impact of hybrid-electric aircraft. Furthermore, *Hoogreef et al.* [8] simulated with dynamic programming the creation of an airline's schedule and fleet assignment while considering both conventional and hybrid-electric aircraft. Although dynamic programming has been used to simultaneously solve the timetable design and the fleet assignment problem before [16][17], this was the first time that this method was used in the context of hybrid-electric aircraft.

Moreover, several researchers have followed a systems-of-systems approach and have created frameworks which allow for the study of the interdependencies between aircraft design and their operational environment. This research domain has even extended to hybrid-electric aircraft in which these were allocated to routes based purely on profit. Furthermore, hybrid-electric aircraft have shown to bring benefits when operated outside their design point and additionally, their environmental impact can be minimized by finding a suitable design cruise altitude-velocity-powersplit combination. Nevertheless, no framework has been created which allows for the study of the potential implications operating hybrid-electric aircraft outside their design point can have on an airline network. Furthermore, shedding light on how these aircraft can be made better suited for operating a certain network in terms of profit and environmental impact. From literature, three variables, were identified to have the largest effect on a hybrid-electric (HE) aircraft's performance. Two variables are design related: the design range and the design powersplit; while one variable is related to how the aircraft is operated: cruise Mach number. With a focus on these three variables, the current work aims to understand how they affect the off-design performance of a HE aircraft and in turn, how these modifications affect the performance of an airline network which includes these aircraft. All in all, the following research objective has been identified:

To create a framework which couples a hybrid-electric aircraft design tool with a fleet assignment and scheduling tool and incorporates the effects of operating hybrid-electric aircraft outside their on-design conditions

Furthermore, with the previous objective in mind, the current work aims to answer the following research questions:

1. *How does the off-design performance of a hybrid-electric aircraft change when it is operated at an off-design cruise Mach number or when it is redesigned for a different design range or design powersplit?*
2. *How is the performance of a network which integrates hybrid-electric aircraft affected by changes in the aircraft's off-design performance?*

To achieve the former objective and answer the research questions, the current work proposes to quantify the off-design performance by exploring the payload-range performance for different cruise velocities of several conceptual designs of hybrid-electric aircraft. These should then be integrated in a fleet assignment and scheduling model which makes use of dynamic programming to select the best schedule which maximizes an objective function.

2 Methodology

The framework was segmented into three separate parts: the *Hybrid-Electric Aircraft Design Module*, the *Off-design Analysis Module* and the *Fleet Assignment and Scheduling Module*. A description of the methodology followed can be found in section 2.1, section 2.2 and section 2.3, respectively. Furthermore, given the interest in studying the interdependencies between aircraft design and the operational environment in section 2.4 a description of the coupling strategy adopted in given.

2.1 Hybrid-Electric Aircraft Design Module

The first element in the framework is the hybrid-electric aircraft conceptual design module. The module developed by *Proesmans & Vos*[18] at the Flight Performance and Propulsion department of the Aerospace Faculty of TU Delft was the foundation for the former. However, the work described in the following subsections is a continuation of that carried out by *Scheers*[14], which had already built upon *Proesmans & Vos*'s work. *Scheers* extended the framework allowing it to be able to design hybrid-electric aircraft. To accomplish this extension, the methodology developed by *de Vries* [7] was used not only to model the hybrid-electric powertrain but also to perform a simplified mission analysis. The adaptations *Scheers* implemented focused on maintaining the computational time to a minimum, hence the mission analysis was conducted with the use of the Breguet Range equation for hybrid-electric aircraft. The reader is recommended to read the work developed by *Scheers* to gain further insight [14].

Given the objective of the current work, the fidelity and accuracy with which the performance of the aircraft can be modelled was increased. This entails further modelling the powertrain system as to comprehend how it behaves under different flight conditions. This allows for a more detailed mission analysis which in turn allows for the off-design performance of the hybrid-electric aircraft to be better understood. In the following subsection, the modifications implemented shall be highlighted.

2.1.1 Module Structure

The structure of the hybrid-electric aircraft design module can be seen in Figure 1. Similarly to the framework developed by *Scheers*, top-level requirements: design range (R_{design}), payload mass (m_{pay}), takeoff length (TOL), approach speed (V_{app}), cruise speed (V_{cruise}) and cruise altitude (h_{cruise}); are used once to run the *Initializer*, which provided with a design mission profile, the total payload mass to be transported and the aircraft type (e.g. turboprop) creates a first estimate of the mass breakdown and the aerodynamic performance of a conventional kerosene aircraft. This is attained based on a Class I weight estimation and statistical aerodynamic data from *Roskam*[19]. Furthermore, the largest changes were implemented within the *Synthesizer*, which is responsible for conceptually designing a hybrid-electric aircraft. The former is composed by a power-loading, an aircraft geometry, a powertrain model, a class II weight estimation and a stepwise mission analysis. As can be noted from the difference in color in Figure 1, the only submodule to which no alterations were applied was the class II weight estimation submodule, and thus no further explanations are given about it. The reader is advised to consult the work by *Scheers* [14] to gain further insight on this topic.

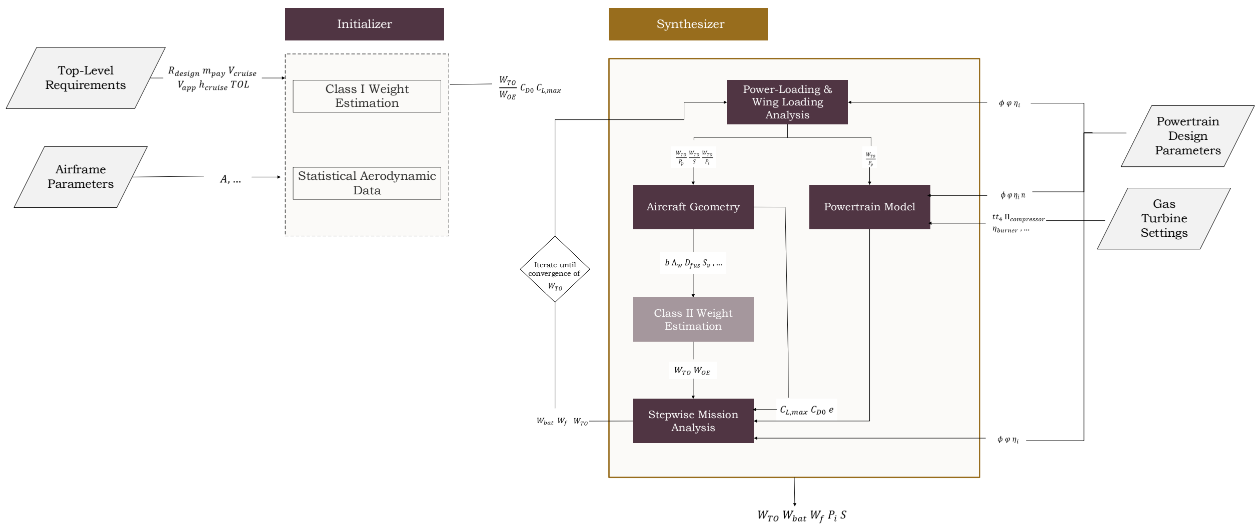

Figure 1: Schematic of the Hybrid-Electric Aircraft Design Module Framework.

2.1.2 Power Loading Diagram

The first discipline within the *Synthesizer* is the power-loading diagram discipline. Here a constraint analysis is performed to determine the hybrid aircraft power-loading (W/P) and wing-loading (W/S) based on several top-level requirements: the takeoff length, the approach speed, the cruise speed and the cruise altitude. Figure 2 is an example of such a power-loading diagram in which one can observe not only the feasible design space in green and the design point in red, but also the different design constraints considered: the stall speed constraint, the approach speed constraint, the takeoff length constraint, the cruise speed constraint and finally the climb gradient in one engine inoperative (OEI) condition constraint. Thus, in contrast with the work developed by *Scheers* [14] the approach speed constraint is now considered to further limit the design space.

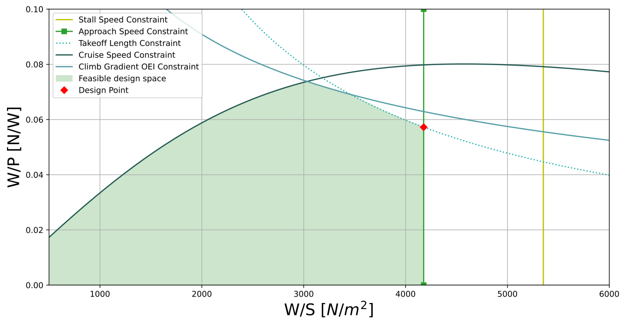

Figure 2: Example of a power-loading-diagram

2.1.3 Aircraft Geometry

The aircraft geometry submodule is used to estimate a preliminary aircraft geometry which is mainly used to update the aircraft aerodynamic parameters (C_D, C_{D0} and e) by making use of the method of *Obert* [20]. Moreover, the sizing equations are based on the method created by *Torenbeek* [21], whereas the turboprop dimensions are based on the method of *Thijssen* [22]. The reader is referred to the work of *Scheers* [14], for further insight.

Fuel Tank Volume

Moreover, as a gate to determining the battery location, a preliminary estimate of the maximum fuel which can be contained in the wings was used. A more accurate result would require more information about the wing planform and a further detailed design. Hence, to estimate the maximum fuel which can be stored in the wings, an adaptation of the method detailed by Torenbeek [21] was used. An estimate for the span occupied by the fuel tanks and the wing area occupied by the fuel tanks was used instead of the entire wing area and the entire wing span. This was achieved by taking the following assumptions into account:

- Fuel tank is split into the centre tank (inside the fuselage) and the main tank (outside the fuselage);
- The main tank begins at the intersection with the fuselage and ends at 85 % of the half-span;
- The main tank and the centre tank are assumed to be constricted between the front and rear spar. These are assumed to be located at 15% and 75% of the local chord, respectively [21];
- The existence of a kink is taken into account by assuming the main wing to be made of two trapezoids;

Battery Location

Furthermore, it is assumed that the aircraft has only one battery. The battery should either be placed in the fuselage compartment or inside the wing. For the case of being placed inside the wing, it is assumed that this is only possible in the portion of the wing inside the fuselage (centre tank), as the remainder of the wing is either occupied by the fuel tank or is too far from the aircraft's centre of gravity, and thus having implications on the aircraft's stability and controllability. Nevertheless, for further detailed designs of hybrid-electric aircraft, it is recommended to revisit this assumption, since placing the batteries on the wing (main tank) not only provides bending relief but also reduces the amount of cables required to be installed.

Finally, when the centre tank volume is larger than the battery volume, the remainder is assumed to be used to store fuel. Moreover, if this is not the case and hence the battery must be stored in the fuselage compartment, the entire tank volume inside the wing (centre and main tank) is assumed to be able to store fuel. Note that, two safety factors are added to the battery volume: a factor equal to 1.2 is added to account for the cables and a factor equal to 1.1 is added to account for the fact that the battery is a solid block and hence some places would not be properly occupied by it [14]. Table 20 in Appendix B provides further details on the geometry assumed to design the aircraft described in section 4.

2.1.4 Powertrain Model & Design

To get a more accurate indication of how a hybrid-electric powertrain would perform at each mission stage, the powertrain model and design submodule had to have the following characteristics. On one hand, it should be able to, given certain flight conditions, determine how much fuel and battery energy is being consumed. On the other hand, it should be able to model the energy and power flow within a hybrid powertrain.

To achieve the former characteristics two models were combined. On one hand, the turboprop engine cycle analysis tool developed by *Thijssen* [22] was used to estimate, among other parameters, the fuel consumption of the gas turbine. On the other hand, an adaptation of the hybrid powertrain model developed by *de Vries* [7] was used to model the energy and power flow within the hybrid powertrain.

Hybrid Powertrain
As in the approach by *de Vries* [7], the powertrain is modelled by a series of simple constituents, namely: energy sources, subcomponents and power and energy paths. It is relevant to note that rectifiers and converters characteristic of batteries and electric motors are not modelled specifically since they do not have an implication on the power transmitted [7]. Cables, switches and other smaller components are gathered in a power management and distribution box (PMAD), which similarly to other electrical subcomponents (batteries and electric motors) is also characterized by its efficiency, specific energy and specific power.

An example of the powertrain model can be seen in Figure 3, specifically for the case of a parallel-hybrid architecture. Each component transmits to the adjacent components a certain amount of power. The direction in which this power flows is determined by which operating mode the powertrain is operating on. For the present work, the only operating mode considered was the fourth operating mode detailed in the methodology of *de Vries* [7]. This operating mode is characterized by the fact that the power provided to the propeller comes from the electric motor and the gas turbine. Moreover, note that the parallel-hybrid architecture was the only architecture considered in the current work.

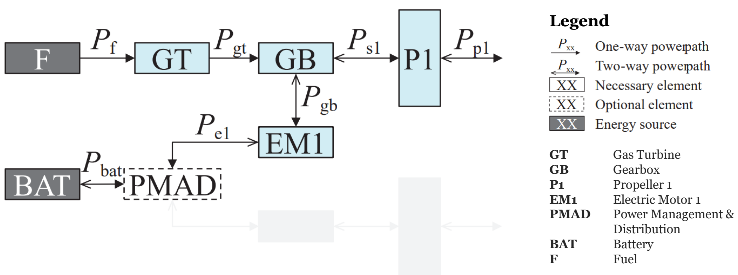

Figure 3: Example of parallel hybrid architecture [7]

Moreover, to attain the powers flowing from and into each subcomponent in the powertrain, a system of equations is solved while attending not only, to the subcomponent efficiencies but also to two power control ratios. These are the supplied power ratio (Equation 1) and the shaft power ratio (Equation 2). The supplied power ratio (ϕ) specifies the split between how much of the system's power is provided by the battery (P_{bat}) and how much is supplied by the fuel (P_f), whereas the shaft power ratio (φ) specifies the amount of shaft power produced by a secondary power path, with respect to the total shaft power produced. Note that some hybrid architectures (e.g. the parallel hybrid architecture) do not have a secondary power path. In these cases the shaft power ratio should be simply set to be equal to zero.

$$\phi = \frac{P_{bat}}{P_{bat} + P_f} \quad (1)$$

$$\varphi = \frac{P_{s2}}{P_{s2} + P_{s1}} \quad (2)$$

Turboprop Engine Cycle Analysis
While maintaining the simplicity of the aforementioned powertrain model, a turboprop engine cycle analysis method is used to design a gas turbine which is capable of producing enough thrust, both at on- and off-design conditions (being cruise the on-design condition). The turborprop engine cycle analysis was implemented based on the method developed by *Mattingly et al.* [23], which had already been used and tested by *Thijssen* [22] for

the design of turboprop engines.

Moreover, given certain atmospheric conditions and several design variables which are summarized in Table 17 in Appendix A, the thrust (T), the specific power ($P_{specific}$) and the specific thrust ($T_{specific}$) are computed and used to quantify the design air mass flow ($\dot{m}_0$) and the design power consumed (P_{design}), according to Equation 3 and Equation 4, respectively.

$$\dot{m}_0 = \frac{1.1T}{T_{specific}} \quad (3) \qquad\qquad P_{design} = \dot{m}_0 \cdot P_{specific} \quad (4)$$

The aforementioned parameters are determined based on a non-dimensional parameter called the work interaction coefficient (C_{total}). This parameter is defined through Equation 5, where C_{prop} (Equation 6) is the work interaction coefficient of the propeller and C_{core} (Equation 7) is the work interaction coefficient of the core. C_{core} is in general much smaller than C_{prop} since for turboprops, the thrust produced by the core (T_{core}) is much smaller than that produced by the propeller. Furthermore, C_{prop} depends on the propeller efficiency η_{prop} and the shaft power provided to the propeller (P_s). Both parameters are normalized with respect to the air mass flow and the specific enthalpy of the air (hs_0).

$$C_{total} = C_{prop} + C_{core} \quad (5) \qquad C_{prop} = \frac{\eta_{prop} \cdot P_s}{\dot{m}_0 \cdot hs_0} \quad (6) \qquad C_{core} = \frac{T_{core} \cdot V_0}{\dot{m}_0 \cdot hs_0} \quad (7)$$

Coupling of Models

As previously mentioned, for the case of a parallel hybrid electric aircraft, the power provided to the propeller is generated by the gas turbine and the electric motor, hence P_s of Equation 6 is no longer only dependent on the work performed by the power turbine. Thus, the shaft power provided to the propeller must comply with Equation 8, where P_{gt} is the power produced by the gas turbine and P_{gb} is the power produced by the electric motor. Note the minus sign, which stems from the sign convention given by *de Vries* 's [7] derivation, where P_{gb} is negative.

$$P_s = \eta_{gb} \cdot \underbrace{\eta_{mL} \cdot \dot{m}_{4.5} \cdot c_{pt} \cdot (T_{t,4.5} - T_{t,5})}_{P_{gt}} - \eta_{gb} \cdot P_{gb} \quad (8)$$

Furthermore, in the approach developed by *de Vries* [7], the powertrain's total output power is known and used to determine all the subcomponent power outputs, including the gas turbine power. In the current work, this no longer applies, since the gas turbine power is computed with the turboprop engine cycle analysis. Hence, an adjustment is made to the system of equations proposed by *de Vries* [7] to determine the battery power, the gearbox power (P_{gb}) and the total powertrain power (P_p), which comply with the selected supplied power ratio, shaft power ratio and power the gas turbine can produce. This is necessary to ensure that the required power equilibrium between the powertrain subcomponents is met. The proposed system of equations can be seen in Equation 9. Furthermore, it is relevant to note that the proposed model can consider other hybrid architectures which do not consider distributed propulsion. Moreover, the assumed powertrain properties can be found in Appendix A on Table 18.

$$\begin{bmatrix} -\eta_{gt} & 0 & 0 & 0 & 0 & 0 & 0 & 0 & 0 & 0 \\ 0 & \eta_{gb} & 1 & 0 & 0 & 0 & 0 & 0 & 0 & 0 \\ 0 & 0 & -\eta_{p1} & 0 & 0 & 0 & 0 & 1 & 0 & 0 \\ 0 & -1 & 0 & \eta_{em1} & 0 & 0 & 0 & 0 & 0 & 0 \\ 0 & 0 & 0 & -1 & -\eta_{pmad} & 1 & 0 & 0 & 0 & 0 \\ 0 & 0 & 0 & 0 & 0 & -\eta_{em2} & 1 & 0 & 0 & 0 \\ 0 & 0 & 0 & 0 & 0 & 0 & -\eta_{p2} & 0 & 1 & 0 \\ \phi & 0 & 0 & 0 & (\phi-1) & 0 & 0 & 0 & 0 & 0 \\ 0 & 0 & \varphi & 0 & 0 & 0 & (\varphi-1) & 0 & 0 & 0 \\ 0 & 0 & 0 & 0 & 0 & 0 & 0 & 1 & 1 & -1 \end{bmatrix} \cdot \begin{bmatrix} P_f \\ P_{gb} \\ P_{s1} \\ P_{em1} \\ P_{bat} \\ P_{em2} \\ P_{s2} \\ P_{p1} \\ P_{p2} \\ P_p \end{bmatrix} = \begin{bmatrix} -P_{gt} \\ \eta_{gb} \cdot P_{gt} \\ 0 \\ 0 \\ 0 \\ 0 \\ 0 \\ 0 \\ 0 \\ 0 \end{bmatrix} \quad (9)$$

Off-design Performance

Once the design of the powertrain is complete, its off-design performance can be assessed by making use of an adaptation of the aforementioned model. Although, the power flow within the powertrain is modelled in the same way (with Equation 9), the state of the gas turbine, meaning how much power it is providing, is determined by making use of the performance analysis developed by *Matingly et al.* [23]. In essence, the gas turbine engine-cycle parameters determined during the engine sizing are adjusted by finding the turbine inlet temperature (tt_4) and thus fuel mass flow which allows the powertrain to meet either a certain total powertrain power (P_p) or a certain low-pressure spool speed, depending on the mission phase.

2.1.5 Mission Analysis

A step-wise approach is adopted, in which the instantaneous point performance of the aircraft at discrete time steps is evaluated and used to estimate the battery mass and the fuel mass required to complete the selected design mission. Compared with an approach which makes use of an adaptation of the Breguet-Range equation, the inclusion of a step-wise mission analysis should be able to more closely represent and demonstrate the tight link between the power control ratios and the block fuel and energy consumption [24].

Mission Profile

The design mission profile used was constructed based on several user-specified parameters. These include the rotational speed of the low-pressure spool, the approach speed, the cruise altitude, the cruise speed, the cruise range and the payload to be carried. Furthermore, the design mission was constructed based on the guidelines provided by the *International Civil Aviation Organization* [25]. An example design mission can be observed in Figure 4 and comprises the segments numbered in Table 1 , which can be divided into the following three main stages:

- **A nominal mission**: Aircraft takesoff, climbs and accelerates until the predetermined cruise altitude and cruise speed. It cruises a distance equivalent to the predetermined design range, descends and attempts to land;
- **A reserve mission**: Aircraft diverts to another airport situated at a maximum distance equal to 185.2 km, while cruising at an altitude equal to 5000 m and speed equal to the nominal cruise speed: *This stems from requirement specified in ICAO Annex 6, 4.3.6.3.d.1*;
- **Endurance mission:** Aircraft loiters for a total of 30 min at an altitude of 450 m above the lading airport: *This stems from requirement specified in ICAO Annex 6, 4.3.6.3.e.2*:

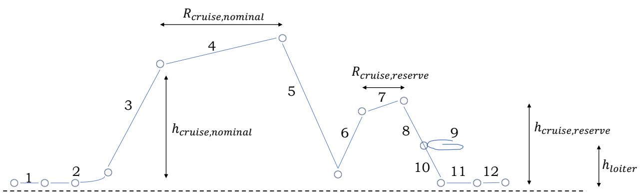

Figure 4: Example mission profile

Table 1: Mission segments and their numbering.

Number	Part	Number	Part
1	Start-up and Taxi	7	Cruise 2
2	Takeoff	8	Descent 2
3	Climb 1	9	Loiter
4	Cruise 1	10	Descent 3
5	Descent 1	11	Landing
6	Climb 2	12	Taxi & Shut-down

Aircraft State

At each time step the aircraft state is quantified, this is achieved by making use of the equations of motion (Equation 10 and Equation 11) in which it is assumed that the thrust vector is aligned with the flight direction and that the change in flight path angle ($\frac{d\gamma}{dt}$) is equal to zero. Furthermore, a quadratic drag polar is assumed, where the aerodynamic parameters C_{D0} and e are taken from the previously described aerodynamic analysis (section 2.1.3) and used to estimate the aircraft's drag. Note that, for each timestep considered the performance of the aircraft is considered constant.

$$T - D - W \cdot sin(\gamma) = \frac{W}{g} \cdot \frac{dV}{dt} \quad (10) \qquad L = W \cdot cos(\gamma) \quad (11)$$

The thrust the powertrain is producing and how much fuel it is consuming is quantified by making use of the off-design performance tool described in section 2.1.4. Depending on the flight phase, either the low-pressure spool speed or the total power the powertrain can produce is taken to be the constraining factor. For the segments of takeoff and climb the former is true, for every other segment the latter applies.

Additionally, since the performance of the aircraft is considered constant for each time step i, the energy drained from the battery and the fuel flow can be computed with Equation 12 and Equation 13, respectively. The power consumptions at the energy sources (P_{bat} and P_f) are attained with the powertrain model described in section 2.1.4 and the value assumed for the fuel specific energy (e_f) can be found in Appendix A.

$$dE_{bat,i} = P_{bat,i} \cdot dt \quad (12) \qquad \dot{m}_{f,i} = P_{f,i}/e_f \quad (13)$$

Furthermore, a numerical integration is used to determine the evolution of the aircraft's state (position, velocity, mass). Equation 14, Equation 15 and Equation 16 are used to compute the horizontal distance (s), the vertical distance (h) and the velocity magnitude (V) at the beggining of the following timestep $i{+}1$, while Equation 17 is used to update the aircraft's mass (m) based on the fuel consumed during the considered timestep i.

$$s_{i+1} = s_i + V_i \cdot cos(\gamma) \cdot dt \quad (14) \qquad h_{i+1} = h_i + V_i \cdot sin(\gamma) \cdot dt \quad (15)$$

$$V_{i+1} = V_i + \frac{dV}{dt}_i \cdot dt = a_i \cdot dt \quad (16) \qquad m_{i+1} = m_i - \dot{m}_{f,i} \cdot dt \quad (17)$$

Finally, the mass of the battery is determined by looking at the total battery energy required to operate the design mission (E_{bat}) and the maximum power the battery must provide ($P_{max,bat}$). If the battery's energy density (e_{bat}) and power density (p_{bat}) are assumed, the mass of the battery (m_{bat}) can be computed with Equation 18 [14]. Note that a minimum state of charge (SOC) was taken into account and set to be equal to 20 %.

$$m_{bat} = \text{Largest of: } \begin{cases} E_{bat}/e_{bat} \cdot (1 + SOC) \\ P_{max,bat}/ep_{bat} \end{cases} \quad (18)$$

Aircraft Emissions
The powertrain emissions were computed by assuming a certain emission index (EI) per combustion subproduct. Furthermore, only CO_2 and NOx emissions were considered. It was assumed that per kg of fuel burnt 3.16 kg of CO_2 would be produced. Moreover, since the emission index of NOx highly depends on the combustion conditions, the method described by *Dallara* [26] was used.

2.1.6 Constraints

Through subsequent iterations the aircraft's parameters, among which the MTOW, are updated until convergence is reached. However, to ensure a feasible design is attained, several constraints were taken into account. Firstly, the maximum allowable cruise lift coefficient is made dependent on the buffet lift coefficient: $C_{L,\text{cruise}} <= \frac{C_{L,\text{ buffet}}}{1.3}$ [27]. To compute the buffet lift coefficient ($C_{L,\text{ buffet}}$) at a specific cruising condition, Equation 19 was used. This relationship is based on a polynomial analysis based on data by *Vos & Farokhi* [28]. Furthermore, the buffet lift coefficient is made dependent solely on the mach number as the aircraft shall have barely any sweep.

$$C_{L,\text{ buffet}} = -0.3624M^2 - 1.8905M + 2.0536 \quad (19)$$

Secondly, due to airport gate constraints, the span of the aircraft is limited to ICAO category C airports (airports capable of accepting narrow-body aircraft. Hence, the wingspan must be smaller or equal to 36 m[1]. Finally, the W/S achieved must be smaller or equal to the W/S_{app}.

2.2 Off-design Analysis Module

Once the synthesis of a hybrid-electric aircraft is complete, its off-design performance is explored. This implies quantifying the fuel consumption, CO_2 and NOx emissions for different payload-range combinations. To achieve this a stepwise mission analysis is used according to the method detailed in section 2.1.5. Moreover, to limit the computational time of the module, only the nominal mission was evaluated for each payload-range combination. The reserve values (fuel consumed, CO_2 emitted and NOx emitted) were assumed to be equal to those of the design mission. Given the conceptual level of the analysis this is an acceptable simplification.

Furthermore, the range of mission lengths analysed can be tailored by the designer but the step taken in the selected interval is always set equal to 400 km. Furthermore, for each range considered, four different payload values were studied, spanning from zero to the maximum feasible payload associated with the range being analysed. This analysis is conducted both for hybrid-electric aircraft and conventional aircraft.

2.2.1 Hybrid-Electric Aircraft

For hybrid-electric aircraft, regardless of the length of the mission and the payload it carries, it must always transport a battery of the same size and thus with the same energy content (if it is assumed that the battery is always fully charged before each flight). Hence, as demonstrated by *Bonnin & Hoogreef* [9], for shorter, lighter

[1] `https://skybrary.aero/articles/icao-aerodrome-reference-code` [Accessed: 05/11/2023]

missions the supplied power split during cruise can increase with respect to that of the design point. More power being drawn from the battery could lead to savings in terms of fuel.

A payload-range analysis is conducted and for each point in the diagram, besides the fuel consumed, the CO_2 produced and the NOx emissions produced, also the maximum viable supplied cruise power split is quantified. Furthermore, the maximum viable supplied cruise power split is attained by finding the cruise power split which minimises the difference between the energy content the battery can supply ($E_{bat,design}$) and the battery energy spent to conduct a certain mission ($E_{bat,mission}$) (Equation 20).

$$\min \mathcal{K}(\phi_{cruise}) = E_{bat,design} - E_{bat,mission} \tag{20}$$

Special attention was given to the fact that there is a physical boundary to the supplied power ratio during cruise, limited by the gas turbine's operational limits. After a certain supplied powersplit the power required to be produced by the gas turbine is so little with respect to its design power, that the gas turbine can no longer physically operate under those conditions. Hence, the maximum feasible supplied powersplit during cruise is limited by both the batteries's energy content but also by the gas turbine's operating envelope.

2.2.2 Mach Number Variation

Besides exploring the variation in aircraft performance within its payload-range limits, it was also considered how the former changes if the cruise Mach number is modified. This variation was attained by varying the cruise velocity and maintaining the cruise altitude constant.

Furthermore, to grasp the effects while maintaining the computational power to a minimum, three different cruise Mach numbers were considered: below the design value, at the design value and above the design value. Moreover, the lower Mach number value was selected to maintain a cruise lift coefficient below the buffet lift coefficient. Thus, it was set to be 0.05 below the design cruise Mach number. Complying with the buffet constraint is not an issue for the upper Mach bound. Nevertheless, it must remain below 0.6 to not compromise the validity of the aerodynamic parameters of the wing. Nonetheless, to keep symmetry a delta Mach (dM) equal to 0.05 was assumed for the upper bound as well.

Ultimately, the goal is to attain for each cruise velocity considered a 2D interpolated function which if provided with a payload-range combination, is able to output the fuel consumed, the CO_2 and NOx produced and finally, for the case of hybrid-electric aircraft the maximum viable cruise powersplit. An example which illustrates the fuel consumed at different payload-range combinations can be visualised on Figure 5. Note that the analysis on the Mach number variation was not conducted for the conventional aircraft. Only the off-design analysis at the design velocity was analysed since it was of interest to compare the performance of the HE aircraft with a fixed baseline case.

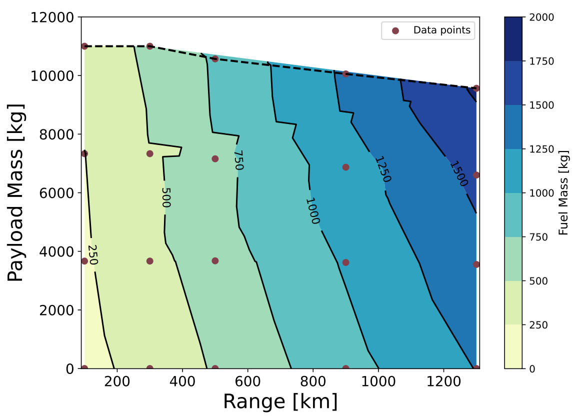

Figure 5: Fuel Mass for different payload-range combinations of example HE Bombardier CRJ1000 aircraft.

2.3 Fleet Assignment and Scheduling Module

The *Fleet Assignment and Scheduling Module* produces the weekly schedule for an airline, assigns aircraft to specific flights and determines the best cruise speed to fly at for each flight. This is possible, if the module is provided with information on which airports the airline wishes to fly to, the length of the runways, the demand to fly between the airports and the performance of all the aircraft to be considered (both on- and off-design). Once a database of aircraft sized with the method detailed in section 2.1 is created and their off-design performance has been explored with the method detailed in section 2.2, the aircraft can be embedded in a simulated network environment according to the model detailed in the following subsections. This module is thus essential to understand how different aircraft designs, including hybrid-electric designs, perform when included in an airline network.

2.3.1 Assumptions

It is relevant to note that during the modelling process, several assumptions were made. These can be summarized in the following manner:

- All airports have recharging stations;
- An operational day begins at 6:00 am UTC and finishes at 00:00 pm UTC, making a total of 17 hours of possible operations;
- Aircraft is always able to land at the largest available runway;
- The electricity price was assumed to be equal to 0.1445 €/kWh [15];
- The fuel price is assumed to be equal to 0.8 €/kg (0.067€/kWh)[15];
- Turnaround time is considered to be equal to 45 min for hybrid aircraft and 30 min for conventional aircraft;
- Battery is always fully charged before each flight;
- Hybrid aircraft ownership cost is assumed to be 20% larger than their conventional equivalent. The assumption is based on the purchasing price difference between electric cars and conventional cars[2];
- Transfer passengers do not have a preference for the amount of transfer time they are to spend at the hub;
- Demand attraction band is considered to be equal to 1 hour;
- The cost per emitted ton of CO_2 is set to be equal to 80 €/ton. This stems from the latest European emission trading scheme prices. [3]
- Network is modelled to be a hub-and-spoke network with one hub.
- Overnight station is not required to be the hub. If overnight airport is not the hub, no overnight parking fee is considered;

2.3.2 Module Structure

The logic and the flow of information within the *Fleet Assignment and Scheduling Module* can be visualized in Figure 6. The module is responsible for simultaneously determining the fleet composition of a certain airline and creating the weekly schedule of each aircraft within the fleet.

The module requires three distinct types of data: demand data, aircraft data and airport data. Firstly, the demand data provides information regarding the number of people who wish to fly between two specific airports. Details regarding the processing and modelling of demand can be found in section 2.3.5. Secondly, the aircraft data comprises information regarding the MTOW, the TOL and the off-design performance of each aircraft considered. Note that the latter is achieved by making use of the method detailed in section 2.2. Finally, the airport data includes which airports are to be considered, how long their runways are and finally whether or not they are operational hubs.

Dynamic programming was selected to solve the integrated fleet assignment and scheduling problem. This approach is an optimization method which separates a large complex problem into smaller sub-problems which can be solved individually and only once, thus avoiding redundant computations [29]. For the current work, the complex problem to be solved consists of constructing an airline fleet and its weekly schedule while maximizing profit and minimising CO_2 emissions. Thus, solving a sub-problem implies creating the weekly schedule of a

[2] `https://www.hdfcergo.com/blogs/car-insurance/electric-cars-vs-petrol-cars`[Accessed: 12/12/2023]
[3] `https://ember-climate.org/data/data-tools/carbon-price-viewer/` [Accessed: 12/12/2023]

single aircraft. All sub-problems are solved in parallel to reduce computational time. Moreover, once all the sub-problems have been solved, the aircraft **a** with the largest objective function is selected and added to the fleet, and its served demand is subtracted from the remaining total. The details of the objective function used for the iterative fleet selection can be found in section 2.3.4. This process is repeated iteratively until it is either not profitable to add a new aircraft or the demand to fly has been served entirely. Note that per iteration there are **m** sub-problems to be solved, where **m** is equal to the number of aircraft types in the database.

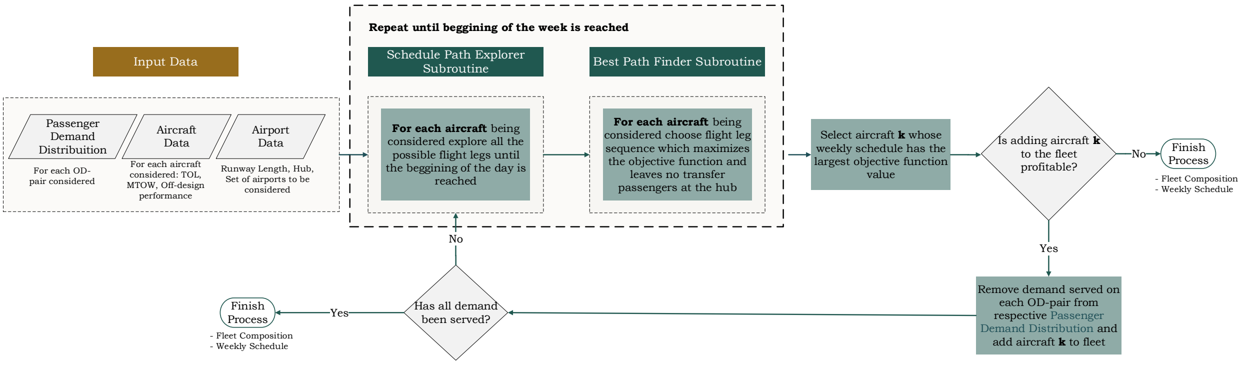

Figure 6: Fleet Assignment and Scheduling Module flowchart

2.3.3 Schedule Synthesizer

The process of creating the weekly schedule for an aircraft is composed of two main elements: the **Schedule Path Explorer** and the **Best Path Finder**. For each day of the week they are employed sequentially: first the former and then the latter.

Schedule Path Explorer

Firstly, the **Schedule Path Explorer** considers one day of the week at a time and examines the demand to fly between each airport in the network at a certain time t during the day, the profit attained and the CO_2 emissions produced for that specific flight. The objective of this element is to explore all the possible schedule combinations for a specific aircraft along a single day. By starting at the end of the day and progressively moving towards the beginning of the day, at each timestep t, the algorithm explores all possible actions within the *action space* (set of actions possible at a certain state). It first selects whether to fly to another airport or to remain at the same airport for the following timestep. In case it chooses to fly to another airport, if instructed by the user to do so, the algorithm explores the possibility of cruising at different cruise velocities. Thus, the algorithm includes an action space with two degrees of freedom: location and velocity.

To capture the spatial and the temporal complexity of the problem at hand, a *time-space network* was used. This has two dimensions: time and space; and two key elements: nodes and arcs. Each node represents a location (airport) and a time t along the day, while an arc connects two nodes. Two types of arcs were considered: flight arcs and ground arcs. On one hand, a flight arc is associated with a flight and represents the transport of a certain amount of passengers from one location to another for a certain time period. On the other hand, a ground arc represents the choice of remaining at the same airport for a certain time period. This can be visualized in Figure 7, where the solid arrow represents a ground arc and the dashed lines represent flight arcs.

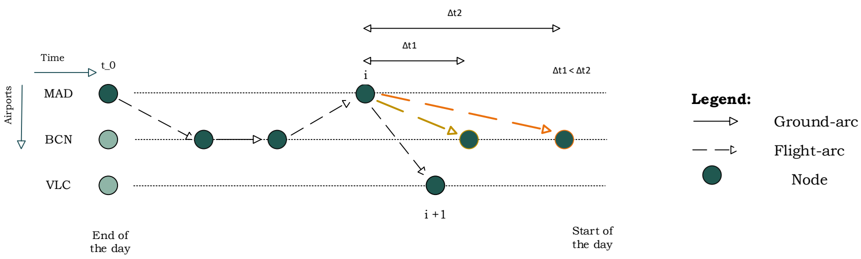

Figure 7: Representation of a time-space network

In this simulation, the minimum timestep between two nodes connected by a ground arc is set to 12 minutes, while the timestep between two nodes connected by a flight arc is modelled depending on the duration of the flight. This contrasts with the approach of having a fixed timestep between each node of, for instance, 30 minutes. This fixed-timestep assumes that, if the departure time of a flight does not exactly coincide with a node in the network, it is taken to be equal to the later node. The approach used in this simulation, without a fixed-timestep, has the potential advantage of better demonstrating the effect of cruise flight speed on the network's performance. The effect of this implementation is highlighted with the yellow and orange arrows. Both flight arcs have the same origin and destination, but the orange flight arc is flown at a lower cruise velocity than the yellow flight arc. Thus, the former must depart earlier than the latter to arrive at the same time. The outcome of the **Schedule Path Explorer** is a time-space network graph (constructed with the *Networkx*[4] Python Package) which spans all the possible flight sequences in a day for a certain aircraft.

Best Pathfinder

Whenever an arc is considered, a weight (W_l) is computed and associated with it. This weight is then used by the **Best Pathfinder** subroutine to determine the sequence of flights which maximize the objective function expressed in Equation 21a. This sequence of flights also has to comply with the set of constraints detailed in Equation 21b-Equation 21g. Moreover, the **Best Pathfinder** makes use of the Bellman-Ford shortest path algorithm to achieve the desired result [29].

After finding the best sequence of flights for one day, the algorithm moves to the next step (previous day) and repeats the **Schedule Path Explorer** and **Best Pathfinder** subroutines until the beginning of the week is reached. Furthermore, note that airport continuity was ensured from one day to the next.

Objective Function

A multi-objective function is considered in which both profit and CO_2 emissions are taken into account. The relative importance of the two separate objectives is controlled with the parameters w_p and w_e, where the former is the relative importance of profit and the latter is that of CO_2 emissions. The sum of the two weights must be equal to one. Furthermore, to maintain a fair comparison between the two objectives, the CO_2 emissions were monetized by making use of a cost per emission C_e [€/ton]. Moreover, the details of how the profit p_l was estimated can be found in section 2.3.6, whereas the details of how the CO_2 emissions (e_l) were estimated can be found in section 2.2. Finally, Table 2 gives the definitions for all the sets used in the model, including set **P**.

Table 2: Model sets

Set	Description
P	All feasible flight schedules
$\mathbf{P}_p$	Sequence p of feasible flights in P, where p = [1,2,3,...]
A	All aircraft types in the database
N	All airports in the network
T	All timesteps in a day of operations

$$\max \mathcal{J} = \sum_{l=1}^{\mathbf{P}_p} W_l = \sum_{l=1}^{\mathbf{P}_p} w_p \cdot p_l - w_e \cdot e_l \cdot C_e \qquad \forall p \in \mathbf{P} \tag{21a}$$

Constraints

A feasible flight schedule is one for which all flight legs l comply with a number of constraints. Firstly, the *Runway Constraints* (Equation 21b and Equation 21c), ensure that the runway length (L_i, L_j) is long enough for a certain aircraft **a** to both takeoff and land at airports i and j, respectively. Additionally, the total number of passengers transported from airport i to airport j is limited by either the demand at time t or by the capacity of the aircraft limited by a certain load factor LF (Equation 21d). Note that a load factor LF is taken into account to model the spoilage of passengers which often occurs in airline operations.

Furthermore, the *Range Constraints* Equation 21e ensure that the range of an aircraft **a** carrying a certain payload m_{pay} (which must comply with the *Capacity Constraint*) is sufficient to travel the distance between airports i and j in feasible flight leg l.

Finally, the two last constraints are the *Transfer Passengers Constraint* Equation 21f and the *Utilization Constraint* Equation 21g. The former ensures that for all flight schedules in **P** no transfer passengers are left at the hub ($w_{l,hub}$) at the end of the day, while the latter ensures that for all flight schedules in **P**, the sum of the

[4] `https://networkx.org/documentation/stable/index.html` [Accessed: 12/12/2023]

flight block time (bt) of all flights in a certain flight schedule p is smaller or equal than the maximum allowable aircraft utilization (UT_{max}).

$$\textit{Takeoff Runway Length Constraint:} \quad L_i \leq TOL_a \quad \forall i \in \mathbf{N} \quad , \forall a \in \mathbf{A} \tag{21b}$$

$$\textit{Landing Runway Length Constraint:} \quad L_j \leq LD_a \quad \forall j \in \mathbf{N} \quad , \forall a \in \mathbf{A} \tag{21c}$$

$$\textit{Capacity Constraint:} \quad u_{ij}^t + w_{ij}^t = \mathbf{min}(CDdemand_{ij}^t, seats_a \cdot LF) \quad \forall i,j \in \mathbf{N}, \quad \forall t \in \mathbf{T}, \quad \forall a \in \mathbf{A} \tag{21d}$$

$$\textit{Range Constraint:} \quad R_a(m_{pay}) \geq dist_{ij} \quad \forall i,j \in \mathbf{N} \quad , \forall a \in \mathbf{A} \tag{21e}$$

$$\textit{Transfer Passengers Constraint:} \quad \sum_{l=1}^{\mathbf{P}_p} w_{l,hub} = 0 \quad \forall p \in \mathbf{P} \tag{21f}$$

$$\textit{Utilization Constraint:} \quad \sum_{l=1}^{\mathbf{P}_p} bt_l \leq UT_{max} \quad \forall p \in \mathbf{P}, \quad \forall a \in \mathbf{A} \tag{21g}$$

2.3.4 Fleet Selection & Airline Schedule

At each iteration, the selection of a new aircraft was made in accordance with the objective function defined by Equation 22. Note that $c_{ownership,a}$ is the cost of owning aircraft **a** from the set of aircraft **A**.

$$\max \mathcal{H} = \mathcal{J} - w_p \cdot c_{ownership,a} \quad a \in \mathbf{A} \tag{22}$$

2.3.5 Demand Modelling

To estimate the number of passengers transported on each flight, the demand to fly between any two airports in the network must be known. In the following sections the demand processing and modelling shall be elaborated. Note that the method considered was based on the work by *Wang* [30].

Unconstrained Demand

The unconstrained demand is the estimated weekly number of passengers that wish to fly from airport i to airport j within the network. This data was attained through an itinerary and passenger flow analysis conducted by *Hoogreef et al.*[8]. People's willingness to fly fluctuates throughout the day and throughout the week. This fluctuation translates into a variation in the demand to fly. Although in reality there are certain days during the week for which there is a larger demand to fly, this was not accounted for. Hence, the weekly unconstrained demand was distributed evenly through the seven days of the week.

Passenger Demand Distribution

To distribute the daily unconstrained demand ($UDemand$) throughout the day, a demand probability function was used ($p(t)$). This function represents the willingness of people to fly at a certain time during the day and it was assumed to have the shape of a normal distribution with the mean equal to half of an operations day and a standard deviation equal to three. In reality, there should be two demand spikes during a single day, one in the morning and one in the afternoon [17], however, the current approximation was considered sufficient for the desired level of fidelity of the *Fleet Assignment and Scheduling Module*. Moreover, as mentioned in section 2.3.1, the total operations day is considered to be equal to 17 hours. In order to construct the *Passenger demand distribution* function (F_t), these 17 hours were split into blocks of 12 min and the probability density function value at each timestep t was multiplied by the unconstrained demand, as per Equation 23. A visual representation of the former can be visualized in Figure 8, for an arbitrary OD-pair. Note that, since it is assumed that there is no demand variation throughout the week, the *Passenger demand distribution* function is the same for all days of the week. Furthermore, for each OD-pair in the network, the *Passenger demand distribution* function must be created.

$$F_t = p(t) \cdot UDemand \tag{23}$$

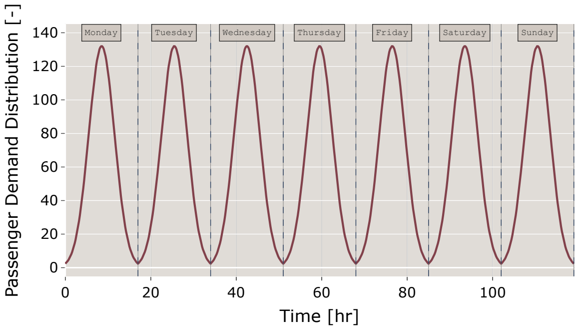

Figure 8: Passenger Demand Function

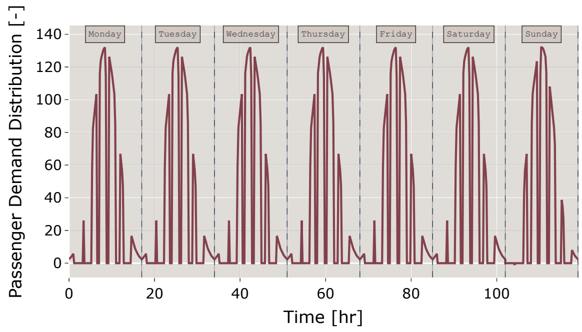

Figure 9: Passenger Demand Function once served demand has been removed.

Constrained Demand

The constrained demand is the demand bounded not only by the passengers' itinerary but also by the capacity of the aircraft being considered. To estimate the total demand which wishes to fly from airport i to airport j at time t it is assumed that all demand comprised within 1 hour of departure time wishes to board the flight. The latter is called the attraction band.

Furthermore, to take passenger itineraries into account a distinction was made between transfer demand and direct demand. A typical transfer passenger itinerary is composed of two flight legs: **spoke-hub** and **hub-spoke**. Given the fact that the flight schedule is created starting at the end of the day (section 2.3.2), for every transfer itinerary, the second flight leg is considered first (**hub-to-spoke**). Hence, to determine the transfer demand of a **hub-to-spoke** flight, the total unconstrained transfer demand wishing to travel from any other spoke in the network to the spoke currently being considered, must be computed. With this knowledge, a *Transfer Passenger Demand Distribuition* function can be created (as per Equation 23) and the constrained transfer demand can be computed according to Equation 24. The constrained direct demand was also computed with Equation 24, however, F_t was created with the unconstrained direct demand of the OD-pair being considered.

$$CDemand = \int_{t-1}^{t+1} F_t \quad dt \tag{24}$$

When considering a **spoke-hub** OD-pair, the constrained transfer demand is calculated differently, whereas the constrained direct demand is not. For this type of OD-pair, special attention is given to the transfer passengers for which a **hub-spoke** leg has been considered already. These passengers are given priority over direct passengers in the flight and thus automatically allocated. This is done to minimize the number of schedule paths for which transfer passengers are left at the hub at the end of the day.

Served Demand

Once a flight is considered, the passengers it transports should be removed from the *Passenger Demand Distribution*. The method used by *Wang* [30] was used to achieve this. *Wang* considers that the demand closer to the departure time is more likely to be captured than the demand slightly further. Hence, starting at departure time t, the *Passenger Demand Distribution* of the OD-pair being considered is set to zero. This is propagated out in both directions (towards earlier in the day and towards later in the day), until the integral under the *Passenger Demand Distribution* is equal to the number of passengers transported. This model was adopted, instead of *Rubbrecht's* [31], because it avoids the simultaneous scheduling of flights for the same OD-pair, which is deemed unrealistic from an airline perspective. Figure 9 displays an example of the *Passenger Demand Distribution*, after the demand served has been removed.

2.3.6 Profit Estimation

The profit of flying a certain flight is dependent solely on the revenue deducted from it and the cost of operating such a flight. The former translates into Equation 25, which demonstrates the total profit p attained in a feasible flight sequence $\mathbf{P}_p$, where r_l and c_l are the revenue and the operating cost of feasible flight leg l.

$$p = \sum_{l=1}^{\mathbf{P}_p} (r_l - c_l) \quad \forall p \in \mathbf{P} \tag{25}$$

Revenue
Revenue depends on the amount of passengers that are being transported and on the fare charged to each of them. All aircraft seats are charged at the same fare. Furthermore, no distinction is made between transfer passengers and direct passengers. Thus, for each flight leg considered the revenue is expressed with Equation 26. The former consideration is taken to avoid having an additional assumption entering uncertainty in the model as considering variable passenger fare is outside the scope of the study. Additionally, since revenue does not change with flight distance, the model has a preference for choosing shorter flights as these are cheaper to operate and generate revenue as in longer routes.

$$r_l = \text{fare} \cdot (u_l + w_l) \tag{26}$$

Operating Cost
The components of operating cost which were considered include not only, the *crew costs*, the *airport costs* and the *navigation fees* but also the *fuel costs*, the *electricity production costs* and the aircraft *ownership cost.*

The crew costs were estimated based on the method given by *Roskam* [32]. It is assumed that the cabin crew is composed of a captain, a first officer and cabin crew members. To determine the required number of cabin crew members the regulations described by EASA were followed, which state that for each 50 seats, there should be one cabin crew member [33]. Furthermore, the crew costs are estimated based on an assumed annual salary (assumed values are summarized in can be found in Table 3), an annual amount of flight hours and the flight's block velocity.

Table 3: Annual salaries of Air nostrum crew members.

Crew Member	Annual Salary [USD]
Cabin Attendant	21700[5]
First Officer	38000[6]
Captain	97900[6]

As far as the airport costs are concerned, these are estimated with the method used by *Wang* [30], which considers two separate types of airport sub-costs: the ground-handling & parking fees and the landing fees; Airport-specific taxes are not taken into account. Furthermore, the key parameters driving these costs on a specific flight are the aircraft's maximum takeoff weight (MTOW) and the number of seats in the aircraft. Note that, to emulate the loss of profit from choosing a ground arc at timestep t instead of a flight arc, it is considered that the cost is equal solely to the ground-handling fees.

As far as navigation fees are concerned, these were also estimated with the method detailed by *Wang* [30], and were made dependent on the aircraft's MTOW and the flight's distance. Moreover, the costs associated with purchasing fuel and purchasing electricity are modelled by assuming a fuel and electricity price and by taking into account the fuel and battery energy consumed during the flight which is being considered.

For the ownership costs, a distinction must be made between conventional aircraft and hybrid-electric aircraft as the latter is likely to be more expensive than the former due to the presence of the battery. The ownership costs of a hybrid-electric aircraft are assumed to be 20 % higher than the cost of owning their conventional counterpart. This assumption is based on the market price difference between normal and electric cars[7]. Additionally, based on the purchasing price of each selected aircraft, the weekly ownership cost is computed with the relationship given by *Jansen & Perez* [34].

2.4 Coupling Strategy

The objective behind devising a coupling strategy lies in the idea of making use of the information attained with the *Fleet & Scheduling Module* and deducting trends and modifications to the aircraft which could potentially benefit the network.

2.4.1 Variables Considered

The two aircraft design variables which were identified to have the largest influence on the performance of the network were the aircraft's design range and the aircraft's design payload. The former directly correlates with

[5] `https://www.salaryexpert.com/salary/job/flight-attendant/spain` [Accessed: 22/12/2023]
[6] `https://worldaviationato.com/en/airplane-pilots-salary/` [Accessed: 22/12/2023]
[7] `https://www.hdfcergo.com/blogs/car-insurance/electric-cars-vs-petrol-cars`[Accessed: 12/12/2023]

route flexibility and servicing while the latter correlates with the amount of demand that can be captured. Additionally, aircraft capacity is related to the amount of profit a given airline makes at any given time while the selection of the design range has an aircraft scaling effect and thus an effect on the fuel consumed. Moreover, this consideration becomes increasingly more relevant when considering hybrid-electric aircraft, as with the addition of the battery, the design range plays a crucial role in the weight penalty the final design suffers from[9]. Furthermore, special attention was given to the assessment on whether to modify the capacity of the aircraft since this would entail a reduction in the possibility to serve demand.

2.4.2 Clustering Method

Given the aforementioned considerations, the flights for each of the aircraft selected during the *Fleet & Scheduling Module* were clustered in terms of passengers carried and distance flown. This should provide insight into what types of routes are flown and whether or not it makes sense to redesign the aircraft for alternative capacities.

Furthermore, to cluster the flights in terms of payload carried and range flown the *Kmeans clustering method*[8] was used. This is an unsupervised machine learning algorithm which clusters data into a specified number of clusters by minimizing the sum of squares within each cluster (Equation 27). This implies dividing a set of **M** samples **X** into **K** separate clusters, for which each has associated with it a mean value μ_j. These mean cluster values are of interest and were used to determine whether modifications to the aircraft design were necessary.

$$\sum_{i=0}^{n} \min(||x_i - \mu_j||^2) \tag{27}$$

Additionally, to determine the best number of clusters which fit the data, the "Kneedle Algorithm" developed by *Satopaa et al.* [35] was used. The algorithm was created to detect the point at which the cost of increasing some parameter in a computer system is no longer worth the improvement in the system's performance. It was conceptualized to be used in situations in which there are two opposing variables, for which a tradeoff is required and a sensible design point must be selected. Thus, for the current application, it can be used to select the number of clusters for which increasing the former by one does not result in a substantial benefit in terms of improving the fit of the "centroids" to the data. This can be visualized in Figure 10, for which the distortion score represents how well the cluster centroids fit the data, and k represents the number of clusters considered. For this specific example, three clusters are the most sensible choice and can be visualized on Figure 11.

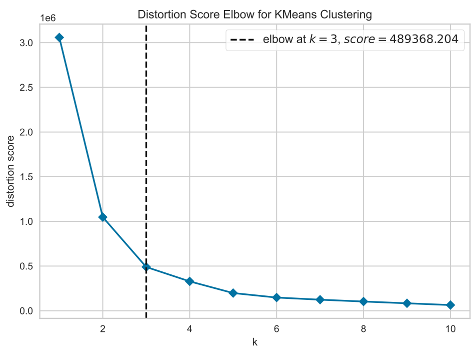

Figure 10: Cluster number versus distortion score for example data

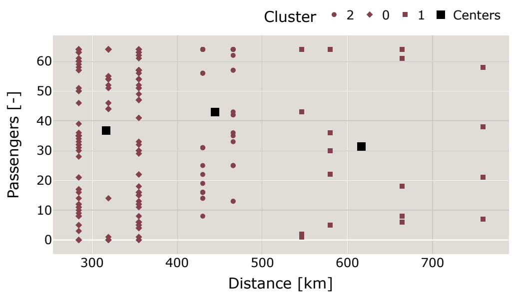

Figure 11: Example of clusters in terms of passengers and distance flown.

3 Case Study Description & Framework Verification

This section elaborates on the case study which was used to verify the framework described in section 2 and answer the research question detailed in section 1. Furthermore, the case study described was used to construct a reference scenario for the analysis in section 4 to be compared with. This same reference scenario was used to verify the *Fleet Assignment and Scheduling Module* by focusing on whether the module is able to correctly represent the decision making process of an airline. Moreover, the hybrid-electric design method has already been partially verified by *Scheers* and *de Vries* [14][7]. Nevertheless, modifications to the powertrain model and

[8] `https://scikit-learn.org/stable/modules/clustering.html` [Accessed: 15/12/2023]

the mission analysis were implemented. Thus, the differences verified in the synthesis of an aircraft resultant of the aforementioned alterations shall be analysed in section 3.2.1.

3.1 Case Study Description

To test the framework described in section 2, an airline case study was selected. The main requirement the selected airline was required to comply with is that it should be a regional airline since this is the target market for hybrid-electric powertrains. In the following subsections, further details are provided.

3.1.1 Airline Characteristics

The case studies constructed to test the framework described in section 2 were based on the Spanish airline **Air Nostrum**. This airline was chosen since it is a regional airline with routes suited for the potential application of hybrid-electric aircraft,and because an unconstrained demand estimate between the OD-pairs in the network was readily available[8]. Furthermore, the airline's network is composed of 40 airports and a total of 109 routes operated by three aircraft. These aircraft are the **ATR 72-600**, the **Bombardier CRJ200** and the **Bombardier CRJ1000**. The characteristics of these aircraft were used as a baseline to produce the hybrid-electric aircraft considered in the current work.

To minimize computational time a subset of the **Air Nostrum** network was used. The airports and routes selected to constitute the subnetwork were required to represent the entire network as much as possible. This implies that the subset of the entire network should represent not only the variation in demand and distance flown of the entire network, but also should allow transfer passengers to flow in between the airports and hence not limit the dynamic programming choices in this matter. Furthermore, it was considered imperative that the subnetwork would include routes with the following demand-distance combinations: (low demand-low distance), (high demand-low distance), (low demand-high distance). Note that the combination (high demand-high distance) is not considered since the Air Nostrum network does not encompass this type of route. Moreover, given the aforementioned considerations, 13 airports were selected, being these the following: MAD, BIO, ALC, VGO, VLC, AGP, BCN, MAH, PMI, MLN, RAK, NCE and NTE. Figure 12 demonstrates the demand to depart from the airports in the Air Nostrum network versus the distance to the hub **MAD** (the only hub in the network). Furthermore, the airports under consideration are highlighted, and the size of the markers indicates the number of transfer routes that end at that airport. The information regarding the airports' geolocation was retrieved from *Openflights*[9], while the runway length was retrieved from *AirportDB*[10]

Finally, it is relevant to note that the **Air Nostrum** network is composed of only brief routes. The longest route is 1186 km while the shortest is 209 km. For this reason, the off-design study (section 2.2) for every aircraft considered (both conventional and hybrid) was restricted to a range between 100 km and 1300 km.

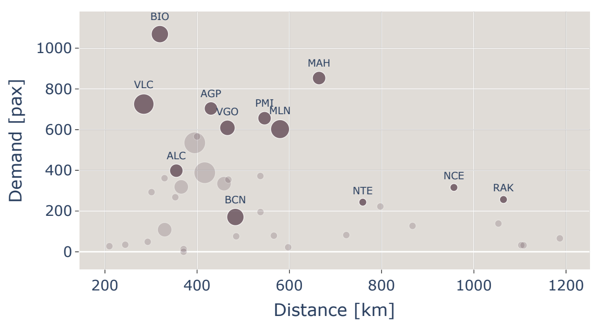

Figure 12: Daily demand from airports in Air Nostrum network versus distance to the hub.

3.1.2 Aircraft Characteristics

As previously outlined, **Air Nostrum**'s fleet includes three types of aircraft: the **ATR 72-600**, the **Bombardier CRJ200** and the **Bombardier CRJ1000**. The conceptual aircraft design tool developed is used not only to size potential hybrid-electric aircraft, but also to replicate **Air Nostrum**'s conventional aircraft. Table 4 summarizes the aircraft characteristics which were considered to prescribe the top-level requirements

[9] `https://openflights.org/` [Accessed: 18/11/2023]
[10] `https://airportdb.io/#findairport` [Accessed: 18/11/2023]

to the conceptual aircraft design tool.

Furthermore, given the scope of the project, although the aircraft *Bombardier CRJ200* and *Bombardier CRJ1000* are both initially turbofans, these were converted into turboprops. Due to the need to limit propeller tip speeds and to avoid loss of efficiency at very high altitudes, both the cruise speed and the cruise altitude were reduced. The cruise altitude and the cruise velocity of the *ATR 72-600* were used as a reference. Moreover, the approach speed (V_{app}) was reduced for both *Bombardier* aircraft. The real approach speed for the *Bombardier CRJ1000* is 65[11] m/s and for the *Bombardier CRJ200* is 69 [12] m/s. This reduction stems from the need to limit the lift coefficient during cruise to below the buffet lift coefficient. The former design modifications have of course implications in the network performance. Due to the difference in cruise velocity, it would be unrealistic to assume it would be possible to serve all the original routes. However, this is not considered to be an issue as the analysis is centred around comparing different case studies, rather than providing absolute results. Thus, the relative difference between the case studies is what is most relevant.

Table 4: Air Nostrum aircraft characteristics.

Parameter	**Aircraft**		
	ATR 72-600	*Bombardier CRJ200*	*Bombardier CRJ1000*
Seats [-]	72 [13]	50[14]	100[15]
R_{design} [km]	1370 [13]	3148[14]	3056[16]
h_{cruise} [m]	7620[17]	8000[a]	8000[a]
V_{cruise} [m/s]	142[13]	140[a]	140[a]
V_{app} [m/s]	58[18]	60[a]	60[a]
AR [-]	12[13]	9.3[14]	8.9[15]
$n[-]$	2[13]	2[14]	2[15]
TOL [m]	1315[13]	1920[14]	2030 [19]
Cost [million €]	24[20]	22.3[14]	23.1[19]

[a] Values adjusted to transform aircraft into turboprop aircraft.

3.2 Verification

The *Air Nostrum* case study was used to create the base case which was used to verify the correct working of the framework.

3.2.1 Verification Hybrid-Electric Design Module

Table 5 summarizes the main variables resultant from the design of a conventional ATR 72-600. Most variables are within acceptable limits, given the conceptual nature of the *Hybrid-Electric Design Module*. The largest discrepancy verified is associated with the power loading which is a result of a lower power setting during cruise. This discrepancy does not however affect the estimation of the fuel consumed during the mission, which is in the current work the most crucial parameter.

3.2.2 Verification Fleet Assignment & Scheduling Module

A reference scenario was constructed not only to serve as basis of comparison for all the scenarios evaluated in section 4 but also to verify the correct working of the *Feelt Assignment and Scheduling Module*. The **Air Nostrum**'s demand data and conventional aircraft along with the airport data detailed in section 3.1.1 were fed as inputs to the *Feelt Assignment and Scheduling Module*. Furthermore, both objectives were considered to

[11] `https://aerocorner.com/aircraft/bombardier-crj-1000/` [Accessed: 20/09/2023]
[12] `https://skybrary.aero/aircraft/crj2` [Accessed: 20/09/2023]
[13] `https://www.atr-aircraft.com/` [Accessed: 20/09/2023]
[14] `https://www.flyradius.com/bombardier-crj200/specifications` [Accessed: 20/09/2023]
[15] `https://www.flyradius.com/bombardier-crj1000/specifications` [Accessed: 20/09/2023]
[16] `https://pdf.aeroexpo.online/pdf/bombardier/crj-series-brochure/169445-101.html` [Accessed: 20/09/2023]
[17] `https://www.caribbean-airlines.com/#/our-fleet/atr-72-600`
[18] `https://skybrary.aero/aircraft/at76` [Accessed: 20/09/2023]
[19] `https://aerocorner.com/aircraft/bombardier-crj-1000/` [Accessed: 20/09/2023]
[20] `https://aerocorner.com/aircraft/atr-72-600/` [Accessed: 20/09/2023]

Table 5: Conventional aircraft synthesis verification, ATR 72-600.

Variable	Reference	Computed	Percentage Difference
MTOM [kg]	23000	24596	+6.9
OEM [kg]	13600	14663	+7.8
M_f [kg]	2000	2013	+0.65
S [m^2]	61	68.3	+11.9
W/S [-]	3698	3540	-4.5
W/P [-]	0.055	0.032	-41.8

be equally important and thus set to be the same and equal to 0.5.

Furthermore, from the results, the *Bombardier CRJ200* aircraft was not selected. Coming back to Figure 12, it is relevant to remember that the analysis was performed on a reduced number of airports, which excluded routes with extremely small demand. Given that the *Bombardier CRJ200* is the aircraft with the smallest capacity out of the three Air Nostrum aircraft, it is reasonable that there is a preference for the other aircraft types. The reference fleet is composed of 4 *ATR 72-600* aircraft and 7 *Bombardier CRJ1000* aircraft, which generate the results summarized in Table 6. Several key performance indicators (KPIs) are used to quantify the performance of the network. These include the total profit (including ownership cost), the total cost (including ownership cost), the percentage of demand served, the number of OD-pairs served, the cost available seat kilometer (CASK), the revenue available seat kilometer (RASK) and finally the total CO_2 and NOx emissions.

Furthermore, it is important to point out that the longest route included in the schedule had a length equal to 664 km, meaning all the longer routes included in the analysis were not considered profitable. Longer routes imply fewer flights can be allocated in one day and since the fare price does not vary with the length of the mission, longer missions end up producing less profit as they generate revenue equivalent to that of shorter routes but consume more fuel and diminish the number of flights in one day.

Table 6: Key Performance Indicators of the Reference Scenario.

Variable	*Profit* [€]	*Cost* [€]	*Demand Served* [%]	*OD-pairs Served* [-]	*CASK* [€/km]	*RASK* [€/km]	CO_2 [kg]	*NOx* [kg]
Value	2059042	1408554	33	8	0.039	0.125	1397029	1838

4 Results & Discussion

The **Air Nostrum** case study described in section 3 was used as a test case to understand how the off-design performance of hybrid-electric aircraft influence the performance of a regional airline network, what are the key variables at play in the trade-off between choosing conventional or hybrid-electric aircraft and finally, how can hybrid-electric aircraft be designed to better suit a regional airline network.

4.1 Hybrid-Electric Design Exploration

The following section aims to shed light on how the off-design performance of a HE aircraft changes for different design ranges and different design powersplits. Furthermore, the effect of cruising at off-design Mach numbers is also considered.

4.1.1 Baseline Exploration

On-Design Performance

Initially, all 3 Air Nostrum aircraft were sized with 5% supplied powersplit in all nominal flight phases. However, for the *Bombardier CRJ200* this led to a battery which did not fit inside the aircraft. Moreover, an analogous issue occurred for the *Bombardier CRJ1000*. Although there was space to store the battery, the span of the aircraft surpassed the ICAO category C airport span constraint of 36 m. Thus, the baseline hybrid-electric design of these particular aircraft was sized for a supplied power split value equal to 4% instead of 5%. This issue stems from the fact that as the supplied powersplit is increased, so does the weight of the battery and in turn the MTOM. Given that the approach velocity constrains the wing loading, the latter remains constant during the aircraft design iteration process. Hence, as the MTOM increases, the wing area must increase accordingly. Since the aspect ratio remains constant throughout the design iterations, the span must ultimately increase.

Furthermore, it was observed that even when setting the design powersplit to a value as little as 5% there was a significant increase in MTOM. Table 7 summarizes the main observations and for the relevant variables provides the Δ in terms of percentage with respect to the correspondent conventional counterpart. It was verified that the larger the design range for which the aircraft is sized the larger the increase in MTOM and consequently the larger the increase in wing span (percentage wise). Moreover, one can also notice the large increase in fuel consumption for the *Bombardier* aircraft. This stems not only from the increase in MTOM but also from the drag penalty due to the low aspect ratio of these aircraft.

Table 7: Initial Hybrid-Electric Aircraft On-design Analysis with battery energy density equal to 350 Wh/kg.

Aircraft	**Powersplit** [%]	$\mathbf{R_{design}}$ [km]	$\mathbf{M_{bat}}$ [kg]	**MTOM** [kg]		**b** [m]		M_f [kg]	
				Value	Δ [%]	*Value*	Δ [%]	*Value*	Δ [%]
ATR 72-600	5	1370	3313	30819	+25	32	+11.8	2088	+3.7
Bombardier CRJ200	4	3148	5974	31233	+66	27	+26.8	4126	+38.4
Bombardier CRJ1000	4	3056	10476	57467	+64.5	36	+26.8	7264	+39.4

Off-Design Performance

With knowledge of the on-design parameters of the baseline HE aircraft, their off-design analysis was constructed. The off-design analysis for the three baseline HE aircraft can be observed in Figure 13. Within the considered range of mission lengths (100-1300 km), Figure 13 provides information on three important variables for each of the *Air Nostrum* aircraft. On one hand, ΔM_{fuel} is the percentage difference in terms of fuel consumed given a certain payload-range combination. $\phi*_{cruise}$ is the maximum attainable cruise powersplit and finally $\eta_{p,climb}$ is the propulsive efficiency during climb (here propulsive efficiency refers to the ratio between $T \cdot V_0$ and the increase in kinetic of the air). The results for different payload masses can be identified by either looking at the color of the lines or by looking at the line dash type.

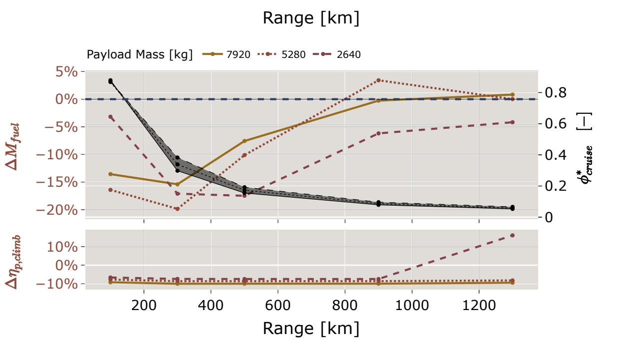

(a) Off-design analysis of hybrid-electric ATR 72-600 aircraft ($\phi = 5\%$, $R_{design} = 1370$ km, Seats = 72)

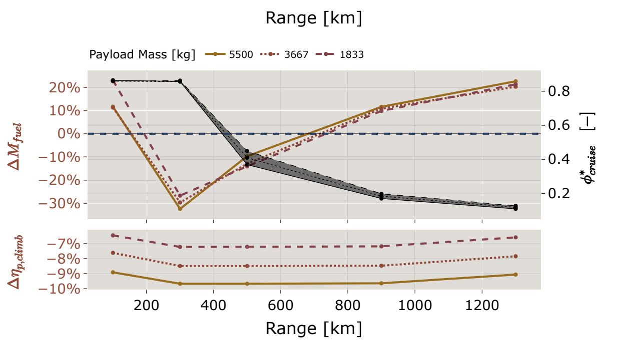

(b) Off-design analysis of hybrid-electric Bombardier CRJ200 aircraft ($\phi = 4\%$, $R_{design} = 3148$ km, Seats = 50)

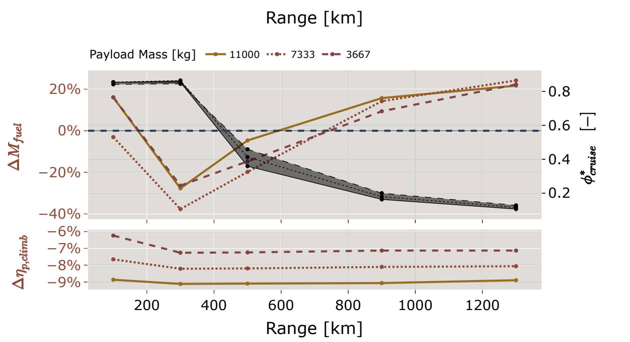

(c) Off-design analysis of hybrid-electric Bombardier CRJ1000 aircraft ($\phi = 4\%$, $R_{design} = 3056$ km, Seats = 100)

Figure 13: Percentage difference of fuel mass consumed of hybrid-electric aircraft with respect to conventional counterpart.

In general, one can observe not only that the baseline HE aircraft fuel consumption gradually reduces with the mission length until it is less than that of its conventional equivalent, but also that there is a non-linear relationship between $\phi*_{cruise}$ and the length of the mission. However, for very short mission lengths, below 300 km, in spite of the maximum attainable cruise powersplit reaching values as high as 80 %, the fuel consumption of the baseline HE aircraft begins to worsen, and for the case of the *Bombardier* aircraft even becomes worse than its conventional counterpart.

Several factors have been identified to come into play such that this phenomenon occurs. On one hand, the maximum attainable supplied powersplit during cruise is limited by the operational envelope of the gas turbine. This limit is found to be roughly equal to 85 % for all baseline HE aircraft and irrespective of the payload mass. This upper bound is clearly visible for the *Bombardier* aircraft. Given that these aircraft were sized for a larger range and thus have a powertrain sized for a larger power than the *ATR 72-600*, it is reasonable that they reach this upper limit before the *ATR 72-600* aircraft. Although not visible on Figure 13a, the *ATR 72-600* aircraft should also reach an upper bound for the maximum attainable cruise powersplit, but for a mission length smaller than 300 km.

Furthermore, the aforementioned behaviour results in the fact that for very small missions the energy stored in the battery is not fully used, since for missions smaller than a certain threshold, the powersplit cannot be increased during cruise. However, this is not sufficient to explain why for very small missions the HE aircraft seem to suffer a toll in terms of performance. Ultimately, this jump is attributed to the fact that HE aircraft suffer from a lower propulsive efficiency during climb and thus require a larger fuel consumption to achieve the same thrust. This is true for all aircraft types and irrespective of the mission length as can be seen from Figure 13. Moreover, as the mission length decreases the climb segment becomes increasingly more dominant in terms of the total fuel consumed. Therefore, once the upper bound for maximum attainable cruise powersplit is reached, as the mission length continues to decrease, the HE aircraft fuel savings during cruise are not sufficient to compensate for the larger fuel consumption during climb.

Moreover, this highlights the importance of the HE aircraft control variables in the minimization of their fuel consumption. To avoid the loss in performance for very short missions, since battery energy usage is not 100%, one can consider two aspects. On one hand, can consider that once the upper bound for $\phi*_{cruise}$ is reached the powertrain can be modelled to operate at fully-electric conditions. On the other hand, one can modify the *Off-design Analysis Module* such that it is also possible to drain more energy from the battery during other flight phases, namely during climb.

Additionally, it appears that for all three HE aircraft, there are similar "switching points". At around 300 km, the fuel consumed by these aircraft shifts from progressively decreasing to progressively increasing as already discussed (with respect to their conventional counterpart). Nevertheless, it is important to note the discrete and coarse nature of the analysis, which does not allow to identify for each aircraft when exactly the largest fuel consumed reduction is achieved. From the observations made about the maximum attainable cruise powersplit and the propulsive efficiency during climb, one can infer, for the *ATR 72-600* aircraft, this "switching point" should occur at smaller ranges than for the *Bombardier* aircraft.

Finally, for smaller design ranges (*ATR 72-600*), it is possible to observe fuel savings already at mission length values close to the design range, while for larger design ranges, (*Bombardier* aircraft) fuel savings are restricted to mission lengths up until roughly 23 % of the design range. When returning to Table 7, and examining the fuel used by each aircraft along with the weight penalty that goes along with it, it becomes evident how aircraft sized for a lesser design range save fuel for a greater area of the domain. Moreover, the small aspect ratio of the *Bombardier* aircraft may also play a role here and shift the curves to higher fuel consumption values. Sensitivity studies would be required to confirm this effect.

4.1.2 Cruise Mach Number Variation

The effect of modifying the cruise Mach number on the off-design performance of HE aircraft was evaluated in the following section. Two aircraft were considered: the baseline *ATR 72-600* and a redesigned *Bombardier CRJ1000*. The redesign of the *Bombardier CRJ1000* has a R_{design} equal to 1370 km and a design powersplit equal to 5%. The redesigned version of the *Bombardier CRJ1000* was considered instead of the baseline version to assess whether the design payload plays a role in the results. Table 19 in Appendix B contains a summary of the on-design characteristics of the redesign *Bombardier CRJ1000*.

Moreover, Figure 14 displays for each of the considered HE aircraft how modifying the Mach number (through the modification of the cruise velocity) affects the fuel consumed when different payload-range combinations are considered. It is relevant to note that all HE aircraft fuel mass profiles (both on and off-design) were compared with the fuel mass profile of their conventional counterpart when flying at the design cruise speed.

In general, modifying the cruise velocity does not affect the relationship between mission length and fuel consumed. It simply shifts the off-design results to higher or lower fuel consumed values. Furthermore, cruising at a higher velocity yields a higher fuel consumed. This can be associated with the fact that accelerating to a higher velocity requires more fuel to be consumed during climb and cruising at a higher velocity implies a higher power required from the powertrain. In turn, more power is required to be provided by the fuel and the fuel consumed during cruise is larger. Logically, when cruising at a lower velocity the opposite reasoning is applied. Nevertheless, for the *Bombardier CRJ1000* this does not seem to apply. When cruising at a lower velocity, more fuel is consumed.

Additionally, it seems that when flying at a lower capacity the aircraft is more sensitive to changes in cruise Mach number. This sensitivity increases as the design payload decreases as can be observed from comparing Figure 14a with Figure 14b. This can be related to the fact that if the aircraft weight is smaller than the lift is also smaller during the cruise phase. Changing the cruise velocity at a low-weight condition results in a larger C_L difference, which in turn implies thrust must increase by a larger amount to keep level flight due to the additional lift-induced drag and hence fuel consumption increases.

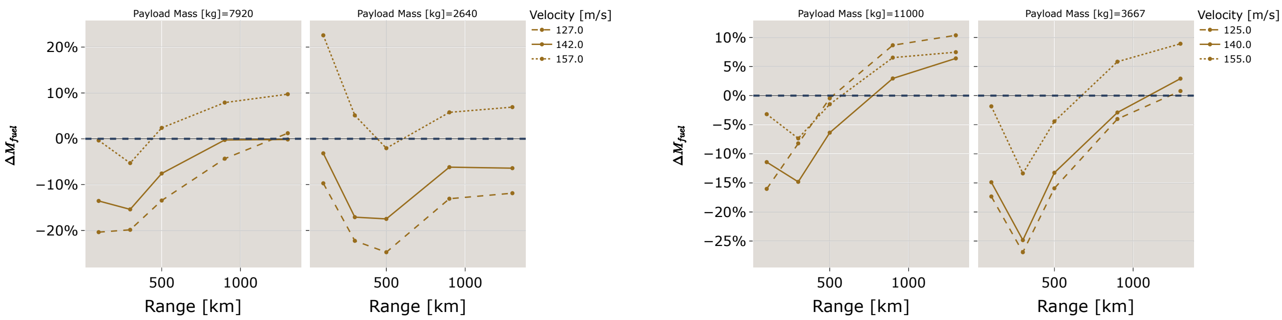

(a) Off-design analysis of hybrid-electric ATR 72-600 aircraft ($\phi = 5\%$, $R_{design} = 1370$ km, Seats = 72)

(b) Off-design analysis of hybrid-electric Bombardier CRJ1000 aircraft ($\phi = 5\%$, $R_{design} = 1370$ km, Seats = 100)

Figure 14: Variation with cruise velocity of off-design analysis for hybrid-electric aircraft.

4.1.3 Design Point Variation

One of the research objectives of the current work is to analyse the effect that modifying the design powersplit and the design range has on the off-design performance of a HE aircraft. In the current subsection these effects shall be quantified. Firstly, the effect of modifying the powersplit is analysed and thereafter the effect of modifying the design range.

Design Powersplit

In order to analyse the effect of modifying the design powersplit on the off-design performance of hybrid-electric aircraft, the design powersplit of the aircraft *Bombardier CRJ1000* and *ATR 72-600* was modified. To isolate this effect the *Bombardier CRJ1000* aircraft redesign with R_{design} equal to 1370 km was considered. Thus, both the *ATR 72-600* and the *Bombardier CRJ1000* are sized for the same design range and the same design powersplit (equal to 5% or 10%). Nevertheless, they have different design payloads. Table 19 in Appendix B provides further details on the performance and characteristics of these aircraft designs at their design point.

Moreover, ΔM_{fuel} in Figure 15 and Figure 16 represents, for the HE aircraft being considered, the difference in total fuel consumed, at a certain payload-range combination, with respect to their conventional counterpart. Thus, for the case of the *Bombardier CRJ1000* it is important to consider the difference in design range between the HE aircraft we are considering and its conventional counterpart. Being that the former is equal to 1370 km and the latter is equal to 3056 km. Anyhow, being sized for a smaller design range simply results in larger fuel savings for a larger portion of the domain considered, as seen in section 4.1.1, thus it does not affect the analysis on the effect of modifying the design powersplit, which is the focus of the current section.

Furthermore, when diving into Figure 15 and Figure 16 one can observe that as the mission length decreases the aircraft sized for a powersplit equal to 10% experiences a much steeper decline in fuel consumed than the aircraft sized for 5%. Furthermore, when looking at larger mission lengths, the former consumes more fuel than the latter. This difference is reduced as the mission length decreases. These considerations show that, interestingly, at the payload-range combinations considered, increasing the design powersplit does not lead to larger savings in fuel. Moreover, similarly to sizing a HE aircraft for a larger range, when sizing it for a larger powersplit, the weight penalty due to the increase in battery weight restricts the savings in fuel to a smaller portion of the domain.

Additionally, the design payload seems to affect the aircraft's sensitivity to modifying the design powersplit. It appears that aircraft with a larger design payload are more sensitive to an increase in design powersplit. This is especially true for larger mission lengths. This phenomenon links once again back to the weight penalty discussion.

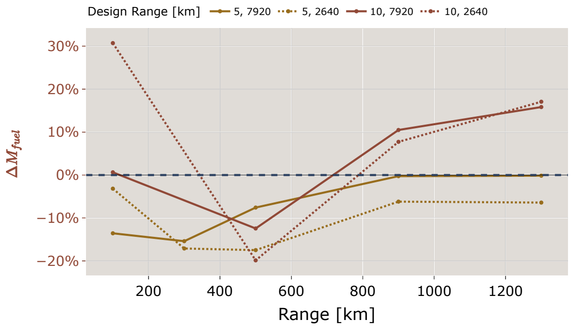

Figure 15: Off-design analysis of hybrid-electric ATR 72-600 aircraft (ϕ = 5%, R_{design} =1370 km, Seats = 72)

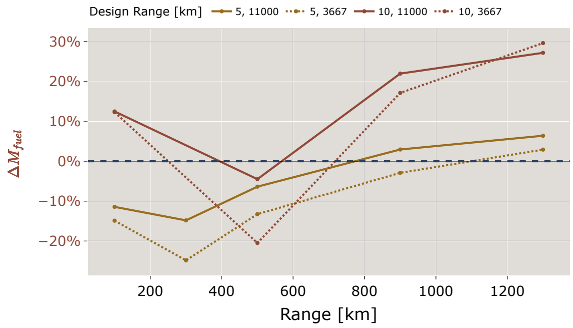

Figure 16: Off-design analysis of hybrid-electric Bombardier CRJ 1000 aircraft (ϕ = 5%, R_{design} =1370 km, Seats = 100)

Design Range

To understand the effect that the design range has on the off-design of HE electric aircraft, four different design ranges are considered. The *Bombardier CRJ1000* HE aircraft redesigned with a design range equal to 1370, 620, 450 and 300 km and a design powersplit equal to 5% are used to draw conclusions. Note that the chosen design ranges are not arbitrary. These were selected by making use of the coupling strategy explained in section 2.4. This procedure shall be further explained in section 4.2, while in the current section, the focus is placed on the evaluation of the off-design performance of these designs. Furthermore, in Table 19 in Appendix B one can find further details regarding the on-design performance and characteristics of the aforementioned *Bombardier CRJ1000* redesigns.

Furthermore, Figure 17 displays for each redesign the change in fuel consumed per payload carried, at different payload-range combinations, with respect to the conventional counterpart. Unlike previous analysis, here the metric of comparison is the change in fuel per payload carried. This is a fairer metric since for the aircraft redesigns with a R_{design} smaller than 1300 km, some of the off-design evaluations are after the harmonic segment of their payload-range diagram and thus the payload mass is smaller than the design payload mass.

Moreover, when inspecting Figure 17 one can note that the trends of fuel savings per payload carried are similar across the aircraft sized for design ranges of 300, 450 and 620 km, especially for large mission lengths. This is not true for smaller mission lengths. As has already been partially observed in section 4.1.1, it appears that aircraft designed for larger ranges experience a stronger decline in terms of fuel consumed as the mission length becomes increasingly smaller. This is then reflected on the fact that at very short ranges (below 300 km) the largest fuel savings are attained by the aircraft with a design range equal to 620 km. Unlike in the case of the aircraft sized for 1370 km, up until 100 km there is no transition from a progressively decreasing fuel consumption to a progressively increasing fuel consumption. This indicates that for these aircraft at a mission length equal to 100 km and above the upper bound for the $\phi*_{cruise}$ has not been reached. Ultimately, the observations made indicate that reducing the design range, up to a certain threshold, yields savings in terms of fuel, after which these savings become increasingly smaller.

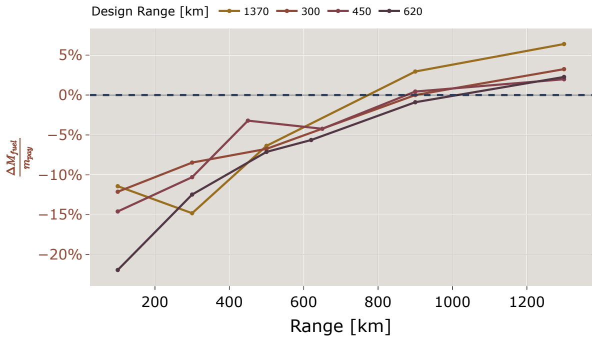

Figure 17: Off-design comparison of Bombardier CRJ1000 for several R_{design} ($\phi = 5\%$, Seats = 100)

4.2 Fleet Assignment and Scheduling Analysis

The following section presents the results which aimed to understand how the performance of an airline is affected when HE aircraft designed for different powersplits and design ranges are considered. In order to conduct the analysis presented in this section, several different HE designs were considered. Already in section 4.1, the off-design performance of these designs has been elaborated. Nevertheless, the way in which these redesigns were selected has not. This shall be elaborated on in section 4.2.1. Furthermore, from these redesigns, several scenarios were constructed. These are analysed in section 4.2.2 and section 4.2.4. Finally, section 4.2.3 elaborates on how cruising at off-design conditions impacts the network performance.

4.2.1 Initial Hybrid-Electric Fleet & Redesigning

The baseline HE aircraft analysed in section 4.1.1 were placed in the network along with their conventional counterparts (**Scenario A**). It was verified that none of the hybrid-electric aircraft were selected and thus the final selected fleet was exactly the same as in the reference scenario (refer to section 3.2.2). This reluctance to choose the HE aircraft is associated with the fact that the ownership cost of the HE aircraft is considered to be 20 % larger than its conventional counterpart. In addition to this, the HE aircraft operating costs consider the cost of electricity, a factor which is non-existent for conventional aircraft. The combination of these two factors overpowers the fuel savings evidenced by the HE aircraft in the range of mission lengths selected (refer to Figure 13).

Coming back to the results from section 4.1.1, and the length of routes which constitute the Air Nostrum network, the unnecessarily large design range of the *Bombardier* aircraft, does not serve the network. In fact, it reduces the range of mission lengths for which there are fuel savings. Given this, the *Bombardier* aircraft were resized for a design range equal to that of the ATR 72-600, thus equal to 1370 km and the powersplit was also kept at 5%.

After the fleet assignment and schedule creation, an analysis on the routes flown and aircraft selected was conducted. It was verified that unlike for **Scenario A**, one HE aircraft was selected. Specifically, the *Bombardier CRJ1000* with R_{design} equal to 1370km. From this observation it was decided to redesign new aircraft in terms of range, while maintaining the capacity of the aircraft the same as that of the original aircraft. This decision stems from the wish to maintain the same ability to capture demand but also from the fact that *Hoogreef & Bonnin* [9], concluded that modifying the design payload of the aircraft has a marginally small effect on the fuel consumed. Since the *Bombardier CRJ200* and *ATR 72-600* were not selected these aircraft were not redesigned and thus not included in further iterations. Furthermore, with the clustering method described in section 2.4, the redesigns summarized in Table 8 were created.

Table 8: Summary of range clusters per aircraft.

Aircraft	**New Range** [km]	**Powersplit** [%]
Bombardier CRJ1000	300	5
Bombardier CRJ1000	450	5
Bombardier CRJ1000	620	5

4.2.2 Fully Hybrid-Electric Fleet

Table 9 summarizes the main characteristics of the different scenarios analysed in the following section. These scenarios were constructed with the aim of understanding on one hand how the performance of the network is affected if only HE aircraft are considered and on the other hand what is the impact of design range and design powersplit on the former. Furthermore, comparing **Scenario B** to **Scenario D** allows for understanding the effect of design powersplit, while comparing **Scenario B** to **Scenario C** allows for analysing the effect of design range on the network's performance. Furthermore, note the naming convention for the different aircraft designs which follows the following logic: Aircraft type- Powertrain type- R_{design} - ϕ_{design}; An example of an aircraft design according to this naming convention is: *Bombardier CRJ1000-HE-1370-5.* Note that this naming convention is used in all the scenarios considered.

Table 9: Characteristics of scenarios B C and D

Scenario	Initial Fleet	Objective Function Weights [w_p, w_e]	Velocity
B	Bombardier CRJ1000-HE-1370-5, Bombardier CRJ200-HE-1370-5, ATR 72-600-HE-1370-5	[0.5,0.5]	Constant
C	Bombardier CRJ1000-HE-1370-5, Bombardier CRJ1000-HE-620-5, Bombardier CRJ1000-HE-450-5, Bombardier CRJ1000-HE-300-5	[0.5,0.5]	Constant
D	Bombardier CRJ1000-HE-1370-10, ATR 72-600-HE-1370-10	[0.5,0.5]	Constant

The different scenarios considered were evaluated according to several key performance indicators and compared to the reference scenario described in section 3.2.2. Figure 18 depicts visually this comparison. Any point outside the black circular line indicates a larger KPI value and vice-versa.

In general, all scenarios suffer from a significant loss in terms of total profit, and at the same time significant savings in terms of CO_2 and NOx emissions. Furthermore, when comparing scenario **C** with scenario **B**, the loss of profit on the former is smaller than the loss of profit on the latter (-20% versus -25%). Furthermore, the total cost of scenario **C** is greater than that of scenario **B** (+5.6% versus -1.3%). This can be attributed to two factors. On one hand, the fact that in scenario **C** the fleet is composed of two extra aircraft and thus ownership costs are larger. The smaller ownership costs of scenario **B** compensate for its larger CASK. Given the fact that in scenario **B** there is a larger reduction in terms of CO_2 and NOx emissions (-36%), the increased CASK can only stem from larger electricity costs or larger airport and navigation costs (due to larger MTOM). On the other hand, scenario **B** has a larger RASK than scenario **C** which indicates more revenue per seat kilometer. This indicates that either scenario **B** has a larger load factor or that on average shorter routes are flown. Given the way in which revenue is modelled, it is reasonable that there is a preference for shorter routes.

Moreover, when looking into the final fleet of scenario **C** (Table 10), only one aircraft type is selected (*Bombardier CRJ1000-HE-300-5*). One might wonder why the *Bombardier CRJ1000-HE-620-5* was left out of the final fleet when according to the analysis conducted in section 4.1.3 this aircraft design yields a lower fuel consumed for most mission lengths. Even though this is true, the *Bombardier CRJ1000-HE-620-5* aircraft does so to the expense of consuming more battery energy than the *Bombardier CRJ1000-HE-300-5* aircraft type (larger electricity costs). Thus the profit and hence the first objective of the *Bombardier CRJ1000-HE-300-5* aircraft is larger than that of the *Bombardier CRJ1000-HE-620-5* aircraft. Furthermore, even though the objective function values are 50-50 the monetization of the CO_2 emissions causes the order of magnitude of the first objective to be larger than that of the second objective (in the order of 20 times in the first iterations) and thus the first objective has a larger contribution to the total objective function value.

When comparing scenario **B** with scenario **D**, the former yields a smaller loss in terms of profit than the latter (-25% versus -39.7%). Both scenarios have CASKs larger than in the reference scenario, this is specially accentuated for scenario **D** and can be attributed to both larger fuel costs (larger CO_2 emissions when compared to scenario **B**) and larger airport and navigation costs. The latter is inferred from the fact that as seen in section 4.1.3, increasing the powersplit from 5% to 10% yields a large weight penalty and a significant increase in MTOW. Furthermore, the larger total cost associated with scenario **D** is also a result of the fact that its final fleet is composed by one extra aircraft when compared to scenario **B**. A fleet composed of HE aircraft with a larger design powersplit requires a larger number of aircraft to serve approximately the same percentage of demand.

All in all, one can observe that both from a profit and a emissions point of view, a fleet composed by aircraft with a smaller design powersplit outperforms a fleet composed by aircraft with a greater design powersplit.

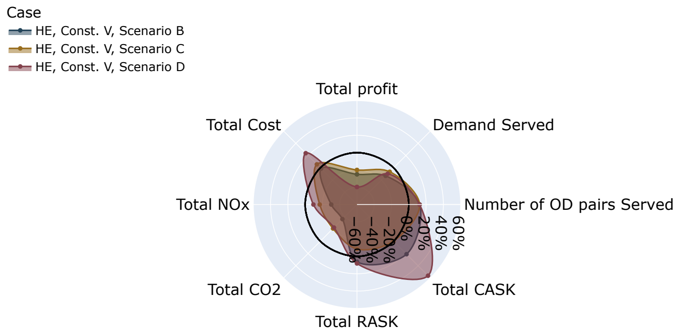

Figure 18: Key performance indicators comparison between scenario B, C and D

Table 10: Fleet composition of hybrid-electric scenarios.

Scenario	Final Fleet
B	(**7**)Bombardier CRJ1000-HE-1370-5, (**3**)ATR 72-600-HE-1370-5
C	(**12**)Bombardier CRJ1000-HE-300-5
D	(**5**)Bombardier CRJ1000-HE-1370-10, (**6**)ATR 72-600-HE-1370-10

4.2.3 Cruise Mach Number Effect

Table 11 summarizes the main characteristics of scenario **J**. The following section elaborates on how the network performance is affected by the change in off-design performance of HE aircraft resultant of cruising at off-design Mach numbers. Here scenarios **B** and **J** are compared. These only differ in the fact that the cruise velocity on each flight is allowed to be selected by the fleet assignment and scheduling module. The reader is referred to section 4.1.2 for further understanding how the off-design performance of HE aircraft is affected by cruising at off-design Mach numbers.

Table 11: Characteristsics of scenario J

Scenario	Initial Fleet	Objective Function Weights $[w_p, w_e]$	Velocity
J	Bombardier CRJ1000-HE-1370-5, Bombardier CRJ200-HE-1370-5, ATR 72-600-HE-1370-5	[0.5,0.5]	Not Constant

When inspecting Figure 19 and Table 12 one can note that when the cruise velocity is allowed to vary the final fleet includes a larger number of *ATR 72-600-HE-1370-5*. As seen in section 4.1.2, both aircraft types yield larger fuel savings when flying slower, however the *ATR 72-600-HE-1370-5* aircraft does so to a larger extent. Furthermore, flying faster allows for a larger flight frequency, but more fuel is consumed. In scenario **J** the framework plays with this paradox and for each flight it chooses to fly slower (thus saving fuel), on another flight it chooses to fly faster (to include an extra flight). Nevertheless, the loss of profit is still larger than for scenario **B** due to a smaller accumulated revenue. Although the total number of flights in both scenarios is nearly the same (644 for scenario **J** and 642 for scenario **B**), due to the smaller capacity of the *ATR 72-600-HE-1370-5* fewer passengers are transported. This is also reflected in a loss of demand served.

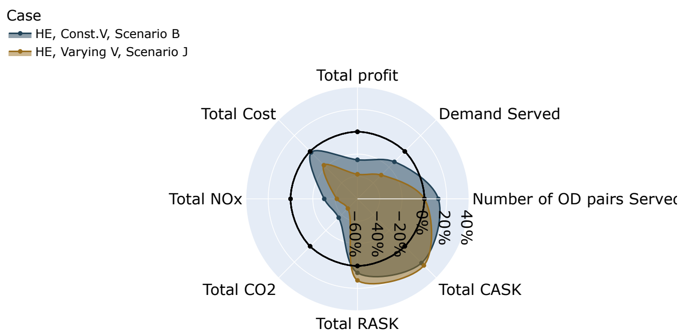

Figure 19: Key performance indicators comparison between scenario B and J

Table 12: Fleet composition of scenarios.

Scenario	Final Fleet
B	(**7**)Bombardier CRJ1000-HE-1370-5, (**3**)ATR 72-600-HE-1370-5
J	(**3**)Bombardier CRJ1000-HE-1370-5, (**6**)ATR 72-600-HE-1370-5

4.2.4 Conventional and Hybrid-Electric Fleet

Table 13 summarizes the main characteristics of the scenarios analysed in the following section. The scenarios were constructed to understand on one hand how the performance of the network is affected if a mixed fleet is considered (both kerosene and hybrid-electric aircraft) and on the other hand how does design range and design powersplit modify the former.

Table 13: Characteristics of scenarios E, F and G. Green color refers to hybrid-electric aircraft.

Scenario	Initial Fleet	Objective Function Weights $[w_p, w_e]$	Velocity
E	Bombardier CRJ1000-KE, Bombardier CRJ200-KE, ATR 72-600-KE, Bombardier CRJ1000-HE-1370-5, Bombardier CRJ200-HE-1370-5, ATR 72-600-HE-1370-5	[0.5,0.5]	Constant
F	Bombardier CRJ1000-KE, ATR 72-600-KE, Bombardier CRJ1000-HE-1370-10, ATR 72-600-HE-1370-10	[0.5,0.5]	Constant
G	Bombardier CRJ1000-KE, ATR 72-600-KE, Bombardier CRJ1000-HE-1370-5, Bombardier CRJ1000-HE-620-5, Bombardier CRJ1000-HE-450-5, Bombardier CRJ1000-HE-300-5	[0.5,0.5]	Constant

Firstly, scenario **F** considered a mixed initial fleet, which includes the HE aircraft redesigns with a design powersplit equal to 10%. When included in the Air Nostrum network, no HE aircraft was selected. This reinforces the conclusion drawn in section 4.2.2: increasing the design powersplit of a HE aircraft does not necessarily bring enough fuel savings such that they become competitive with respect to kerosene aircraft.

Furthermore, Figure 20 displays the KPIs percentage difference between scenarios **E** and **G** and the reference scenario. When looking at scenario **E**, the final fleet composition differs from the reference scenario by only one aircraft: the *Bombardier CRJ1000-HE-1370-5* was selected at the last iteration. From this modification, even though the *Bombardier CRJ1000-HE-1370-5* aircraft has a larger ownership cost, total profit remains virtually the same (-0.01%). Although CO_2 emissions are reduced by 1.3%, scenario **G** yields a much larger reduction in CO_2 emissions (-15%). In scenario **G** a larger number of HE aircraft are selected. In spite of their larger ownership costs, with six *Bombardier CRJ1000-HE-300-5*, total profit is reduced by only 1.35%. The increased ownership costs are mostly compensated by a reduction in operating cost. The latter stems from a reduction in fuel costs and airport costs (smaller MTOW). This indicates that if ownership costs were to be the same between HE and KE aircraft, a mixed-fleet would yield larger profits. Nevertheless, further studies are required to confirm this. Moreover, the reduction in demand served with yet an increase in RASK indicates that shorter routes are flown. This would be reasonable since due to the small design range of the *Bombardier CRJ1000-HE-300-5* aircraft short routes (below 300 km) allow for the aircraft to fly at maximum capacity while yielding large savings in fuel.

Combining KE and HE aircraft with a network-specific design range allows for initially capturing more demand (due to the reduced turnaround time of KE aircraft) at the expense of additional emissions. There are then compensated for by the HE aircraft flying short routes frequently and inexpensively. Furthermore, it is relevant to note the characteristics of the airline network being considered: many short routes with high demand. From both the off-design analysis conducted in section 4.1 and the observations made in this section it is clear how a network with these types of routes directly benefits from the introduction of HE aircraft.

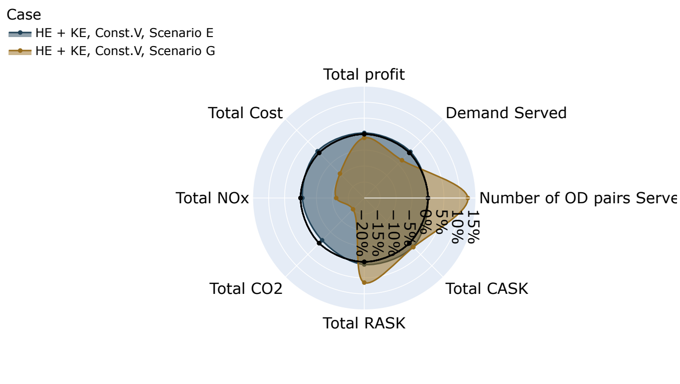

Figure 20: Key performance indicators comparison between scenario E and G

Table 14: Fleet composition of mixed fleet scenarios.

Scenario	Final Fleet
E	(**6**) Bombardier CRJ1000-KE, (**4**) ATR 72-600-KE, (**1**) Bombardier CRJ1000-HE-1370-5
F	(**7**) Bombardier CRJ1000-KE, (**4**) ATR 72-600-KE
G	(**2**) Bombardier CRJ1000-KE, (**2**) ATR 72-60-KE, (**6**) Bombardier CRJ1000-HE-300-5

4.3 Sensitivity Analysis

In the current work, as described in section 2.3, the fleet is chosen based on a weighted objective function, which considers both profit and CO_2 emissions. Thus, a sensitivity study was conducted to understand how the trade-off between these two objectives affects the performance of the network. Table 15 summarizes the characteristics of scenarios **H** and **I**, which were constructed based on scenario **G**. The only difference between these scenarios is the objective function weights.

Table 15: Characteristics of scenarios H and I. Green color refers to hybrid-electric aircraft.

Scenario	Initial Fleet	Objective Function Weights $[w_p, w_e]$	Velocity
H	Bombardier CRJ1000-KE, ATR 72-600-KE, Bombardier CRJ1000-HE-1370-5, Bombardier CRJ1000-HE-620-5, Bombardier CRJ1000-HE-450-5, Bombardier CRJ1000-HE-300-5	[0.2,0.8]	Constant
I	Bombardier CRJ1000-KE, ATR 72-600-KE, Bombardier CRJ1000-HE-1370-5, Bombardier CRJ1000-HE-620-5, Bombardier CRJ1000-HE-450-5, Bombardier CRJ1000-HE-300-5	[1.0,0.0]	Constant

In general, attributing more importance to the profit-related objective (scenario **I**) leads to an increase in total profit (+26.5%) with a larger percentage of demand served (+29.5%). Evidently, this causes there to also be an increase in CO_2 (+26.6%) and NOx emissions. A 1% increase in profit induces a 1% increase in CO_2 emissions. It is interesting to see that HE aircraft are selected after the first fleet iterations. This is once again related to the turnaround time effect discussed in section 4.2.4.

Counterintuitively, when giving larger importance to the emissions objective than to the profit objective (scenario **H**), the reduction in CO_2 emissions is less than when equal importance is given to both objectives (-4.5% in scenario **H** and -15% in scenario **G**). Moreover, note that in scenario **H** there is a growth in demand served (+9%) and yet the selected fleet outputs a reduction in CO_2 emissions. Given the characteristics of the Air Nostrum network: many short routes with high demand; the most profitable routes are also those that require less time and costs to be operated. As seen in section 4.1, within short mission lengths some yield larger reductions in fuel consumed than others. Furthermore, both objectives are not entirely uncorrelated, since reducing emissions also implies reducing the fuel consumed and thus the fuel costs. When prioritizing the emission objective the "greenest" routes within the short routes are selected which in turn not only yields lower emissions but also a higher profit. As the iterations progress this effect compiles and a larger number of aircraft are selected and more demand is served.

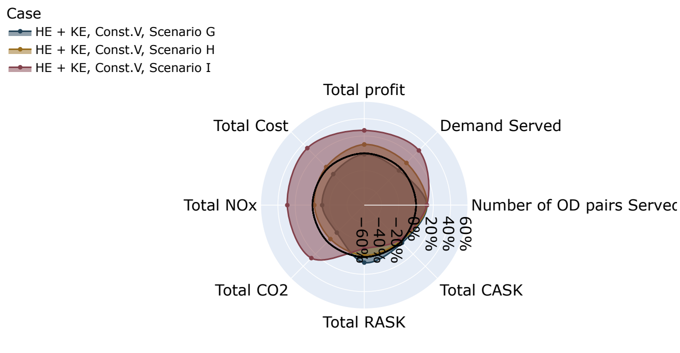

Figure 21: Key performance indicators comparison between scenarios G,H and I

Table 16: Fleet composition of scenarios.

Scenario	Final Fleet
G	(**2**) Bombardier CRJ1000-KE, (**2**) ATR 72-60-KE, (**6**) Bombardier CRJ1000-HE-300-5
H	(**4**) Bombardier CRJ1000-KE, (**1**) Bombardier CRJ1000-HE-620-5, (**7**) Bombardier CRJ1000-HE-300-5
I	(**4**) Bombardier CRJ1000-KE, (**4**) ATR 72-60-KE, (**7**) Bombardier CRJ1000-HE-300-5, (**1**) Bombardier CRJ1000-HE-620-5

5 Conclusions & Recomendations

The objective of the current work was: *To create a framework which couples a hybrid-electric aircraft design tool with a fleet assignment and scheduling tool and incorporates the effects of operating hybrid-electric aircraft outside their on-design conditions.* The framework created consists of three parts. Firstly, the *Hybrid-Electric Aircraft Design Module*, includes a modified powertrain model which is able to evaluate emissions, fuel consumption and for the case of hybrid-electric aircraft the battery energy spent both at on-design and off-design conditions. Secondly, the *Off-design Analysis Module* evaluates the maximum attainable powersplit during cruise for different payload-range combinations. This permits the quantification of how much fuel is consumed, and how much CO_2 and NOx is emitted when a hybrid-electric aircraft is considered. Finally, the *Fleet Assignment & Scheduling Module* relies on dynamic programming to select the fleet composition and their associated weekly schedule which maximizes profit and minimizes CO_2 production during the operations of an airline. The aforementioned modules are then coupled through a clustering method, which makes use of the passenger-distance data retrieved from the *Fleet Assignment & Scheduling Module* to explore new HE aircraft designs.

Moreover, a subset of the **Air Nostrum**'s network was used as a case study. The original Air Nostrum aircraft were redesigned to incorporate a hybrid-electric powertrain, their off-design performance was quantified and a new fleet composition was selected. In general, several HE aircraft designs were considered, spanning design ranges ranging from 300 km to 3000km and design powersplits either equal to 5% or 10%.

From the analysis conducted, several conclusions can be drawn. Firstly, hybrid-electric aircraft sized for a larger design range suffer from a large weight penalty at the design point. This weight penalty results in the fact that for the same reduction in mission length a larger reduction in fuel consumed is attained. Thus, for short missions these aircraft achieve larger absolute fuel savings than aircraft sized for a smaller range. However, these fuel savings span fewer mission lengths. Furthermore, the combination of the gas turbine operational limits and the lower propulsive efficiency during climb of HE aircraft yield, for these aircraft, a worse performance, than their conventional counterparts, for short missions. The larger the design range the greater the former effect.

Furthermore, increasing the design powersplit from 5% to 10% does not yield larger savings in terms of fuel at the payload-range combinations which were considered. The weight penalty which stems from increasing the powersplit depletes the aircraft from experiencing fuel savings for a large range of mission lengths. Moreover, when the design powersplit is kept at 5% and the design range is progressively reduced, the aircraft which experiences the largest fuel savings (for the largest amount of payload-range combinations) is not the aircraft sized for the lowest range. For the case considered the design range which maximizes fuel savings is 620 km. This is of course case specific but highlights a non-linear relationship between the design range and the off-design fuel savings directly attained.

The aforementioned conclusions are reflected in the fleet assignment and scheduling analysis. In general, a fully HE fleet yields a lower profit than a mixed-fleet or a fully kerosene fleet. Moreover, from a profit and emissions point of view, a fleet composed by aircraft with a smaller design powersplit outperforms a fleet composed of aircraft with a larger powersplit. In addition, modifying the design range outputs a smaller loss of profit when compared to increasing the design powersplit. If the change in aircraft performance from cruising at off-design Mach numbers is considered, less demand can be captured and the total profit attained decreases.

When considering a mixed-fleet, it has been shown in scenario **G** that a fleet composed by kerosene aircraft and HE aircraft redesigned with a small design range can achieve savings in terms of CO_2 emissions in the order of 15% while only experiencing a reduction in total profit equal to 1.35%. From this result, total profit and total demand served can be increased by attributing larger importance to the objective associated with emissions. Moreover, for both fully-hybrid and mixed fleets modifying the design range seems to be a larger predictor than design powersplit on whether HE aircraft are a competitive option to kerosene aircraft.

Finally, for future work, several activities are recommended. Firstly, it would be interesting to include the aero-propulsive benefits associated with propeller aircraft. This would open the way for investigating, for example, architectures which make use of distributed propulsion. From an off-design analysis point of view, it is recommended to evaluate the possibility of flying fully electric or making use of the battery in other phases besides the cruise phase. This is thought to have the potential to increase the fuel savings of HE aircraft for very short missions. Finally, to improve the fidelity of the fleet assignment and scheduling module, the costs associated with interest, depreciation and insurance should be taken into account. The current models would need to be adjusted in order to properly take the hybridization of the powertrain into account.

Moreover, given the conclusions of the current work, it is recommended to further explore how the design powersplit and the design range can be concurrently modified to control by how much and at which mission lengths the aircraft experiences fuel savings. It would also be relevant to consider airline networks with different demand-route length distributions. This could extend the knowledge on the extent of HE aircraft applicability.

References

[1] Boieng. *Commercial Market Outlook*. URL: `https://www.boeing.com/commercial/market/commercial-market-outlook/index.page` (visited on 05/04/2023).

[2] Airbus. *Global Market Forecast | Airbus*. en. June 2021. URL: https://www.airbus.com/en/products-services/commercial-aircraft/market/global-market-forecast (visited on 05/04/2023).

[3] United Nations. *The Paris Agreement*. en. URL: https://www.un.org/en/climatechange/paris-agreement (visited on 05/04/2023).

[4] NLR - Royal Netherlands Aerospace Centre and TU Delft. *Towards a Sustainable Air Transportation System*. White paper. 2021.

[5] Venkatasubramanian Viswanathan et al. "The challenges and opportunities of battery-powered flight". In: *Nature* 601.7894 (Jan. 2022), pp. 519–525. DOI: 10.1038/s41586-021-04139-1.

[6] Giuseppe Palaia and Karim Abu Salem. "Mission Performance Analysis of Hybrid-Electric Regional Aircraft". In: *Aerospace* 10.3 (Mar. 2023), p. 246. DOI: 10.3390/aerospace10030246.

[7] R. de Vries. "Hybrid-Electric Aircraft with Over-the-Wing Distributed Propulsion: Aerodynamic Performance and Conceptual Design". Dissertation (TU Delft). 2022. DOI: 10.4233/uuid:ef87dc11-e7b2-4726-a41f-28588d64c58d.

[8] M. F. M. Hoogreef et al. "Scalability Assessment of Hybrid-Electric Technology Application to Various Aircraft Classes - an Overview of Opportunities and Challenges". In: *Aerospace Europe Conference 2023 – 10 EUCASS – 9 CEAS* (2023). Publisher: EUCASS. DOI: 10.13009/EUCASS2023-260.

[9] Vincent Bonnin and Maurice Hoogreef. *Deliverable D3.3 - Report on opportunities for cross-vehicle class and technology synergies*. Tech. rep. May 2023.

[10] Peter Jansen and Ruben Perez. "Coupled Optimization of Aircraft Family Design and Fleet Assignment for Minimum Cost and Fuel Burn". In: *12th AIAA Aviation Technology, Integration, and Operations (ATIO) Conference and 14th AIAA/ISSMO Multidisciplinary Analysis and Optimization Conference*. Aviation Technology, Integration, and Operations (ATIO) Conferences. American Institute of Aeronautics and Astronautics, Sept. 2012. DOI: 10.2514/6.2012-5495.

[11] Christine Taylor and Olivier de Weck. "Coupled Vehicle Design and Network Flow Optimization for Air Transportation Systems". In: *7th AIAA ATIO Conf, 2nd CEIAT Int'l Conf on Innov and Integr in Aero Sciences*. American Institute of Aeronautics and Astronautics, Sept. 2007.

[12] Peter W. Jansen and Ruben E. Perez. "Coupled Optimization of Aircraft Design and Fleet Allocation with Uncertain Passenger Demand". In: *2013 Aviation Technology, Integration, and Operations Conference*. Los Angeles, CA: American Institute of Aeronautics and Astronautics, Aug. 2013. DOI: 10.2514/6.2013-4392.

[13] Satadru Roy et al. "A Mixed Integer Efficient Global Optimization Algorithm for the Simultaneous Aircraft Allocation-Mission-Design Problem". In: *58th AIAA/ASCE/AHS/ASC Structures, Structural Dynamics, and Materials Conference*. American Institute of Aeronautics and Astronautics, Jan. 2017. DOI: 10.2514/6.2017-1305.

[14] Elise Scheers. "Coupled hybrid electric aircraft design and strategic airline planning". MA thesis. TU Delft, 2023.

[15] Noa Zuijderwijk. "Study to the adaptation of electrified aircraft by regional airlines: using strategic airline planning and aircraft design". MA thesis. TU Delft, 2022.

[16] Maria Seoane Álvarez. "Assessment of the Climate Impact Mitigation Potential of Intermediate Stop Operations: A Dynamic Programming Approach". MA thesis. Delft, The Netherlands: TU Delft, 2021.

[17] Mahdi Noorafza et al. "Airline network planning considering climate impact: assessing new operational improvements". In: (2023).

[18] Pieter-Jan Proesmans and Roelof Vos. "Airplane Design Optimization for Minimal Global Warming Impact". English. In: *Journal of Aircraft* 59.5 (2022), pp. 1363–1381. DOI: 10.2514/1.C036529.

[19] Jan Roskam. *Airplane design. Pt. 1. Preliminary sizing of airplanes*. English. Ottawa, Kansas: Roskam Aviation and Engineering, 1985.

[20] E. Obert. *Drag polars of nineteen jet transport aircraft at mach numbers m=0.40-0.60*. Technical Report. (unpublished). 2013.

[21] Egbert Torenbeek. *Synthesis of subsonic airplane design: an introduction to the preliminary design, of subsonic general aviation and transport aircraft, with emphasis on layout, aerodynamic design, propulsion, and performance*. English. Delft: Delft University Press, 1982.

[22] Roel Thijssen. "Propeller Aircraft Design Optimization for Reduced Climate Impact". MA thesis. 2022.

[23] Jack D. Mattingly et al. *Aircraft engine design*. Third edition. AIAA education series. Reston, Virginia: American Institute of Aeronautics and Astronautics, Inc., 2018.

[24] A.T. Isikveren et al. “Pre-design strategies and sizing techniques for dual-energy aircraft”. In: *Aircraft Engineering and Aerospace Technology: An International Journal* 86.6 (Jan. 2014). Ed. by Riti Singh, pp. 525–542. DOI: 10.1108/AEAT-08-2014-0122.

[25] ICAO. *Annex 6 - Operation of Aircraft. Part I - International Commercial Air Transport*. July 2018.

[26] Emily Dallara. “AIRCRAFT DESIGN FOR REDUCED CLIMATE IMPACT”. PhD Thesis. Stanford, Feb. 2011.

[27] EASA EASA. *Certification Specifications and Acceptable Means of Compliance for Large Aeroplanes (CS25)*. Tech. rep. Dec. 2023.

[28] Roelof Vos and Saeed Farokhi. *Introduction to transonic aerodynamics*. volume 110. Dordrecht: Springer, 2015.

[29] Richard Ernest Bellman. *The Theory of Dynamic Programming*. Tech. rep. RAND Corporation, Jan. 1954.

[30] Xueying Wang. “Development of a dynamic operations optimization modelling framework”. MA thesis. Delft, The Netherlands: TU Delft, 2016.

[31] P. Rubbrecht. *Development of an Airline Systems Simulation Program*. Tech. rep. Delft, The Netherlands: TU Delft, 1989.

[32] Jan Roskam. *Airplane design. Pt. 8. Airplane cost estimation: design, development, manufacturing and operating*. English. Ottawa, Kansas: Roskam Aviation and Engineering, 1990.

[33] . *Commission Regulation (EU) No 965/2012*. Mattingly. Legislative Body: COM. Oct. 2012.

[34] Peter W. Jansen and Ruben E. Perez. “Coupled Optimization of Aircraft Families and Fleet Allocation for Multiple Markets”. In: *Journal of Aircraft* 53.5 (Sept. 2016), pp. 1485–1504. DOI: 10.2514/1.C033646.

[35] Ville Satopaa et al. “Finding a "Kneedle" in a Haystack: Detecting Knee Points in System Behavior”. In: *2011 31st International Conference on Distributed Computing Systems Workshops*. ISSN: 2332-5666. June 2011, pp. 166–171. DOI: 10.1109/ICDCSW.2011.20.

[36] Yorick Teeuwen. “Propeller Design for Conceptual Turboprop Aircraft”. PhD thesis. 2017.

Appendices

A Powertrain Assumptions

The following appendix outlines the assumptions considered when designing the hybrid-electric powertrains. Table 17 outlines the assumptions of the gas turbine and Table 18 outlines the assumptions of hybrid powertrain overall.

Table 17: Gas turbine design variable assumptions retrieved from *Thijssen* [22]

Variable	$\Pi_{compressor}$	tt_4	Π_{burner}	Π_{inlet}	Π_{nozzle}	$\eta_{compressor}$	η_{hpt} [a]	η_{lpt} [a]	η_{burner} [a]	η_{mH}	η_{mL} [a]
Value	14.3	1200	0.96	0.98	0.99	0.9	0.89	0.91	0.99	0.975	0.99

[a] hpt - High-pressure spool; lpt - Low-pressure spool; mH - Mechanical High-pressure spool; mL - Mechanical Low-pressure spool; burner - Combustion chamber.

Table 18: Hybrid powertrain properties. Estimates as of 2035, retrieved from *de Vries.*[7] and from *Scheers* [14]

Variable	Value	Units
Fuel Density, ρ_{fuel}	775[21]	[kg/m^3]
Specific Energy Fuel, e_{fuel}	11900	[Wh/kg]
Specific Energy Battery at pack level, e_{batt}	350	[Wh/kg]
Specific Power Battery at pack level, ep_{batt}	1000	[W/kg]
Energy Density Battery at pack level, ρ_{batt}	1000	[Wh/l]
SOC	20	%
Specific Power EM, ep_{em}	5940	[W/kg]
Efficiency GT, η_{gt}	40	[%]
Efficiency GB, η_{gb}	96	[%]
Efficiency EM, η_{em}	97	[%]
Efficiency PMAD, η_{pmad}	99	[%]
Maximum Efficiency Propeller, $\eta_{p,max}$	88[a]	[%]

[a] Used in combination with the flight mach number to estimate the propeller efficiency η_P according to model by *Thijssen* [22]. Optimistic value, according to projections for the future [36].

B Aircraft Designs

Table 19: Hybrid-Electric Aircraft On-design Analysis with battery energy density equal to 350 Wh/kg.

Aircraft	Powersplit [%]	$\mathbf{R_{design}}$ [km]	$\mathbf{M_{bat}}$ [kg]	MTOM [kg]		b [m]		M_f [kg]	
				Value	Δ [%]	*Value*	Δ [%]	*Value*	Δ [%]
ATR 72-600	5	1370	3313	30819	+25	32	+11.8	2088	+3.7
ATR 72-600	10	1370	8102.0	41268.8	+67.8	36.0	+25.8	2674.8	+32.8
Bombardier CRJ1000	5	1370	4821.8	41225.0	+17.9	30.6	+7.7	3118.4	-40.1
Bombardier CRJ1000	10	1370	12307	57379	+64.1	36.0	+26.7	3953.7	-24.1
Bombardier CRJ1000	5	300	1491.7	31824.1	-8.9	26.95	-5.1	1338.5	-74.3
Bombardier CRJ1000	5	450	1710.7	32629.7	-6.6	27.3	-3.9	1530.6	-70.6
Bombardier CRJ1000	5	620	2215.5	34000.9	-2.7	27.8	-2.1	2215.5	-57.4
Bombardier CRJ200	5	1370	2635.6	21793.3	+15.8	22.8	+7.0	1703.0	-42.9

Table 20: Aircraft geometry characteristics.

Parameter	Aircraft		
	ATR 72-600	*Bombardier CRJ200*	*Bombardier CRJ1000*
Wing Configuration	High	Low	Low
Empenagge Configuration	T-tail	T-tail	T-tail
Engine Placement	Wing	Wing	Wing
Undercarriege Configuration	Belly-fairing	Belly-fairing	Belly-fairing

[21] https://exolum.com/wp-content/uploads/2021/06/AVIATION-KEROSENE-JETA1_issue-12.pdf

II

Literature Study

(Previously graded under AE4020)

1
Summary

The interest in looking at the aviation industry as a system of systems has grown in the last years. There has been a realization that coupling aircraft design with the design of networks in which such aircraft would operate can lead to not only identifying design trends but also has the potential of improving the efficiency of the entire network. With the pressure which stems from the ambitious climate goals of limiting the average global temperature increase to 1.5 degrees Celsius above pre-industrial levels, it becomes increasingly interesting to study how the benefit of new and disruptive technologies changes when its operations are considered.

In the current literature review, three different disciplines are coming together and the way these have been coupled thus far shall be analysed. The disciplines that shall be considered are: Conceptual design of hybrid-electric aircraft, optimization of airline fleet and schedule planning and finally in-flight power management optimization.

Firstly, with the growing interest in decarbonizing the aviation industry, electrified propulsion systems, specifically hybrid-electric aircraft, present themselves as one of the promising technologies that could potentially move aviation towards this goal. With the fact that there are no commercially tested hybrid-electric aircraft, it is not possible to follow traditional design methods. For example, attaining the battery mass and the fuel mass can no longer be done by the use of fuel fractions, one must either do an energy-based step-wise analysis or use a modified Breguet range equation.

Secondly, the adoption of future technologies, such as hybrid-electric, requires airlines to consider various aspects from an operational standpoint. The cost of choices made by airlines, including route selection, flight frequency, and aircraft type, is a major driving factor in strategic and tactical planning to ensure profitability and a sustainable network. This involves deciding which routes to add or remove, determining flight departure times, assigning specific aircraft to flights, and considering the routing of each aircraft in the fleet. An integrated scheduling, fleet assignment and routing of aircraft method should provide significantly accurate modelling of airline operations, crucial for a relevant study of the existent trade-off between maximizing profit and minimizing environmental impact. The modelling of the integrated scheduling fleet assignment and routing of aircraft problem has been explored in the research industry, both by modelling it as a mixed-integer linear programming problem but also as a dynamic programming problem. In general, only profit is taken into account as an objective. There is a lack of research on how accounting for the environmental impact affects the results.

Thirdly, the propulsion system of a hybrid-electric aircraft has a new degree of freedom which affects its fuel consumption. This new degree of freedom is called the degree of hybridization. It allows to design how much energy/power should be provided by the battery and how much should be provided by the fuel on each flight step. Furthermore, the three main ways in which the power management unit can be designed are the following: rule-based design, optimal control design and dynamic programming design. Although the last two methods output the largest savings in fuel, they are also the most computationally expensive options. Moreover, besides the degree of hybridization also altitude and speed have a significant effect on an aircraft's

climate impact.

Furthermore, there is an absence of research on the coupling of an integrated scheduling, fleet assignment and aircraft routing framework with a hybrid-electric aircraft design module while attending to the effect of certain mission parameters on the network's environmental impact.

Finally, given the aforementioned discussion, a research objective was identified. An effort should be made to create a framework which couples hybrid-electric aircraft design and mission variables to a dynamic programming integrated scheduling and assignment of aircraft to flights method, that allows to study and identify the existing interdependencies and trade-offs in terms of profit and environmental impact.

2

INTRODUCTION

2.1. CLIMATE GOALS

Aviation has experienced steady traffic growth in the last decades and this is forecasted to continue to grow in the years to come [10] [11]. Boing's commercial market outlook forecasts that in the period between 2022 and 2041, there will be an annual traffic growth equal to 3.8% [1], while its competitor Airbus forecasts that in the same period, the traffic will grow annually by 3.6% [2].

Furthermore, as the traffic volume increases so does aviation's contribution to climate change. With the ambitious goals to limit the increase of the earth's average temperature to 1.5 degrees above pre-industrial levels, there is evident pressure on aviation to reduce its emissions [3]. With the goal of supporting the aforementioned target, the European Commission has established a set of goals to aid in the neutralization of aviation's emissions by 2050. The ambition is to be able to reduce by 75% the carbon dioxide (CO_2) emissions per passenger kilometre and by 90% the nitrogen oxide (NOx) emissions. As highlighted by the goals, in order to properly assess and reduce the environmental impact of aviation it is required to also take into consideration the non-CO_2 emissions.

2.2. TECHNOLOGY IMPROVEMENTS

In general, there are several factors which affect the environmental impact of an aircraft. For conventional aircraft, limiting fuel consumption has a direct correlation with limiting the volume of emissions. Furthermore, this can be done in numerous ways. On one hand, a smaller aerodynamic efficiency implies that the aircraft's drag is larger and hence more thrust is required. This in turn means that the propulsion system is heavier, consumes more fuel and thus emits more. A similar reasoning can be made with the weight of the aircraft, a heavier aircraft requires a heavier and more fuel-consuming propulsion system. However, one could argue that neither the aerodynamic efficiency nor the weight of the aircraft would be a problem if the fuel combustion would not produce such harmful agents (at least the in-flight emissions would be limited). Given this realisation, there have been multiple efforts all over the industry to create conceptual designs of aircraft which run on alternative fuel sources. Electrified powertrains and propulsion systems is one of the technology areas which promises the largest development towards creating sustainable aircraft [4].

2.3. PROPULSION SYSTEM ELECTRIFICATION

When it comes to electric flight, the largest challenge lies in attaining a safe and usable specific energy density to cover enough profitable missions [12]. Current battery-specific energy densities are not large enough to power a commercial aircraft, however, there has been a large investment in battery research in the last couple of years [13]. The most promising battery technology so far is the Lithium-Air battery developed in Japan by the National Institute for Materials Science (NIMS). An energy density at cell level equal to 500 Wh/kg was achieved [14].

Furthermore, electric powertrains have a much larger efficiency in converting stored energy to shaft power than fuelled aircraft [12]. In spite of the former, the weight of an electric powertrain is in general higher to that of a conventional propulsion system due to the additional components, such as generators or electric motors. Adding this to the insufficient specific energy density of batteries significantly limits the visibility of electric flight. For this reason, it is believed that the first missions for which electric flight will be visible are regional missions [12]. Moreover, electric vehicles could potentially serve smaller markets for which using conventional aircraft is neither profitable nor advantageous from an environmental perspective.

Hybrid architectures have as an energy source both a battery and kerosene and hence are able to serve missions with a larger range than a fully electric aircraft. It has been shown that, if properly designed, integrating hybrid-electric propulsion in regional aircraft not only can lead to benefits in terms of environmental performance, (savings in terms of fuel) but can also extend the operating envelope of such aircraft [15]. Hybrid-electric aircraft could therefore serve regional missions far earlier than fully-electric aircraft and potentially make advancements towards a carbon-neutral industry. This would not only have environmental benefits, but it would also smooth the transition (in terms of infrastructure) to the use of fully electric aircraft.

2.4. AIRLINE OPERATIONS

From an operations point of view, there are several aspects that need to be taken into account if a specific airline should adapt to future technologies, for instance, hybrid-electric or fully-electric aircraft. The major driving factor in the business choices that an airline undertakes (e.g. which routes to fly, how often, which aircraft to purchase, among others) is the cost of making those choices. Ensuring profitability and a sustainable network is one of the main goals of the strategic and tactical planning of an airline [16].

When making strategic decisions, an airline decides which routes to add/remove from its network, how often it should fly those routes and which aircraft type it should use for those specific routes [16]. In a subsequent step, the timetable design is constructed. For a certain time period (week or day) the departure times of all the network flights are determined. Simultaneously the fleet assignment is conducted. To each flight in the timetable, a specific aircraft is assigned. Furthermore, airlines take into account the routing of each of the aircraft in their fleet, as there should be continuity and circularity [16].

Furthermore, an airline purchases a certain aircraft as its specifications, in terms of payload and range, serve their network in a profitable manner. Although flexibility, in terms of range and payload, is highly appreciated by the airline industry, over-exploring it, results in the fact that many times aircraft operate outside their design point, and hence are less efficient, which in turn leads to a larger fuel consumption. This is not only negative from a profit point of view but also from an environmental point of view. This argument is verified by *Cruz et al.* [17], which presented a data-driven approach to be able to assess the impact that considering realistic mission constraints has on the concurrent aircraft design and network optimization problem. From their case study, it was concluded that real mission profiles result in a smaller profit than if great-circle distances are considered. As previously mentioned, this is related to the fact that in reality many times, aircraft operate outside of their design point. Moreover, it highlights the importance that the flight profile has on the key performance indicators of an airline.

2.5. SYSTEM OF SYSTEMS

The term system of systems does not have a widely accepted definition. Nevertheless, it has been defined as a "set of systems or system elements that interact to provide a unique capability that none of the constituent systems can accomplish on its own" [18]. Furthermore, to further define this concept *Maier* [19] determines that a system of systems must have the following characteristics:

- Operational independence of the components: if the individual systems are disassembled from eachother, they should be able to operate individually;
- Managerial independence of the components: individual components continue to manage their own operations even if together;

Moreover, if one analyses the case of the aviation industry, it is possible to acknowledge that it is a complex system of systems. It is driven by several factors and thereby has multiple stakeholders. For instance, airlines are interested in maintaining a cost-efficient network, manufacturers compete for safe and efficient aircraft designs, air traffic management must find strategies to comply with the ever-growing air traffic, and people wish to limit their waiting time at the airport, among others. Being a complex system makes it difficult to accurately model its dynamics, nevertheless, without this perspective it is not possible to study and identify the interdependencies and hence important decisions, such as investing in new technologies, may be taken without the full comprehension and knowledge about the practical outcome.

One example of a difficult trade-off in aviation is that between emissions and profit. As previously mentioned, to properly assess aviation's environmental impact, one should consider not only the CO_2 emissions but also the non-CO2 emissions, such as NOx emissions. Simultaneously minimizing emissions and costs is a tricky task as the operating costs of an airline are inversely related to its NOx emissions, which in turn is also inversely related to the CO_2 emissions [20].

2.6. GOAL AND SCOPE

As highlighted in this chapter, there are ambitious climate goals which have been set for all industries, including aviation. The only realistic way in which these are going to be attained is if the way the industry operates is completely revolutionized. This revolutionary change mainly stems from altering the aircraft configurations and specifically the energy source. Several promising technologies have been identified, among which are electrified powertrains. These bring to the table the potential of reducing the consumption of fuel while maintaining a competitive range.

From an airline perspective, this change would require some adjustments. The need to recharge the batteries highly influences the scheduling of aircraft but also influences the way in which the aircraft can be flown, which in turn influences pilot training. All in all, these changes can result in additional costs. This is where the concept of system of systems analysis comes in. Being able to study the interdependencies between these two systems and how to manage the trade-off between reducing the environmental impact of aviation while maintaining the costs at a manageable level should be addressed. Hence, the goal of the current literature study is to review what has been done thus far in terms of the design of aircraft with electrified powertrains, how can the split between fuel and battery energy be managed, how does an airline schedules and assigns aircraft to flights and finally in what way have these disciplines been coupled so far.

Given the former, the literature study is structured in the following way: In chapter 3 one can find not only a review on the new design considerations that hybrid-electric aircraft require but also a discussion on the design methods which have been created thus far; An extensive discussion on the airline planning process, especially during the scheduling phase can be found in chapter 4. In addition to this, chapter 4 also motivates why looking at the fleet assignment and aircraft routing problem for the current literature review is especially relevant. In what way this problem has been addressed by the researched community is also discussed; Then in chapter 5, one can find a brief discussion on how to assess the climate impact of aviation, along with a discussion on how the power management can be optimized and what are the implications of speed and altitude on the climate impact of aviation; chapter 5 is followed by chapter 6, which reviews in what ways aircraft conceptual design has been coupled with fleet planning activities and with mission profile parameters; Finally, from the analysis of the previously mentioned chapters, in chapter 7, the main conclusions are addressed and a research gap, a research question, a research objective and a preliminary planning are provided.

3

Hybrid-electric aircraft

In the following chapter, a review of the state-of-the-art hybrid-electric aircraft architectures is provided (section 3.1). In addition to this, several conceptual examples of hybrid-electric aircraft are provided (section 3.2). Then, the different design methods encountered in the literature are compared and discussed (section 3.3), which is followed by a review on battery technology (section 3.4). Finally, a review on how the aero-propulsive benefits of propeller aircraft have been included in the design of hybrid-electric aircraft is provided (section 3.5)

3.1. Classification of architectures

There are several electric aircraft architectures. The metric which is most commonly used to distinguish these from each other is the degree of hybridization. It determines how much of the total power and the total energy is provided by the battery and how much is provided by the liquid fuel.

The first metric is that which was developed by *Isikveren et. al* [21]. Its definition can be observed in Equation 3.2. It relates the energy provided by the battery E_b with the total energy required E_{tot}. This can also be expressed in terms of power, as it was done by *de Vries* [5].

Furthermore, *de Vries* [5] created an additional metric to characterize hybrid-electric powertrains. The author called it the "shaft power ratio" (Equation 3.1) and it represents the amount of shaft power which is produced by a secondary thrust source with respect to the total shaft power produced (both a gas turbine and isolated electric motors). This formulation is particularly useful if one decides to consider a distributed propulsion system as a secondary propulsion system. Evidently, the choice of shaft power ratio becomes trivial if one chooses there not to be a secondary power source. Furthermore, analogously to the degree of hybridization, the shaft power ratio should also be between zero and one during normal operations.

$$H_{P2} = \frac{P_{\text{shaft},2}}{P_{\text{shaft},2} + P_{\text{shaft},1}} \quad (3.1)$$

$$H_E = \frac{E_b}{E_{tot}} \quad (3.2)$$

Table 3.1 summarizes the differences between the different architectures in terms of degrees of hybridization. Note that only the primary architectures are included and reviewed. Several other architectures can be derived from these primary architectures by for instance considering two propulsion systems or by combining two primary architectures.

For conventional aircraft, no electric power or electric energy is used to propel the aircraft. On the other end of the spectrum, there is the fully-electric architecture, in which all the power and energy are provided by an electric motor and the battery, respectively.

Furthermore, there is also the possibility to create hybrid architectures. These are those for which there are two energy sources and two power sources. The first type of hybrid-electric aircraft is the turboelectric aircraft (Figure 3.1c). It uses combustible fuel for energy storage but uses electric power transmission instead of mechanical power to drive the propulsors.

Table 3.1: Classification of electric propulsion architectures [22].

Architecture	H_E
Conventional	0
Fully-electric	1
Turboelectric	0
Series hybrid	<1
Parallel hybrid	<1

Then, there is the series-hybrid architecture (Figure 3.1a). For this configuration, the propeller is fully driven by the electric motor. The power derived from combustion is converted to electric power via a generator. The power retrieved from combustion can be used to directly drive the electric motor or can be stored in the battery. This type of hybrid-electric architecture is that which is most easily extended to a distributed electric powertrain [23]. Moreover, the main advantage of this architecture is the fact that the engine is completely decoupled from the propeller, this means that it can run at its optimal operating condition regardless of the working condition. However, it suffers from poor system efficiency as there are major losses during combustion and electrical energy conversion. In addition to this, it requires multiple elements (engine, generator and electric motor) which makes this architecture heavy and thus costly. Furthermore, with the decoupling between the engine and the electric motor, it is not possible to make use of the maximum combined power [23].

In contrast, there is the parallel-hybrid architecture (Figure 3.1b). In this architecture, both the engine and the electric motor are mechanically connected to the propeller and hence both can provide power simultaneously. It is also possible that only one of the two provides power. This flexibility allows for an unique power management. This characteristic will be further explored in a subsequent chapter (chapter 5). Much like the series-hybrid configuration, it is also possible that the engine simultaneously drives the propeller and the electric motor and thus charges the battery mid-flight. In addition, one of the advantages of the parallel architecture in comparison to the series architecture is the fact that it only requires an engine and an electric motor. It does not require a generator. Hence, this configuration is lighter. Furthermore, the power losses are smaller as there is no mechanical to electrical energy conversion. Nevertheless, the rotational speed of the propeller is not always the optimum speed of the engine, which may lead to sub-optimal engine conditions. One way to manage this is by including a gearbox which decouples the propeller and the engine's rotational speed. On the other hand, it is also possible to develop a power management strategy which determines how much power is delivered by the electric motor and how much is delivered by the engine [23].

3.2. ELECTRIFIED AIRCRAFT CONCEPTS

In order for electrified propulsion to become a reality, there is still a long road ahead. The following section discusses and exposes the electrified aircraft which have been designed so far. This includes both conceptual designs and practical examples. The goal is to get an understanding of the design decisions so far and hence which technologies and assumptions have been considered. Later on in section 3.3 a review of the methods used to design the aircraft shall be given.

3.2.1. FULLY ELECTRIC

As far as fully electric aircraft go, there are already a couple of models in the market which have successfully flown while using only batteries. However, the capacity of these aircraft is very limited (mostly one or two-seaters) and could never be used for commercial purposes, even if used on regional routes. Some examples of these aircraft are the Lange Antares 20 E, the Fishman Electraflyer C, the Yuneec E430 and more recently the Airbus E-Fan, the Pipistrel Alpha Electro and the Siemens Extra 300 (330LE) [22].

Nevertheless, certain companies are already making conceptual designs of fully-electric aircraft which should have a capacity which is large enough for them to be commercially feasible. Some examples of these aircraft are summarized in Table 3.2. As a first example, there is the Eviation Alice commuter aeroplane. With a maximum capacity of 11 seats, it has successfully flown in 2022 for eight minutes. Furthermore, its

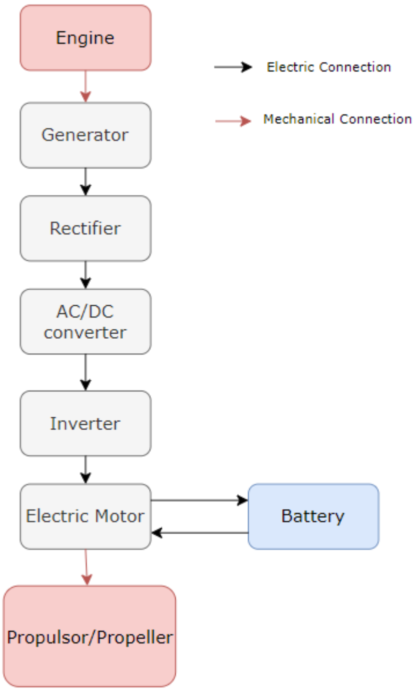

(a) Series hybrid architecture

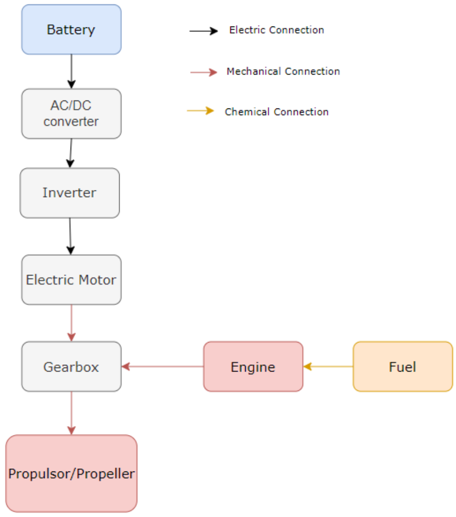

(b) Parallel hybrid architecture

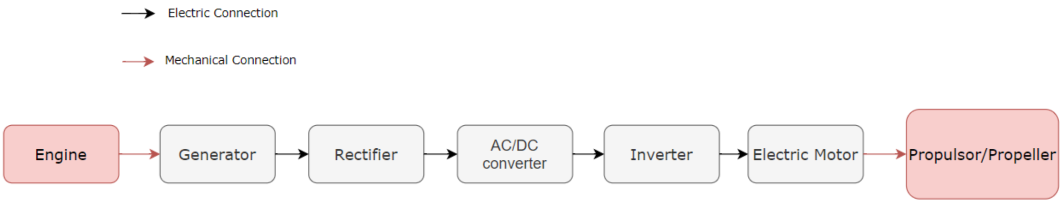

(c) Turboelectric architecture

Figure 3.1: Hybrid-electric propulsion architectures

two propellers are placed at the rear of the fuselage and are powered by Kokam Li-Ion batteries [24] [25]. Furthermore, there have also been several conceptual designs for a capacity of nearly 200 passengers. One of these is the Ce-Liner, developed by the Bauhaus Lufthart. The concept was developed in 2013 and there have been no further developments. Interestingly enough both of its engines are also placed at the rear of the fuselage, and it has a very distinctive C-wing [26]. Moreover, it is assumed that by 2035 it will be possible to produce batteries with a specific energy of roughly 2000 Whr/kg, which according to the *National Academy of Engineering* [27], it should only be possible to reach 400-600 Whr/kg. Moreover, Airbus has also developed a concept, VoltAir [28], which was designed to carry roughly 68 passengers while requiring a battery specific energy density of more than 1000 Whr/kg. On top of this, the aircraft is designed to include other complex and expensive technologies such as a boundary layer ingestion engine at the rear of the fuselage and a laminar flow wing. It is possible to observe that scaling up the usage of fully-electric aircraft (larger capacity and range) incurs the need to make use of advanced technologies, such as boundary layer ingestion to attain a reasonable design. Achieving these designs would require not only a massive improvement of battery technology but also massive research in terms of alternative aircraft configurations.

Table 3.2: Fully-electric aircraft design concepts.

Name	EIS	Seats	MTOW (kg)	Max. power(MW)	e_b (Whr/kg)	Range (nmi)	Reference
Eviation Alice	2027	11	8346	0.78	260	560	[24] [25]
Bauhaus Luftfahrt Ce-Liner	2035	189	109300	33.5	2000	900	[26]
Airbus VoltAir	2035	68	33000	NA	>750	900	[28]

3.2.2. HYBRID-ELECTRIC

There has been a larger investment in the investigation of hybrid-electric aircraft as they could, to a certain extent, provide some of the benefits of fully-electric flight while maintaining competitive ranges and payload capacity.

TURBOELECTRIC

One of the turboelectric concepts that have been developed is the NASA STARC-ABL [29], and it consisted of a tube-fuselage with two turbofans under the wing equipped with generators which could extract power from the fan shaft and transmit it to a boundary layer ingesting fan located at the rear of the fuselage. At the other end of the spectrum, the largest hybrid aircraft designed so far is the N3-X aircraft designed by NASA. It was designed based on the capacity and range of the Boing 777. Besides being turboelectric, this aircraft has a blended wing body shape, makes use of boundary layer ingestion and uses liquid hydrogen as a fuel. It was estimated that the combined effect of the previously mentioned technologies would amount to a reduction in fuel burn equal to 70% when compared to the fuel burn of the Boing 777. Furthermore, Empirical Systems Aerospace developed an aircraft concept named Eco-150 where electric generators are employed on the turbofan engines mounted on the wings. These generators power electric fans which are distributed along a split-wing configuration [30].

Table 3.3: Parallel hybrid-electric aircraft design concepts.

Name	EIS	Seats	MTOW (kg)	Max. power(MW)	Range (nmi)	Reference
NASA STARC-ABL	2035	154	60000	2.6	3500	[29]
NASA N3-X	2045	300	227000	50	7500	[31]
Eco-150R	2035	150	60000-75000	0.78	1650	[30]

SERIES HYBRID

Similarly to fully-electric aircraft, there are some aircraft models which employ a series-hybrid architecture but have a limited capacity [22]. Besides the testbed aircraft developed by Airbus, E-Fan X and E-Thrust [32] the Zunum Aero aircraft was found to use a series hybrid-electric architecture. With a capacity to transport 12 passengers and a design range equal to 700 nmi it should allow for a lower flying fare in regional American routes [33]. Further specifications can be found in Table 3.4. Furthermore, with the aim of expanding the knowledge on hybrid-electric propulsion systems, *Pornet & Isikveren* [34] developed a hybrid-electric aircraft with two advanced geared turbofans (GTf) and two electrical fans (EF).

Table 3.4: Series hybrid-electric aircraft design concepts.

Name	EIS	Seats	MTOW (kg)	Max. power(MW)	e_b (Whr/kg)	Range (nmi)	Reference
Zunum Aero	2020s	12	5216	1	NA	700	[33]
Conceptual Aircraft	NA	NA	77730	NA	1500	1300	[34]

PARALLEL HYBRID

One example of a hybrid-electric aircraft with a parallel architecture is the SUGAR Volt aircraft developed by Boing [35]. With a design range equal to 3500 nmi and a trussed-braced wing, it requires a battery specific energy equal to 750 Whr/kg. Furthermore, NASA also developed another aircraft concept named PEGASUS [36]. This aircraft is characterized by parallel hybrid electric propulsors at the wing tips and two electric propulsors inboard of the wing.

Table 3.5: Parallel hybrid-electric aircraft design concepts.

Name	EIS	Seats	MTOW (kg)	Max. power(MW)	e_b (Whr/kg)	Range (nmi)	Reference
Boing SUGAR Volt	2035	154	68040	1	750	3500	[35]
Pegasus	>2030	48	24058	1.1	500	>174	[37] [36]

3.3. DESIGN METHODS

Validation and verification of hybrid-electric aircraft design methods is a complicated task. This is due to the lack of available validation data. Most researchers are not explicit about the assumptions they assume or do not provide sufficient data to replicate the analysis [38]. Furthermore, hybrid-electric technology has not been extensively explored. Hence, as verified in section 3.2, there are a limited number of designs in the market which have undergone flight testing.

Furthermore, the design of hybrid-electric aircraft also poses other challenges. In the beginning of the design process, the initial estimate of the aircraft's empty weight is typically based on statistical data from similar aircraft. This is not possible for electrified aircraft as there are not enough models available. Additionally, unlike fuel, the battery mass remains unchanged throughout the flight. Hence, the traditional method of using fuel fractions also cannot be used. These and other limitations are addressed by the methods discussed in the following section. These shall be compared, their limitations shall be outlined and the points of improvement shall be discussed.

3.3.1. CONSTRAINT ANALYSIS

Typically one of the first steps in aircraft conceptual design is the creation of the constraint diagram (Power-to-weight ratio versus wing loading). The goal is to attain the limits of the feasible design space. The design space is constrained by, for instance, the take-off distance, the cruise speed, the rate of climb, the stall speed and the one engine inoperative condition. Other constraints can be applied, however, these were the constraints that were considered in the FH Aachen methodology [39]. Furthermore, this specific methodology sizes the propulsive system as a whole (engines, motors, motor controllers, gearboxes, generators, power distribution systems, cables, among others) by making use of the maximum attainable power (Equation 3.3). The former methodology does not consider the different components of the propulsion system individually. However, in another method by *de Vries* [5] each component of the powertrain is sized with its own loading diagram.

$$P_{max} = \frac{P}{W} \cdot MTOM \cdot g \tag{3.3}$$

Moreover, the way the design space is constrained (through the constraint functions) can also differ. For example, in the method developed by *Finger et al.* [39], most of the constraint functions are adaptations of the equations developed by *Gudmundsson* [40]. For instance, the take-off distance constraint is adapted to be sensitive to both drag ($C_{D,TO}$) and rolling friction (Equation 3.4). In a different approach, *de Vries* [5], simply made use of the Raymer's take-off parameter [41].

$$\left(\frac{T}{W}\right)_{\text{TOD}} = 1.21 \cdot \frac{(W/S)}{g \cdot s_G \cdot \rho \cdot c_{L,\text{TO}}} + 1.21 \cdot \frac{c_{D,\text{TO}}}{c_{L,\text{TO}}} - 0.21 \cdot \mu \tag{3.4}$$

Furthermore, as evidenced in section 3.1, a hybrid-electric aircraft has two additional degrees of freedom: the degree of hybridization of power and the degree of hybridization of energy. In the methodology developed by *Finger et al.*, the area below the design line (considered as the infeasible region for conventional aircraft, as at least one performance constraint is not met) is considered to be the design space of hybrid-electric aircraft. Note that the constraints are still required to be met, however, one is now able to play with the degree of hybridization of power to meet these constraints.

Additionally, as will be further explained in section 3.5, the use of electric motors opens the door to many new aircraft configurations which leverage from favourable aero-propulsive interactions. For the case of the *Finger et al.* framework these benefits are not taken into account. Conversely, in the framework developed by *Zamboni* [42], these effects are reflected in the constraint analysis by shifting the constraint functions towards conditions with a larger lift coefficient and a smaller induced drag. This originates a larger design space. Moreover, these effects are also taken into account by *de Vries* [5] and *Orefice et al.* [43] in a similar fashion.

3.3.2. MISSION ANALYSIS

As far as the mission analysis is concerned, two main methods have been identified. On one hand, using a modified Breguet Range equation which is able to take into account the particularities of hybrid-electric propulsion. On the other hand, the use of energy methods, in which the mission is broken down into several small steps and the energy equations are solved.

ENERGY-BASED METHOD

When the mission is broken down into several small segments, it is important to make sure that the flight profile correctly describes the type of mission for which we are designing our aircraft. For the case of the methodology developed by *Finger et al.* [39], the mission is divided into several time steps. For each time step, the required energy for that specific timestep is determined. Generally speaking, Equation 3.5 is used to compute the change in energy required. As can be seen, three separate components can be identified. Firstly, there is the aerodynamic drag component, which during cruise is the only factor which influences the energy demand. Secondly, there is the kinetic energy component, which is associated with the flight phases in which the aircraft is required to accelerate: take-off, climb, and descent. Finally, there is the potential energy component, which is added or subtracted depending on whether the climb or the descent phase is being considered.

$$\Delta E = \underbrace{\frac{m \cdot g \cdot v}{(L/D)} \cdot \Delta t}_{\Delta E_{\text{Acro.Drag}}} + \underbrace{\frac{m \cdot \Delta v^2}{2}}_{+\Delta E_{\text{Kinetic}}} + \underbrace{m \cdot g \cdot \text{ROC} \cdot \Delta t}_{+\Delta E_{\text{Potental}}} \tag{3.5}$$

Once the energy required at each time step is known, the degree of hybridization of energy (H_e) determines how much energy must be provided by the battery and how much must be provided by fuel. Furthermore, the fuel mass required at each time step and the battery mass are determined with Equation 3.6 and Equation 3.7, respectively.

$$\Delta m_{\text{Fuel,ICE}} = (1 + \text{tf}) \cdot P_{\text{ICE}} \cdot \text{NOD} \cdot \text{BSFC} \cdot \Delta t \tag{3.6}$$

$$\Delta m_{\text{Battery}} = (1 + \text{DDP}) \cdot \frac{\Delta E_{\text{nc}}}{\eta_{\text{BtT}} \cdot E_{\text{Battery}}} \tag{3.7}$$

Irrespective of the specifics of the previously described methodology, several papers have adopted energy-based methods. In general the aircraft is treated as a point-mass and the X and Z equations of motion are considered [44]. For example, in the methodology developed by *Zamboni* [42], a point performance analysis is also conducted to determine how much power is required at each time step of the mission. In general, this is computed as the product of flight speed and thrust required (Equation 3.8). Similarly to the methodology developed by *Finger et al.* [39], the components of the powertrain are sized by backpropagating the power required to be delivered by the propeller until the battery and/or turbine. This is possible by assuming the efficiency of the components within the powertrain.

$$P = T \cdot V \tag{3.8}$$

MODIFIED BREGUET RANGE EQUATION

It is possible to follow a different approach if the cruise phase is dominant in the overall energy consumption. Although less accurate, making use of a modified Breguet range equation, could be applicable. *de Vries* [5] [45], derived an equation (Equation 3.9) which can be used to compute the range of a conventional, a serial, parallel, turbo-electric or fully-electric aircraft. However, it is assumed that the power split, the flight speed, the lift-to-drag ratio, and the powertrain efficiencies are constant. Furthermore, *de Vries* was not the only author that derived a hybrid-electric aircraft range equation. *Voskuijl et al.* [46] also derived an equation based on similar assumptions (power split and the angle of attack are kept constant during the cruise phase).

$$R = \eta_3 \frac{e_f}{g} \left(\frac{L}{D}\right) \left(\eta_1 + \eta_2 \frac{H_E}{1 - H_E}\right) \ln \left[\frac{W_{OE} + W_{PL} + \frac{g}{e_{bat}} E_{0,\,tot} \left(H_E + \frac{e_{bat}}{e_f}(1 - H_E)\right)}{W_{OE} + W_{PL} + \frac{g}{e_{bat}} H_E E_{0,\,tot}} \right] \tag{3.9}$$

Finally, Table 3.6 provides a summary of the main differences between the several papers which were reviewed.

Table 3.6: Summary of main characteristics of hybrid-electric aircraft design methods.

Authors	Constraint diagram	Mission analysis	Aero-propulsive correction	Reference
Finger et al.	One	Energy-based	No	[39]
de Vries	Multiple	Energy-based/Breguet Range	Yes	[5]
Zamboni	One	Energy-based	Yes	[42]
Orefice et al.	Multiple	Energy-based	Yes	[43] [47]

3.4. ENERGY SOURCE

In order for electric flight to become a reality, the energy storage unit must be reliable, compact and light. This is a great challenge as most of the energy storage options have low specific energy, face thermal management issues or have a low volumetric specific density. Furthermore, the two most promising technologies which have been identified are batteries and fuel cells.

Fuel cells are an alternative to batteries. Have a larger specific fuel density. However, are less efficient in converting the hydrogen energy into shaft power. Battery efficiency is 73 % while that of the fuel cells is 44% (the entire powertrain is considered). Regardless of the former, the efficiency of a fuel cell driven propulsion system is still larger than turbofan engines [48].

Furthermore, electrically driven propulsion systems face the problem of overheating of components and potential fire [49]. This problem is common for both battery and fuel-cell-driven propulsion systems. In addition to this, since fuel cells operate on hydrogen, and hydrogen has a low volumetric energy density, accommodating hydrogen inside the aircraft adds to the complexity of the problem. The hydrogen has to be either stored in a high-pressure tank or needs to be carried in liquid form. Although the latter allows to accommodate a larger amount of hydrogen, it requires additional components such as a heat exchanger, which adds complexity and weight to the aircraft. Given the aforementioned discussion, fuel cells will not be considered in the current study and focus shall be put on battery technology.

3.4.1. BATTERIES

The major challenge of using batteries is their low energy density when compared to liquid fuel. Besides this metric, according to *Zamboni* [42], there are a number of other battery parameters which should be taken into account when designing a battery-driven aircraft. These are used in literature to compare different battery technologies and identify the most promising technologies.

Currently, the most promising batteries are those based on lithium: Lithium-ion, Lithium-sulfur and lithium-air/oxygen [49]. Hence, the focus will be placed on these battery technologies.

These technologies differ from each other in terms of the materials that are used. For example, Li-Ion batteries are made of a graphite anode, a lithium metal oxide cathode and an electrolyte [50]. They are reaching the maximum possible level of maturity and hence further improvements in the battery performance can

Table 3.7: Main battery parameters. [42]

Parameter	Description	Units
Gravimetric energy density	Amount of electrical energy stored per unit battery mass. It is dependent on battery chemistry and can be computed by multiplying the cell voltage (V) with its specific capacity (Ah/kg)	Wh/kg
Specific capacity	Amount of amp-hours that can be used when the battery is discharged at a certain current, per unit of mass. Just like for the gravimetric energy density, it is bounded by the cell chemistry.	Ah/kg
Specific power	Determines how much power can be delivered based on the weight of the battery. There is a trade-off between the specific power and specific energy as, during peaks of power demand, the battery capacity drops considerably.	W/kg
Volumetric energy density	Similar to the gravimetric energy density, it determines how much volume the battery occupies if it needs to provide a certain amount of energy	Wh/m^3
State of charge (SOS)	Ratio between the remaining capacity (Q, Ah) and the nominal capacity. It should never exceed a certain lower bound level, as afterwards the battery is permanently damaged.	%
Depth of discharge (DoD)	Rate of discharged capacity over the nominal capacity. It is related to the state of charge through: DoD = 1 - SOS.	%
Cost	Cost of acquiring a certain battery. It is dependent on the materials used and the manufacturing process	$/Wh

only be marginal [51]. Studies show that experimenting with the chemical combinations of lithium-based batteries is necessary if one wishes to significantly improve the battery's performance [49]. Thus, in the latest years, there has been an effort towards this goal. An example, are the lithium-sulfur batteries, which theoretically would be able to achieve a specific energy density greater than 2000 Wh/kg [49]. However, this battery technology has a major pitfall. The number of charge/discharge cycles which it is able to endure before it starts losing capacity is fairly limited as of now. The same is true for Lithium-air batteries, which in addition to this also faces issues in terms of safety. All-in-all, within battery research, improving safety, improving charge/discharge capabilities and improving specific energy density are the three main research focus.

Table 3.8 provides an overview of the state of the art and the future projections of the specific energy and the number of life cycles for each of these technologies. Note that the specific energy values are in terms of cell level, not in terms of pack level. The specific energy density at cell level is always larger than that that can be achieved at pack level. In spite of this, Table 3.8 still provides a term of comparison between the different battery technologies. Furthermore, two future projections are provided, a short-term projection around the year 2035 and a long-term projection, around the year 2045. These projections were retrieved from two separate sources. While the information on Li-Ion batteries was retrieved from a study by *Armand et al.* [52], the information for both the Lithium-Sulfur and Lithium-Air batteries was retrieved from a NASA study conducted by *Dever et al.* [49].

As has been previously indicated, one of the major concerns and limitations that stops electric aviation from becoming a reality is the specific energy density of batteries. However, as has been highlighted in the current section, other major factors such as the number of cycles is also fairly limited as of now. As a step forward, although this aspect does not directly limit the design-space of a hybrid-electric aircraft if one also considers the design for sustainable operations, it becomes a highly limiting factor. From analysing Table 3.8, if one would prioritize only the specific energy density of batteries, then Lithium-air batteries would appear to be the best choice, however, it is possible to see that even in 2035 the projections for the number of cycles the battery will be able to undergo before losing capacity is fairly limited. Both variables should be taken into account when making assumptions about the performance of batteries.

Table 3.8: State-of-the-art specific energy and specific power for the three most promising battery chemistries at cell level.

Battery Chemistry	Specific Energy (Wh/kg)			Number of cycles ([-])	
	State-of-the-art	Future projection (2035)	Future projection (2045)	State-of-the-art	Future projection (2035)
Lithium-Ion	160-260	275-320	>350	>300	400-450
Lithium-Sulfur	250-300	500-650	800-950	NA	1000
Lithium-Air	300-350	600-750	1300-1600	>50	500

3.5. AERO-PROPULSIVE EFFECTS

The aerodynamic interactions between the slipstream created by the propeller and the wing can be used to improve the aerodynamic performance of a wing and hence reduce the required wing area. At the conceptual design level, the former effect can only be quantified by a change in the lift-over-drag of the aircraft.

As has been highlighted in section 3.3, some design methods for hybrid-electric aircraft have already considered the possibility to take into account the aero-propulsive benefits of propeller-driven aircraft. One of these examples is the methodology developed by *de Vries* [53], which has also been used by*Orefice et al.* [43]. In this methodology, the aerodynamic benefits derived from making use of propeller-driven aircraft are taken into account by considering three different effects. The effect on the lift ΔCL, the effect on the induced drag ΔC_{D_0} and the effect on the zero-lift drag ΔC_{D_i}. These are estimated based on an approach suggested by *Patterson et al.* [54]. Patterson's model considers several assumptions, namely:

- Velocity increase at the actuator disk is computed while assuming uniform axial inflow;
- Swirl is assumed to not have an effect on lift;
- The flow over the wing is attatched;
- The effect of each propeller on the adjacent one (in case of distributed propulsion) is neglected;
- The effect of the propellers on the wing is limited to the spanwise interval occupied by the disks;
- Within the spanwise interval at which the propellers are located, their effect is considered to be uniform in the spanwise direction;
- Wing is assumed to be fully immersed in the slipstream, half of the slipstream flows under the wing and half flows over the wing;

Under these assumptions, the method is mainly only valid under clean configuration conditions, nevertheless, it is suitable for the conceptual design phase [53]. Furthermore, the model represents the propellers as actuator disks and the wing as a flat plate. The change in sectional lift caused by the propeller slipstream is computed with Equation 3.10, where α is the angle of attack, β is the finite-slipstream correction factor, i_p is the incidence angle of the propeller and a_w is the axial induction factor caused by the propeller. Furthermore, the sectional lift coefficient Δc_l is related to the wing's lift coefficient increase through the spanwise interval occupied by the disks.

$$\Delta c_l = 2\pi\left[(sin\alpha - a_w sin i_p)\sqrt{(a_w)^2 + 2a_w cos(\alpha + i_p) + 1} - sin\alpha \right. \tag{3.10}$$

Additionally, the change in sectional zero-lift drag and sectional induced drag is accounted for through Equation 3.11 and Equation 3.12, respectively. Note that, c_f is the skin friction coefficient and $C_{Lairframe}$ is the lift produced by the airframe without the propellers.

$$\Delta c_{d_0} = a_w^2 c_f \tag{3.11}$$

$$\Delta c_{d_i} = \frac{2C_{Lairframe}\Delta c_l}{\pi A} \tag{3.12}$$

Moreover, the finite-slipstream correction factor is critical in the estimation of Δc_l. Hence, *Patterson* [55], generated a surrogate model based on CFD simulations of an actuator disk in front of a two-dimentional wing. This same model is also used and validated by *de Vries et al.* [53]. By comparing the lift estimations of the model with CFD simulations of the NASA X-57 demonstrator, *de Vries* concluded that the model is applicable to high-aspect-ratio wings at high lift coefficients with a large number of propellers. However, it is not so accurate at low angles of attack and with propellers of large dimensions.

Furthermore, using distributed propulsion in hybrid-electric aircraft implies that there needs to be two separate propulsion systems. On one hand, a propulsion system whose power is supplied by the turbine and on the other hand a propulsion system whose power is supplied by electric motors. *de Vries* [5] derives a metric dependent on the shaft power ratio (H_{P2}) which allows to determine the thrust ratio between the two propulsion systems (conventional and distributed). Depending on whether the distributed propulsion is part of the primary or the secondary powertrain, Equation 3.13 can be used.

$$\chi = \begin{cases} \dfrac{1}{1+\frac{\eta_{p2}}{\eta_{p1}}\left(\frac{H_{P2}}{1-H_{P2}}\right)}, \text{ if the DP system belongs to the primary powertrain,} \\ \\ \dfrac{1}{1+\frac{\eta_{p1}}{\eta_{p2}}\left(\frac{1-H_{P2}}{H_{P2}}\right)}, \text{ if the DP system belongs to the secondary powertrain,} \end{cases} \tag{3.13}$$

4

FLEET ASSIGNMENT & AIRCRAFT ROUTING

Within the airline planning process there are several steps to be followed. One of these steps is the fleet assignment and the routing of aircraft through an airline's network. The goal of the following chapter is that one is able to get a grasp of the current state-of-the-art literature on the topic of fleet assignment and aircraft routing. To do so section 4.1, highlights the main steps during the airline planning process and puts special attention on the fleet assignment and aircraft routing problem. Then, in section 4.2, a review of the methods which have been used to solve the fleet assignment and aircraft routing is provided, namely mixed-integer linear programming and dynamic programming. Finally, in section 4.3, a comparison of the aforementioned methods and a review of the literature which made use of them to solve the fleet assignment and aircraft routing problem is given.

4.1. AIRLINE PLANNING PROCESS

As briefly outlined in chapter 2, and as explained by *Belobaba et al.* [16] the most important planning decisions faced by airlines are the following:

- **Fleet Planning:** Deciding when and how many aircraft to acquire;
- **Route Planning:** Deciding which routes to fly;
- **Schedule Planning:** Deciding how frequently and when should the airline fly a certain route;

Further tactical decisions are planned closer to the departure date of the aircraft, namely maintenance checks or other revenue management decisions. These will not be reviewed. Furthermore, Figure 4.1 summarizes the entire airline's planning process. For the scope of the current work, from the diagram, only the following processes shall be reviewed: Fleet planning, network development, frequency planning and scheduling planning. In the following subsections (subsection 4.1.1-subsection 4.1.3), these processes are described based on the description given by *Belobaba et al.* [16].

4.1.1. FLEET PLANNING

The fleet planning process is a long-term strategic process in which, an airline decides which and how many aircraft of each type to acquire or retire. Deciding whether to acquire an aircraft is not a decision which is taken lightly by airlines as it represents a large financial stress.

Besides the range and the capacity of an aircraft, other performance parameters are taken into account when deciding if a specific aircraft fits the requirements of the airline's network. Such parameters are for instance, the maximum take-off weight, as it affects the maximum runway length and hence which airports the aircraft can fly to, but also the span, due to gate or taxiway limitations and airport fees.

Additionally, it is in the interest of an airline to limit its fleet diversity as different aircraft increase the costs associated with pilot training but also the costs associated with maintenance. Besides costs, there has been an increase in considering the environmental effects of aircraft in the decision-making process of which aircraft to acquire. Besides the political pressure for airlines to adopt greener operations, there is also a financial

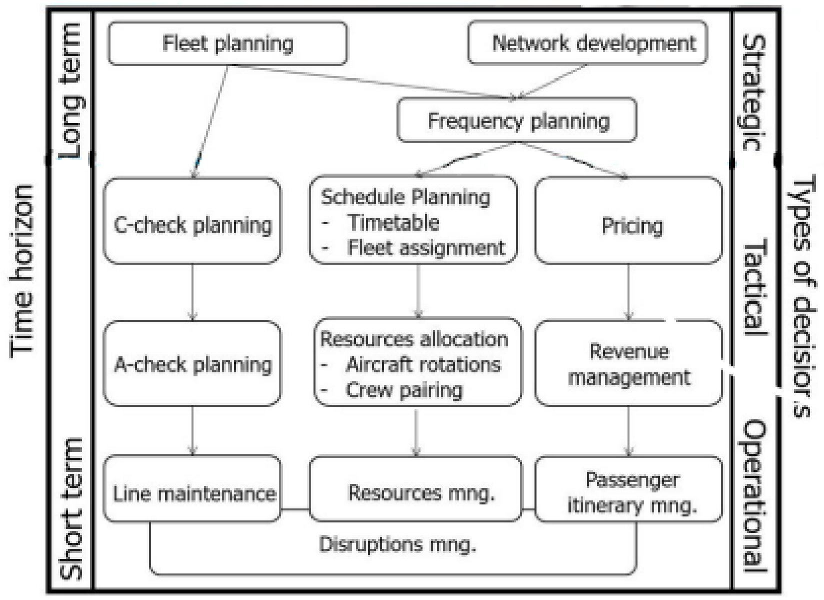

Figure 4.1: Airline's planning process. [56]

aspect to be considered. Several airports already have in place fees for the noise and emissions (such as NOx) of aircraft.

Moreover, the quality of the fleet plan is highly dependent on the quality of the future demand forecast. Two approaches can be adopted: top-down approach (high-level analysis) and the bottom-up analysis (much more detailed analysis of data); In contrast to the former, in the latter detailed models are used to forecast the demand, which makes this a more computationally expensive method. Given, that it is quite difficult to forecast future competition and account for the uncertainty associated with demand, the top-down approach is more commonly used.

4.1.2. ROUTE PLANNING

The route planning process is also a long-term strategic process in which an airline decides which routes would be profitable to fly based on an analysis of the market. One of the steps in route planning is to decide the airline structure to be selected. Two of the most commonly used structures are the hub-and-spoke and the point-to-point.

The hub-and-spoke architecture is characterised by having a main airport (the hub) which is the airline's center of operations. In a hub-and-spoke structure, flights are flown from the hub to a spoke airport and back. This structure has several benefits. It allows not only, for routes with a small demand to be chosen while maintaining profitability but also for lower maintenance costs. Conversely, it also has several drawbacks namely reduced aircraft and crew utilization when compared to the point-to-point structure. Furthermore, the turnaround time is also larger to allow for connecting passengers and their luggage to board the aircraft. Often, this leads to substantial delays.

Furthermore, the point-to-point structure is characterized by having only direct flights in between two O-D pairs. for this architecture, virtually every airport in the network could be a transferring airport for a passenger who wishes to fly between two airports for which there is no direct flight. The former adds substantial complexity to the problem. Nonetheless, regardless of the type of airline structure which is adopted, the choice of routes highly depends on the forecast of demand, costs and revenue.

4.1.3. SCHEDULE PLANNING

According to *Belobaba et al.* [16], the schedule planning of an airline can be split into four phases. First, an airline should determine how often it wishes to perform flights on a certain route. Then, it should create a timetable and determine the times at which it will provide a certain flight. Following this, the airline should assign aircraft types to specific routes and finally the airline should concern itself with the routing of a specific aircraft throughout its network.

Furthermore, if one wishes to explore the trade-off between profit and environmental effects of aviation there are two problems within airline planning that one should look at: the fleet assignment problem and the aircraft routing problem. These are directly associated with the missions that an aircraft performs and often include additional constraints such as mandatory maintenance checks. These two problems shall be discussed subsequently.

FLEET ASSIGNMENT & AIRCRAFT ROUTING

Solving the fleet assignment problem means assigning, in a profitable manner, aircraft to flight legs in the airline's network. There are two aspects to take into account when solving the fleet assignment problem. On one hand, it is important to consider the available aircraft types. On the other hand, it is necessary to consider the fleet balance, which makes sure that a flight schedule can be repeated periodically. This is achieved by maintaining in equilibrium the number of aircraft arriving at an airport and the number of aircraft departing from that same airport during a specific time period [16].

To be able to capture not only the temporal but also the spacial component of the fleet assignment problem, *Hane et al.* [57], came up with the concept of a time-space network. An example of a time-space network can be visualised in Figure 4.2. This is an expansion of the static representations of an airline network, in which each node represents not only a location (airport) but also a point in time.

Furthermore, in the context of the fleet assignment problem finding a feasible fleet assignment is comparable to finding a feasible path (for each aircraft in the fleet) within the time-space network which fulfils the requirement of continuity and minimizes spillage and spoilage.

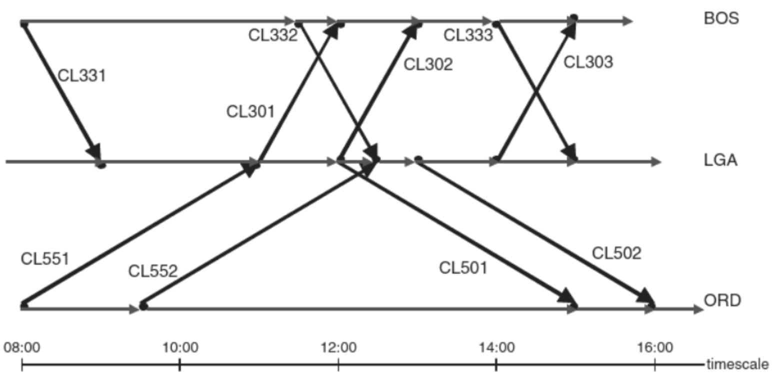

Figure 4.2: Example of a time-space network [57]

As a step further in the fleet scheduling and planning of airlines, there is the aircraft routing problem (ARP). First envisioned by *Daskin & Panayotopoulos* [58], this involves assigning specific aircraft to a specific set of flights, while attending to the required flight coverage and ensuring that continuity to the next time period is possible. This is usually the step at which mandatory maintenance checks are taken into account [16].

4.1.4. INTEGRATED AIRLINE PLANNING

The joint optimization and planning of all the aforementioned disciplines would bring substantial benefits for an airline [16]. This is however difficult to achieve. On one hand, there is a lack of detailed demand and cost data which can accurately represent the market dynamics. On the other hand, from the airline side, there is a lack of trust in a large-scale framework which solves all the main airline problems at once. Nevertheless, there has been research on the possibility of performing it simultaneously. For the scope of the current literature review, the focus is placed on the fleet assignment and routing of aircraft. As described in section 4.3, there has been research in terms of simultaneously creating the timetable design, assigning aircraft to flights and considering their routing.

4.2. METHODS

With knowledge of the main problems that the operations department of airline faces, one should be aware of the different methods which can and have been used to solve them. A description of mixed-integer linear programming (MILP) and dynamic programming (DP) is given.

4.2.1. MIXED-INTEGER LINEAR PROGRAMMING

In general, problems which have a linear objective function and are subject to linear constraints can be solved with linear programming (LP). This optimization technique was first envisioned by *Dantzig & Ferguson* [59] for which the objective function always assumes the form present in Equation 4.1 [60]. Mixed-integer linear programming (MILP) is in a way a type of linear programming (LP) with the difference or particularity that the decision variables can be binary, integer and continuous, whereas in linear programming they can only be continuous.

$$\text{Min} c_1 x_1 + c_2 x_2 + c_n x_n \tag{4.1}$$

Moreover, given the simplicity of the models that can be solved using MILP, they can be solved by making use of the simplex algorithm, which was first developed in 1947 by *Dantzig* [61]. This makes this optimization technique computationally efficient, even if it is required to solve a large system with hundreds of equations. In addition to this, MILP problems can be solved in exponential time by making use of the branch-and-bound technique [62] and are nearly guaranteed to output an optimal solution.

However, the simplicity of the problem formulation comes at a price. The dynamics and the interactions within the problem at hand need to be made into linear form, which is sometimes impossible or quite difficult. In addition to this, the formulation of the problem is static in time. In the case of problems which evolve over time, this becomes an issue. It is however possible to overcome this problem by adding a new set of constraints at each time step. It is important to highlight that, the entire problem is still solved as one large problem (all time steps are solved in one go)[60]. In addition to the aforementioned issues, in an attempt to reduce the inaccuracies resultant of assuming linear constraints and objective function, often more variables are added to represent the system. This, in turn, increases the dimensionality of the problem and thus computational time.

4.2.2. DYNAMIC PROGRAMMING

Dynamic programming is a mathematical technique used to solve large complex problems. It was first envisioned by *Bellman* [63]. Typically dynamic programming tackles problems with **discrete** states and decisions, meaning problems in which the moments to make a decision are clearly distinguishable from each other. Thus, one of the core concepts of dynamic programming lies in dividing a complex problem into smaller sequential sub-problems, which can be solved individually to find the optimal solution based on the system's current state. Moreover, dynamic programming relies on a fundamental concept: the principle of optimality; which says that:

> *"An optimal policy has the property that whatever the initial state and initial decision are, the remaining decisions must constitute an optimal policy with regard to the state resulting from the first decision"*

Furthermore, an important underlying assumption of dynamic programming is that it is a Markov decision process: Decision at each state only depends on the current state, it does not depend on the previous state. While making use of this assumption, most dynamic programming problems are solved backwards, meaning starting at the final known state and making way to the initial system state. This is advantageous as it allows for the cost function to be optimized, without the need for an extensive analysis of every possible outcome [63]. Furthermore, the fact that dynamic programming allows for a big problem to be fractured into smaller sub-problems and their solutions to be stored for later, significantly reduces computational time.

Each dynamic programming problem requires a specific formulation, nevertheless *Powell* [64], created a general formulation which can be used to formulate most dynamic programming problems:

- **State variable** $(s_1,...,s_N)$: Contains information on the system at each stage. Represents all the information which is required to make the next decision.
- **Decision variable** $(x_1,...,x_N)$: Tracks the decisions which are made at each stage.
- **Exogenous information** $(p_1,...,p_N)$: Information that becomes available at stage n.
- **Contribution function** $C_n(s_n, x_n)$: Represents the immediate contribution cost (to the cost function) of taking decision x_n at stage n given the state s_n.
- **Transition function** $S^T(s_n, x_n)$: Defines the evolution of the system from state s_n to state s_{n+1} given decision x_n.
- **Objective function** min $\sum_{n=1}^{N} C_n(s_n, x_n)$: Minimization of the costs which are a result of all decisions.

Additionally, it is important to address the dimensionality issue that dynamic programming poses. A problem can easily become difficult to solve if the number of variables, dimensions, possible states and possible decisions increases [64]. In contrast to mixed-integer linear programming, there is little documentation or readily available commercial software that provides an easy and comprehensible way of using dynamic programming.

4.3. METHOD COMPARISON FOR SOLVING FAP & ARP

As defended by *Dreyfus* [60], and in the aforementioned analysis, if a problem is mostly linear in its assumptions, then mixed-integer linear programming has superior characteristics than dynamic programming. However, if the problem is of multi-stage nature or non-linear, then dynamic programming is a superior method.

Both methods have been used to solve the fleet assignment problem, the aircraft routing problem and a combination of the two. Nevertheless, whereas the use of MILP has been extensively researched, the same is not so true for dynamic programming. This section exposes relevant literature that has made use of both methods to solve the fleet assignment and aircraft routing problems and highlights their points of improvement.

MIXED-INTEGER LINEAR PROGRAMMING

MILP has been extensively used in literature to solve the fleet assignment problem. *Abara* [65], was one of the pioneers in using MILP to solve fleet assignment problems. At this stage the concept of a time-space network was still not known, hence this method uses a connection-based network structure. The former is based on nodes, where each node represents the arrival and departure times of flights. This method is limited as it requires that all the feasible connections between nodes are known a priori. In addition to this, it only works for homogeneous fleets.

Since then, several advancements have been done in terms of using MILP for solving the fleet assignment problem. For example, *Barnhart et al.* [66], developed an itinerary-based fleet assignment model which combines the classical leg-based fleet assignment model with the passenger mixed flow model. This allows to recapture demand which is not allocated in the classical fleet assignment model and hence produces higher profits. Building upon this model, *Lohatepanont & Barnhart* [67] created a framework which simultaneously optimizes the flight legs that should be flown to maximize profit and assigns aircraft to them. Similarly to the model built by *Barnhart et al.* [66], the time frame considered is of only one day and the schedule design is incremental, meaning it is not built from scratch.

Following the trend of combining the scheduling of flights with the fleet assignment problem, *Justin et al.* [68], propose a half-leg half-itinerary MILP formulation to simultaneously optimize the scheduling of flights, the assignment of aircraft gauges to flights, the size of the sub fleets, and finally the itineraries of passengers.

Furthermore, both profit and environmental impact are considered as objective functions. It is important to note, that a predefined fleet or schedule blueprint was not required. This makes this framework, suitable for evaluating the profitability and environmental impact of new aircraft and airline concepts. Given this, the framework was tested by considering the demand in the Northeast Corridor of the United States and 3 baseline aircraft (a 9 seater, a 19 seater and a 48 seater). The latter were based on existing aircraft and either a fully electric or a hybrid electric propulsion system was integrated. Furthermore, it is important to note a large limitation of this framework. It does not account for demand variability throughout the week and it does not employ a wraparound fleet-size constraint which equates the aircraft subfleet sizes at each location between the previous evening and the morning after.

On another front, *Barnhart et al.* [69] was a pioneer in simultaneously solving the fleet assignment problem and the aircraft routing problem while making use of MILP. These efforts were followed by *Unal et al.* [70], which concurrently optimized the costs of fleet assignment and aircraft routing for a hub & spoke airline. It is important to note that this approach was quite computationally expensive. Attaining a feasible solution for a 2-day fleet schedule took 2.5 hours. Which poses the question: How feasible is it to make use of MILP to combine fleet assignment and aircraft routing if one wishes to consider a larger time span or a larger network?

DYNAMIC PROGRAMMING

As highlighted by *Woudenberg* [71], using dynamic programming within airline planning has not been as explored as the use of linear programming. Nevertheless, one of the first efforts made to make use of dynamic programming to solve the fleet assignment problem was done by *Hyman & Gordon* in 1968 [72]. The developed framework had as its objective to maximize revenue by allocating aircraft to specific flights. Several inputs are taken into account. Besides the turn-around time, the aircraft types available, preliminary maintenance plans and the desired frequency per available route in the network, also the demand throughout the day was considered. To determine the demand the authors made use of a survey. Furthermore, an attraction band was considered to determine how many passengers would be assumed to be captured around a certain time of the day. This can be visualized in Figure 4.3 where an attraction band around 9:30 am can be seen. Moreover, the authors highlight the importance of good demand data throughout the day.

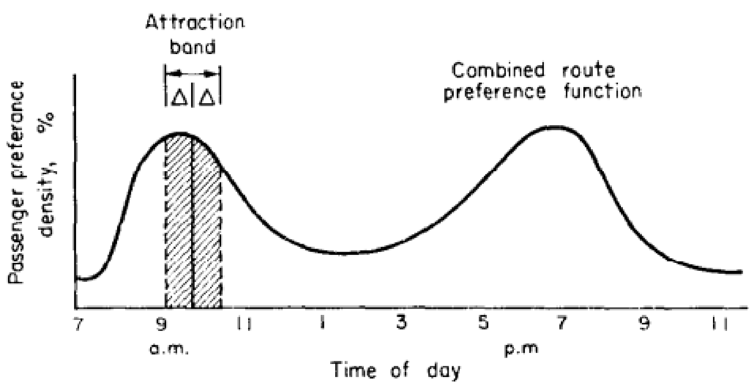

Figure 4.3: Time of the day passenger preference function [72].

Furthermore, *Hersh* [73], combined dynamic programming with a heuristic approach with the goal of maximizing profit when assigning aircraft to routes in a network. The author tries to build on top of the work developed by *Hyman & Gordon* [72], by tackling two additional aspects which had not been considered: 1. The fact that there is competition and passengers may choose the competitors flight over yours; 2. The existence of intermediate flights, meaning the possibility that on a specific flight leg, there are passengers who started their journey at a different location or are ending their journey at different locations. Moreover, the heuristic approach that was employed can be summarized in the following 4 steps: 1. Creation of feasible routes; 2. Assignment of aircraft to routes; 3. Assignment of passengers to flights; 4. Sequential reassignment of passengers to routes;

More recently, the concurrent integration of schedule design, fleet assignment and aircraft routing has been explored. *Wang* [74], created a framework which makes use of dynamic programming to optimize for profit the schedule and fleet assignment. The model takes into consideration several aspects which had been lacking thus far. Firstly, it allows for the consideration of both local and transfer passengers. This is done by making a distinction between the flights flying to the hub and those flying from the hub. Furthermore, the constraint that all the aircraft must return to the hub at the end of the day, is also relaxed. Whenever flying back to the hub at the end of the day leads to negative profit, it is considered if there exists any schedule that covers the same sequence of flights with any of the available aircraft type for which it is more profitable to leave the aircraft overnight at an outstation. Finally, the model also considers the possibility of spoke-to-spoke flights, meaning passing through the hub is not mandatory. Thus, the model could be used to explore hub-and-spoke airline operations or point-to-point. However, only one day of operations is considered. This is a fairly limited time span if realistic operations are to be captured. Nevertheless, the fact that it is not mandatory that all aircraft must return to the hub at the end of the day may form the basis for a multi-day aircraft routing routine to be created.

In spite of the innovative features, a major limitation has been identified. The first limitation is related to the transfer passengers. Due to the sequential nature of dynamic programming and considering that the schedule of each aircraft type is constructed independently (one at a time), it is not possible to know all the possible connections until the program is finished. This means that it is quite hard to ensure that all the connecting passengers will be provided a connection. When compared to linear programming, this is the largest disadvantage of dynamic programming.

Furthermore, *Woudenberg* [71] made use of dynamic programming to optimize the schedule and rotation of individual aircraft during a week of operations of a cargo airline. The problem was modelled as a time-space network and the methodology followed builds on previous research performed by *Rubbrecht* [75] and *Wang* [74] . The high-level architecture of the framework can be visualised in Figure 4.4. The results showed that the framework was able to create a realistic schedule for cargo airline operations.

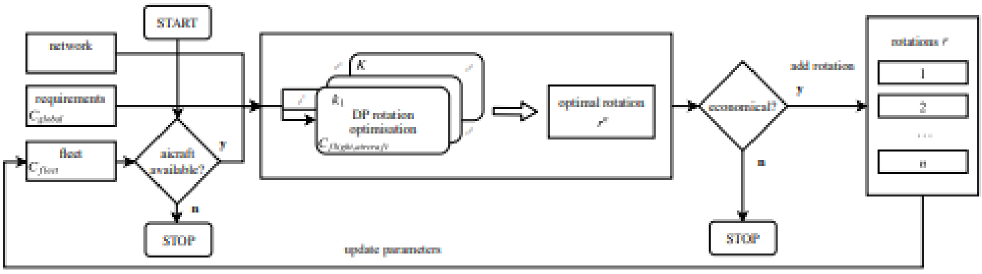

Figure 4.4: *Woundenberg* framework architecture [71].

In a posterior effort, *Seoane Álvarez* [76], used dynamic programming to assess the environmental benefits of intermediate stop operations, by optimizing a week-long schedule and fleet assignment. Since one of the goals of the paper is to quantify the potential environmental savings of intermediate stop operations, the environmental effects are not taken into account in the objective function. Rather they are assessed posteriorly.

As a step forward, in a publication which is soon to be published, *Noorafza et al.* [77], created a multi-objective framework which considers the interdependencies between network planning and flight scheduling decisions. The framework is able to consider the operations of several airline types and several operational improvements such as intermediate stop operations. Going against common practice, the authors considered a modified profitability metric which considers profit per climate impact unit (ATR20) as the objective function. Through means of an integrated network planning model, the framework outputs the network design, flight schedule, aircraft routes and a set of climate and non-climate KPI's to evaluate the output quality. At the core of the integrated network planning model, which can be visualized in Figure 4.5, lies a dynamic programming algorithm which decided which aircraft to use on which flights and when.

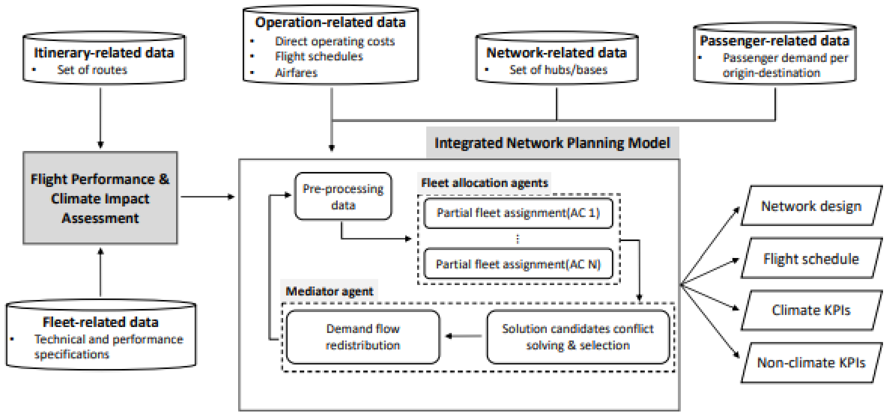

Figure 4.5: Diagram of the multi-objective framework for integrated network planning and flight scheduling. [77]

In contrast, *Khoo & Teoh* [78], explored the possibility of constructing a bi-objective dynamic framework to find an optimal aircraft acquisition strategy. Even though it is not directly related to the fleet assignment problem or aircraft routing problem it serves as an example of the possibility to construct a dynamic programming framework which abides by two separate objective functions. The objective in question was to maximize an airline's environmental performance and operational profit by determining the type and amount of aircraft that should be purchased and/or leased to meet the demand. The interesting part about the method in question is that it allows to select which of the objectives: maximising profit or maximising environmental performance; should be considered a priority. Although, in the framework by *Noorafza et al.* [77], both profit and environmental impact are considered in the objective function, this is done through considering a ratio between the two variables. Hence, only one objective function formulation is considered.

DISCUSSION AND COMPARISON

Furthermore, in a study by *Kannon et al.* [79], a comparison was drawn between using a MILP and dynamic programming to solve the aircraft routing problem with aerial refuelling. The following problem was solved separately by the two methods: Route an aircraft with a certain fuel capacity, from one pre-designated node in the network to another with the possibility to air-refuel at certain intermediary nodes. The objective was to minimize a weighted combination between the total distance travelled and the number of aerial refuelling operations conducted. The authors found that the dynamic programming method is robust for both network size and required computational time to achieve a solution whereas MILP struggled to find a solution for larger networks within the 1 hour time limit they imposed. Although this is a specific case, it brings to light once again how dynamic programming is a feasible and beneficial alternative to mixed-integer linear programming.

5

Climate optimization

The climate impact of aviation is directly linked to how much energy an aircraft needs to perform its missions. There are several ways one can attempt to limit the energy consumption of aviation. On one hand, there is the optimization of the aircraft design. This includes improving the aerodynamic efficiency, improving the structural efficiency and reducing weight, or even limiting the in-flight emissions by optimizing the propulsion system or choosing an alternative energy carrier altogether. On the other hand, operational changes such as flying at a lower/higher speed, climbing faster, and cruising at a lower/higher altitude greatly influence the conditions at which the aircraft's propulsion system operates and thus indirectly influence the aircraft's energy consumption.

Furthermore, the aircraft's energy consumption is related to its climate impact. However, this is not necessarily an easy relationship to derive as there are other factors at play. Given this, section 5.1, gives a brief overview of how the climate impact of aviation can be quantified.

Moreover, the inclusion of batteries and electric systems in hybrid-electric aircraft poses a massive increase in their empty weights, which could impact negatively the aircraft's mission performance. For the specific case of hybrid-electric aircraft, according to *Zhang et. al* [80], the benefit of using hybrid-electric aircraft highly depends on the energy management strategy applied (balance between battery and fuel energy). Hence in section 5.2 methods which have been used to optimize the hybridization of hybrid-electric shall be reviewed.

Finally, as parameters such as altitude and cruise speed have an influence on the design of the propulsion system but also on the climate effect of the combustion products, section 5.3 reviews literature which has looked at the effect of these parameters on the fuel consumption of an aircraft, but also on the propulsion system design.

5.1. Climate Impact Assessment

In addition to CO_2 and NOx, other pollutant compounds resulting from aviation are sulfur oxides (SOx), water vapour (H_2O) and in smaller amounts unburnt hydrocarbons (UHC), carbon monoxide (CO) and soot. In Table 5.1, a summary of the typical emission indexes for each of the different products of aviation can be visualized. Furthermore, there is also an indication in what ways they are sensitive to the current flight condition.

Estimating the impact that these products have on the environment is quite complex and there is a large uncertainty associated with it. The effects of CO_2 are the most well-known as they have been researched the most. Although it may be tempting to neglect the effects of other combustion products it has been shown by *Lee et al.* that the total climate impact of aviation is about three times larger than that of CO_2 alone [81]. Considering the additional products adds complexity to the problem as their effect on climate depends on the geographical location, altitude and the weather. Moreover, there are several climate impact metrics which can and have been used to assess the climate impact of aviation, which shall be discussed.

Table 5.1: Typical emission indexes of aviation products per kg of JetA1 and their dependencies on the propulsive conditions [81].

Compound	Emission Index (kg/kg)	Dependencies
CO_2	3.16	Thrust setting
NOx	0.01514	Thrust setting (equivalence ratio, temperature), combustion technique
H_2O	1.231	Thrust setting
Soot	0.00003	Thrust setting (equivalence ratio, temperature, pressure), condition of fuel injection
SO_2	0.0012	Content of sulphur in the fuel

RADIATIVE FORCING

Radiative forcing is a net flux imbalance at a location in the atmosphere, which is caused by a change in the atmospheric composition. Without entering a detailed analysis, there are several specific definitions which differ mainly on the assumptions on how the atmospheric temperature changes along a vertical atmospheric segment [82]. Furthermore, this is a backwards-looking climate metric which may raise the question of how suitable it is to be used to forecast the future climate impact of aviation.

GLOBAL WARMING POTENTIAL

The global warming potential (GWP) measures how much the radiative forcing caused by a one-time emission of a specific species contributes to global warming (at a specific time horizon) as compared to the radiative forcing of the reference gas CO_2. Furthermore, this can be translated into Equation 5.1, where i is a specific gas, H is the time horizon, t the time and RF is the radiative forcing. Moreover, this climate metric was first created in 1990 by *Rodhe* [83] and although it is the most commonly used climate metric as of now [84], its applicability has been extensively criticized. On one hand, it has been criticized because of its dependency on the time horizon H, for which 100 years is the most commonly used timeframe. The choice of such a time horizon has been criticized as there seems to not be any scientific reason for this specific choice [85]. In addition to this, the global warming potential does not actually give an indication of the change in the earth's temperature. It is based on quite an abstract concept: an integration overtime of the radiative forcing of a specific species.

$$GWP(H)_i = \frac{\int_0^H RF_i(t)dt}{\int_0^H RF_{CO_2}(t)dt} \tag{5.1}$$

GWP*

A modified application of Global Warming Potentials (GWPs), called GWP*, provides a way to express emissions of both short-lived and long-lived climate pollutants (SLCPs LLCPs) in a consistent way while using a single measure. This is achieved by considering a change in the emission rate of an SLCP as equivalent to a single emission pulse of a long-lived pollutant. In other words, it is a method to compute CO_2- equivalent emissions as a function of time, which can then be translated into a change in atmospheric temperature at a specific time t.

EGWP*

As part of his thesis work *Megill* [84], created a new climate metric which is a derivative of the GWP* metric. In addition to the aspects that GWP* takes into account, EGWP* considers the efficacy of the different emissions: the effectiveness of a climate agent in leading to a temperature change when compared to the effectiveness of the reference gas CO_2. The author defends that the absence of this consideration leads to the overestimation of the temperature induced by contrail formation and an underestimation of the temperature induced by ozone reduction, caused by NOx emissions.

GLOBAL TEMPERATURE-CHANGE POTENTIAL

The global temperature change potential (GTP), was first created in 2005 by *Shine et al.* [86] and in contrast to the GWP metric it is an endpoint climate metric. The GWP is defined as the ratio between the absolute global temperature-change potential of gas i ($AGTP_i$) and the AGTP of the reference gas CO_2. In essence, the AGTP of a gas is the temperature change (ΔT) at the time horizon H. In contrast to the GWP metric it gives an indication of the atmospheric temperature change.

AVERAGE TEMPERATURE RESPONSE

The average temperature response (ATR) metric was first developed by *Dallara* [87] and it was specially designed for aircraft design. ATR considers average, sustained emissions over the lifetime of an aircraft instead of considering only a pulse, as is the case of GWP and GTP. This can be translated into Equation 5.2, which considers the time horizon H and the change in atmospheric temperature at time t (ΔT).

$$ATR_H = \frac{1}{H}\int_0^{\infty} \Delta T(t)dt \tag{5.2}$$

COMPARISON

For his master thesis *Megill* [84] compared and analysed the aforementioned metrics based on a set of requirements to determine which is the best-suited climate metric. The requirements for which each climate metric wwas analysed are the following:

- Shall correctly represent the temperature change
- Shall be easy to understand and implement.
- Shall be largely independent of the time horizon.
- Shall be largely independent of the background emissions scenario.
- Shall have low inherent biases towards changes in aircraft design or trajectory.
- Shall be appropriate for different emission profiles.

For the analysis, different use cases were considered. Two are of relevance for the current literature study. The first one regards aircraft design optimization, and the second one regards trajectory optimization. Regarding the first use case, the author concludes that the climate metric ATR_{100} is the most suitable. From analysing the results and taking into consideration the pre-defined requirements, the author concludes that this metric is especially good for comparing the performance of different fleets (fleets which use different technologies, e.g. hydrogen fuel cell versus SAF). For the case of trajectory optimization the author still suggests the use of ATR, but this time with a time horizon equal to 20 years.

5.2. HYBRIDISATION OPTIMIZATION

As discussed in chapter 3, there are several propulsion system architectures that a hybrid-electric aircraft can have. Furthermore, these architectures can be characterized by two variables: the degree of hybridization of power or power split (H_p) and the degree of hybridization of energy or for short energy split (H_e) [21]. Given the duality of hybrid-electric aircraft (two sources of energy), there are several power settings allowed that output the same required power. Furthermore, a larger hybridization also implies a larger battery and a heavier powertrain. The negative effects of the additional weight may outweigh the positive effects of the increase in powertrain efficiency and potential reduction in fuel consumption. Thus, studying how to effectively make use of a hybrid propulsion architecture and sizing it accordingly is a trade-off worth investigating.

Overall there are two main groups of methods which can be employed to optimize the use of battery energy during a mission. The first one is rule-based methods, which as the name indicates determines when to make use of the battery's energy based on a set of premisses or conditions. The second group of methods is the optimization-based methods. These aim at minimizing an objective function (typically fuel consumption) which depends on the degree of hybridization.

5.2.1. RULE-BASED

According to *Çaugatay Bayindir et al.* [88], there are two main types of rule-based power management strategy: deterministic and fuzzy rule-based methods. Whereas deterministic rule-based methods are guided by extremely precise and strict rules, fuzzy-logic rule-based methods, accommodate uncertainty and allow for flexibility in the controller's decisions.

Furthermore, unlike conventional aircraft, the weight of electric or hybrid-electric aircraft does not vary much during a mission, as the source of energy is a battery or a battery-fuel combination. Logically, in the case of hybrid-electric aircraft, it should be beneficial, from an efficiency point of view, to consume as much fuel at the beginning of the mission and minimize the weight of the aircraft for the remainder of the mission. This is supported by *HyunKi et al.* [89], where the power split during the climb of a series-hybrid electric aircraft was optimized. It was found that the trajectory which minimizes the fuel burn is that in which the use of electric power is delayed until the end of climb. From this conclusion, a rule-based strategy could be derived. The decision of whether or not to make use of the electric motor power could be guided, for instance, by the current flight stage or by the current thrust required.

5.2.2. OPTIMIZATION-BASED

As far as optimization-based methods are concerned, there are three main categories: the global optimization methods, the instantaneous optimization methods and the real-time optimization methods. An example of a global optimization method is dynamic programming and an example of an instantaneous optimization method is optimal control. Furthermore, real-time optimization methods put a special focus on the required assumptions to be able to in real-time control the vehicle and deliver the specified power management strategy. As the focus of the current review is placed on sizing aircraft at a conceptual level, rather than controlling it, these methods will not be reviewed.

OPTIMAL CONTROL METHOD

Although other power management strategies were considered, namely rule-based strategies, the main focus of a study performed by *Trawick et. al* [90] was put on comparing dynamic programming with optimal control for the power management of a parallel hybrid-electric aircraft. These strategies resulted in the largest reduction in fuel burn. In spite of the marginally better performance, the dynamic programming method is more computationally expensive than the optimal control method. Given this, one could argue that adopting an optimal control strategy is a better choice.

The optimal control method bases itself on the Pontryagin's minimum principle [91] and as previously mentioned it is particularly attractive when compared to dynamic programming as it is far less computationally expensive. This strategy has been applied in the literature to optimize the degree of hybridization of power throughout a hybrid-electric aircraft mission [92] [90]. To help solve the optimal control problem, one should make use of a Hamiltonian function which is minimized by the control inputs. Equation 5.3 is an example of a Hamiltonian function which is used in literature to solve the power split problem. Note that, P_{bat} is the power of the battery, $\dot{m}_f$ is the aircraft's fuel consumption, SOC is the state of charge of the battery and finally λ is the costate factor. In this case, the costate factor determines the relative importance/cost of electric power to fuel power, or in other words the power split between the two energy sources.

$$H = \dot{m}_f(P_{bat}) + \lambda \cdot S\dot{O}C(P_{bat}, SOC) \tag{5.3}$$

Furthermore, *Swannet* [93] made use of optimal control to optimize the flight path and the energy management of two aircraft: a hybrid electric aircraft based on the panthera aircraft and a hybrid fuel cell aircraft. Only the modelling of the former is relevant for the current literature study. The states which were kept track of are the distance travelled, the altitude, the indicated airspeed of the aircraft, the fuel mass and finally the state of charge of the battery. Additionally, the control variables considered were the shaft power, the propeller rpm, the flightpath angle and the engine rpm. The author found that when trying to minimize fuel consumption, approximately 23 % of the battery's energy is used during climb, while for the remainder of the flight, its use is more or less constant, leading to them being at their minimum state-of-charge at the beginning of descent.

DYNAMIC PROGRAMMING METHOD

The bases of dynamic programming has been explained in subsection 4.2.2. Furthermore, it can be applied to solve other problems besides fleet assignment, namely a hybridization optimization problem.

Soares Pinto Leite & Voskuijl [94], used dynamic programming to optimize the usage of battery energy on board of a serial hybrid-electric aircraft. Furthermore, the optimisation was conducted for a prescribed flight profile. This means that the altitude, speed and flightpath angle were not considered state variables. Only the state of charge and the weight of the aircraft were considered as states. By using a simple aircraft performance model (specific fuel consumption and efficiency of powertrain components considered constant), the optimizer chooses, at each time step, the power that should be delivered by the turbine as to minimize fuel consumption. Additionally, one particular aspect of the modelling is the fact that during descent a propeller is used as a windmill to reacharge the battery.

Moreover, the authors compared a non-optimal control strategy (engine is kept at 80% of the throttle for most of the flight and during descent the engine is at idle) with an optimal control strategy (using dynamic programming to reach a solution) and concluded that for a 200 min flight, the difference in fuel mass consumption between the two strategies is nearly negligible. Without giving any indication of the amount of energy stored in the batteries, the authors state that the difference between the two strategies could be more significant if the energy stored in the batteries were to be larger.

5.3. FLIGHT PROFILE OPTIMIZATION

The flight profile affects the block energy consumption during a flight. This is because the engines are designed to be the most efficient at specific operating conditions, thus if these conditions are not entirely met then the engine's efficiency decreases. Furthermore, variables such as altitude or required aircraft speed are examples of variables which indirectly affect the performance of engines. For example, reducing the thrust level at the top of climb which in turn reduces the rate of climb, leads to reductions in the block fuel consumption of aircraft [95].

Additionally, in general, cruising at a lower altitude leads to a higher fuel consumption due to the higher atmospheric density and hence higher drag. Nevertheless, as investigated by *Dahlmann et al.* [96] it has been shown that although the fuel consumption increases, the climate impact (average temperature response) of one mission decreases. The authors attribute this phenomenon to the fact that at lower altitudes NOx emissions have a lower climate impact. From an airline perspective, the additional fuel consumption from cruising at a lower altitude would entail an unnecessary increase in operational costs. However, with the introduction of hybrid-electric aircraft, as described in section 5.2, there is significant potential to limit the additional fuel consumption while benefiting from the lower climate impact of cruising at a lower altitude.

While following the aforementioned reasoning, *HyunKi et al.* [89], concurrently optimized the power split and the flight path trajectory and concluded that the simultaneous optimization of both aspects results in the largest fuel savings. Note that the optimization was only conducted for the climb phase, furthermore they made use of differential dynamic programming (DDP), which evidenced benefits in terms of computational speed.

6
Coupling of disciplines

Following from the discussion in chapter 2 it is of interest to couple aircraft conceptual design with fleet planning considerations. Furthermore, in chapter 3 and chapter 5 it has become apparent that for the specific case of hybrid-electric aircraft, it is especially important to take into consideration certain mission parameters and how varying these affects the design of aircraft. Hence, the following chapter reviews in what ways aircraft conceptual design has been coupled with fleet planning activities and with mission profile parameters (e.g. altitude and speed). In section 6.1 literature which has looked at coupling aircraft design with the fleet allocation problem is reviewed, in section 6.2 a review of the literature which has coupled aircraft design with mission profile variables is reviewed and finally in section 6.3 a review is given of the literature which has coupled aircraft design, fleet allocation and mission profile variables.

6.1. Aircraft design & Fleet allocation

Literature has evidenced that the coupling between aircraft design and fleet allocation can be done in numerous ways. On one hand, the coupling could be sequential (two problems solved separately, results interchanged and iterated [97], or it could be done simultaneously (both problems are solved together, the solver has full knowledge of both problems at all times [98].

Taylor & Weck [99] were pioneers in looking at the aviation system as a system of systems (SoS). They coupled aircraft design considerations with network flow considerations and operations considerations (aircraft capacity and range). Moreover, they embedded a linear-programming solver (LP) within a Simulated Annealing (SA) optimization algorithm. The simulated annealing algorithm perturbs the design vector and evaluates how likely it is that the objective function is improved by moving to a different condition. Furthermore, as the number of iterations increases it becomes increasingly more difficult for a new state to be accepted and hence possible to converge. Furthermore, it is important to note two aspects of this framework: the demand was assumed to be static and it was only tested for a small network with seven cities.

Building on top of the former, *Jansen & Perez* [97], were one of the first to create a multidisciplinary framework for the coupled optimization of aircraft and their allocation to routes in an operator's network with uncertain passenger demand. The framework is divided into two problems: a system-level problem and a sub-level problem. For the former, the goal is to minimize the network's energy intensity and for the latter, the goal is to minimize the network's operating cost. These problems are solved sequentially and their results are interchanged according to until convergence.

6.2. Aircraft design & Mission profile

It has been revealed that when optimizing the mission of an aircraft for climate, there is a tendency for the aircraft to fly slower and lower [100] [87] [97] [101]. This results in an increase in block time, which could affect the productivity of airlines. Based on this reasoning, *Proesmans & Vos* [**proesmans_airplane_nodate**], optimized a narrow-body medium-range aircraft, by allowing not only design variables such as the aspect ratio or the bypass ratio to vary but also by allowing mission variables such as the cruise altitude and Mach

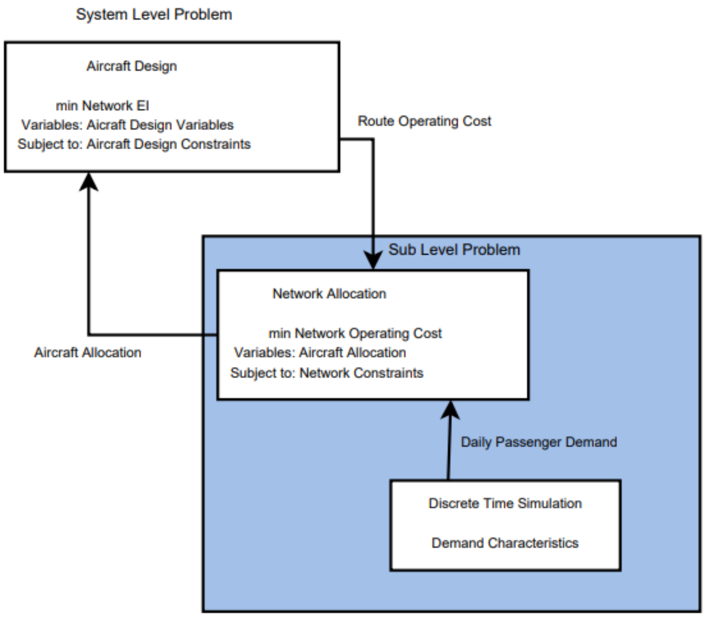

Figure 6.1: Framework for a coupled aircraft design and allocation decomposed optimization [97].

number to vary. A bi-objective objective function was considered. Both the operating costs and the average temperature response (ATR) were minimized. Furthermore, it was concluded that it is possible to largely reduce the ATR of a fleet while incurring a minimal cost increase of roughly 2%. Evidently, there is a large uncertainty associated with these results, as there still is a big incertitude in the quantification of the climate impact of emissions. Adding to this, the operating costs highly depend on the cost model assumptions.

6.3. Aircraft design, Fleet allocation & Mission profile

Hwang & Martins [102], simultaneously optimized the design of a next-generation aircraft, along with the mission profile, and the allocation of aircraft to routes in an airline network. Although the allocation model considered was quite simple, a surrogate model for lift and drag, dependent on Mach number and angle of attack was considered. To create the surrogate model, a CFD simulation was realized. Adding to this expensive simulation, with the goal of maximizing profit, a total of 6061 design variables were considered. Evidently, such a large problem incurs large computational disadvantages and makes it hard to track the relationship between design variables and outcome. Nevertheless, the results demonstrated that coupling the aforementioned disciplines can lead to a substantial increase in the airline's profit. When comparing the profit attained from considering the allocation-only optimization versus that attained by considering the simultaneous allocation-mission-design optimization the authors found an increase of 27%.

In a subsequent study, the same authors *Hwang & Martins*, improved even further the fidelity of the previously described framework [103]. Besides including an aerodynamic surrogate model (attained through RANS CFD simulations), the authors also include a propulsion surrogate model and improve the atmospheric models considered.

Roy et. al [98], developed a framework which couples aircraft design with fleet allocation while maximizing profit. Similarly to *Hwang & Martins*, this is done simultaneously. Furthermore, they developed an algorithm that is able to handle the fully coupled design-allocation-mission, that respects the integrality of the allocation variables, can overcome poor initial guesses, can accommodate a big continuous design space and can make use of parallel design space. Given the former, the authors created a framework which combines branch and bound, efficient global optimization, Kriging partial least squares (surrogate model) and gradient-based optimization to solve design-allocation-mission as an MINLP. Furthermore, a large number of variables are used to describe the shape of the aircraft. Adding to this, the cruise Mach number and altitude were also allowed to vary. This framework, A Mixed Integer Efficient Global Optimization (AMIEGO), can be visualized in Figure 6.2. It is another example of how increasing the accuracy of the description of the aircraft and the network dynamics has a significant computational cost.

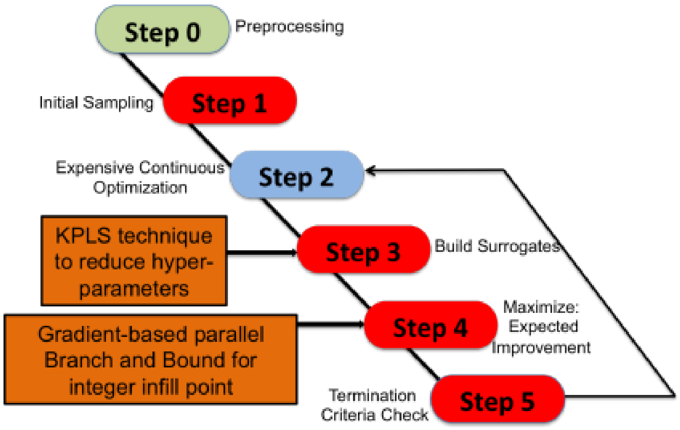

Figure 6.2: Overview of AMIEGO framework.[98]

In a subsequent study, *Roy et. al* [104], built upon the effort described previously [98]. The use of the AMIEGO framework (simultaneous approach) to optimize the aircraft design of a single-aisle aircraft while attending to airline operations and economics was compared with a sequential approach. The results evidenced that a simultaneous optimization approach yields a much larger profit than the sequential approach. Irrespective of the numbers themselves, as these highly depend on the assumptions and modelling which was used, this study comes to demonstrate that simultaneous coupling allows to capture the synergies between these disciplines with a higher degree of accuracy.

As evidenced in chapter 5, taking into consideration the mission profile and the power management during the mission has large benefits in terms of emissions reduction. This is especially true for hybrid-electric aircraft, due to their unique characteristics. While taking this into account, *Scheers* [8], coupled a hybrid-electric conceptual design tool to a fleet-and-network allocation model. The former was based on an already existing conceptual design tool created by *Proesmans & Vos* [**proesmans_airplane_nodate**] and was modified to be able to design parallel hybrid-electric aircraft. Furthermore, the fleet-and-network allocation model was based on a model developed by *Zuijderwijk* [9] which differs from other models because it considers the existence of battery charging stations within the network. Moreover, the hybrid-electric aircraft were also optimized for minimal climate impact (measured through CO2 emissions). This was done by allowing the cruise velocity, the cruise altitude and the cruise power split to be changed.

The coupling of the three different disciplines is performed sequentially. An iterative process is followed between the aircraft design module and the fleet-and-network allocation module. Convergence is reached when no new aircraft designs are chosen to operate within the network. Posteriorly, the mission profile of these aircraft is optimized in terms of cruise altitude, velocity and power split. Finally, the framework was tested by considering the SATA Air Açores regional airline network. Results show that hybrid-electric aircraft have the potential of reducing the network's emissions by 11% if the aircraft are designed particularly for the specified network. Furthermore, changing the cruises' altitude, velocity and power split resulted in a reduction in emissions larger than that verified by the coupling between the aircraft design and the network design. This supports the conclusions taken in chapter 5, by once again demonstrating the benefits that mission profile optimization has in terms of emissions reduction.

Table 3.6 summarizes and provides a visual comparison between the literature which was reviewed in this section.

On a last note, only one paper was found to couple in a simplistic manner aircraft design and fleet assignment of aircraft to flights. *Govindaraju & Crossley* [105], examined the effects of coupling the conceptual design of a cargo aircraft with the fleet assignment problem while attending to design parameter uncertainties and demand uncertainties. The optimization problem is decomposed into three smaller problems. The

Table 6.1: Comparison of literature which addresses the coupling between aircraft design, fleet allocation and mission profile

Authors	Objective function	Fleet allocation	Aircraft design	Mission profile	Fidelity	Coupling type	Reference
Sheers	Profit, CO_2 emissions	✓	✓	✓	Medium	Sequential	[8]
Hwang & Martins	Profit	✓	✓	✓	High	Simultaneous	[102]
Roy et al.	Profit	✓	✓	✓	High	Simultaneous	[98] [104]
Taylor & Weck	Operating cost	✓	✓		High	Simultaneous	[99]
Jansen & Perez	Energy intensity & operating cost	✓	✓		Medium	Sequential	[97]
Proesmans & Vos	Operating cost & ATR		✓	✓	Medium	Simultaneous	[**proesmans_airplane_n**

top-level problem aims to exploit new aircraft's requirements space, the aircraft sizing subspace, which determines the optimum aspect ratio, thrust-to-weight ratio and wing loading ratio for minimizing operating cost on a specific route. Finally, the assignment subspace determines which aircraft are operated on which flights.

7

Conclusions & Research Proposal

In the following chapter the main conclusions derived from the review carried out in chapter 3-chapter 6 are detailed in section 7.1. Furthermore, from these, the research gap which was identified can be found in section 7.2. Finally, the research questions and research objective as well as a preliminary planning are detailed in section 7.3, section 7.4 and section 7.5.

7.1. Conclusions

From the analysis and review in chapter 3-chapter 6 several conclusion were drawn. These can be summarized as follows:

Hybrid-electric aircraft

- From chapter 3, it became evident that the design of hybrid-electric aircraft comes with additional challenges: traditional design methods must be altered because there is no statistical data on commercial hybrid-electric aircraft, the propulsion system has multiple new degrees of freedom: architecture, degree of hybridization and shaft power ratio; and finally, the specific energy of the current state-of-the-art batteries is limited.
- The propulsion system of hybrid-electric aircraft has two energy sources (e.g. battery and kerosene). There are several possible ways in which the energy is harvested and transformed into shaft power (different architectures). The main hybrid-electric aircraft architectures are: turboelectric, serial and parallel; from these several derivatives can be created. On one hand, it is possible to combine two or more of these "base" architectures and on the other hand it is possible to play with the fact that there may be more than one powertrain path (e.g. if there is a main engine and a distributed propulsion system composed of several electric motors).
- The two main design methods which were identified were created by *Finger et al.* [39] and *de Vries* [5]. From the analysis of these methods two conclusions were drawn. On one hand, the sizing for power of each of the subcomponents in the propulsion system can be accounted for by taking the total power required to be provided by the propeller and through a step-back approach (in which the efficiencies of the components are assumed) move towards the energy sources. on the other hand, when sizing the battery and fuel mass for a specific design mission, there are two main approaches which can be followed: energy-based and through a modified Breguet range equation.
- The aero-propulsive effects of propeller aircraft (especially if distributed propulsion is considered) should not be ignored. Even if at the conceptual level, accounting for the propeller effect on lift and drag and thus extending the design space of hybrid-electric aircraft should not be neglected.

Fleet assignment & Aircraft routing

- There are several phases within an airline's planning process: strategic planning (long-term), tactical (medium to short term) and finally operational (short-term). Within tactical planning, the fleet assignment and routing of aircraft provide a significantly accurate approximation of the airline's operational process which allows for the study of the existent trade-off between profit and environmental impact.

- To solve the fleet assignment and aircraft routing problems it is possible to model them in several ways, namely by modelling them as mixed-integer linear programming problems or as dynamic programming problems. The main advantage of mixed-integer linear programming is the fact that it is guaranteed that it will converge to an optimal solution. However, it comes at the cost of not allowing non-linear behaviours (such as) to be modelled and is often computationally expensive for large problems. Dynamic programming on the other hand, allows for the modelling of non-linear behaviours and can lead to savings in terms of computational time as it fractures a big problem into several small problems.

- The use of mixed-integer linear programming to solve the fleet assignment problem and the aircraft routing problem has been more researched than the use of dynamic programming. Recently, an MILP formulation was created which simultaneously optimizes the scheduling of flights, the assignment of aircraft to flights, the subfleets size and the passengers itinerary [68]. A similar effort was made with dynamic programming [74], however only profit was considered as the objective function.

Climate optimization

- It is extremely important to take into account not only the CO_2 effects of aviation but also the non-CO_2 effects, as these account for two-thirds of the climate impact of aviation [81]. Furthermore, the climate effects can be quantified in several ways. For the specific case of the current literature study, it was found that the average temperature response metric is the most suited [84].

- For the specific case of hybrid-electric aircraft deciding when during a mission the battery energy should be used, is an important design parameter. There are two main groups of methods which can be used to optimize the energy management during a mission. First, rule-based (guided by a set of premisses and conditions) and optimization-based (aim to minimize an objective function, usually fuel consumption)

- Playing with altitude and speed can be used to reduce the climate impact of aviation. Although flying lower leads to a larger fuel consumption, it has a lower climate impact associated with it [96].

- Concurrently, taking into account the energy management and the flight path of hybrid-electric aircraft leads to the largest fuel savings. However, this has only been performed with complex techniques, such as differential dynamic programming which probably are difficult to integrate as part of a large framework.

Coupling of disciplines

- The combination of aircraft design with strategic airline planning (specifically allocation of aircraft types to routes) has been quite investigated. The same is not true for the coupling of aircraft design with the assignment of those aircraft to flights. Specifically, the feedback from network design towards aircraft design has not been explored.

- Most of the frameworks created attempt to automize the link between aircraft design and airline planning by running a multidisciplinary optimization problem. This makes it difficult for the authors to identify the interdependencies between the variables and the trade-offs required.

- Profit is the most commonly used objective function, however also environmental trade-offs have been considered. Furthermore, most of the studies only consider the aircraft design of conventional aircraft, not hybrid-electric aircraft. Furthermore, only one study [**proesmans_airplane_nodate**] was identified to take into account the average temperature response as one of the objective functions.

7.2. Research Gap

Given the aforementioned conclusions, a research gap can be identified:

Coupling hybrid-electric aircraft conceptual design with flight scheduling and fleet assignment while allowing for the possibility to manipulate certain mission parameters, such as altitude, speed and degree of hybridization.

7.3. RESEARCH QUESTION

All in all, given the aforementioned research gap, the following research question was formulated: Given the gap identified in section 7.2, the main research question to be answered can be formulated as follows:

What is the effect on network's profitability and environmental impact if the effects of altitude, speed and hybridization are directly coupled to hybrid-electric conceptual aircraft design?

This research question can be further split into the following sub-research questions:

1. What is a coupling strategy which is computationally inexpensive, useful, feasible and accurate?
2. Depending on a network's structure and type of mission (length), how does the choice to use the battery change?
3. What are the trade-offs between altitude, speed, and degree of hybridization in terms of network profitability and environmental impact?
4. How can altitude, speed and degree of hybridization be effectively incorporated into conceptual design for improved network profitability?
5. How does demand affect the top-level requirements of the hybrid-electric aircraft?
6. How scalable (towards large networks) is using dynamic programming for solving the fleet assignment and aircraft routing problem?

7.4. RESEARCH OBJECTIVE

All in all, the research objective of the current research can be formulated in the following way:

To create a framework which couples hybrid-electric aircraft design and mission variables to a dynamic programming integrated scheduling and assignment of aircraft to flights method, that allows to study and identify the existing interdependencies and trade-offs in terms of profit and environmental impact.

7.5. PRELIMINARY PLANNING

In order to answer the research question and fulfil the research objective, a preliminary planning was constructed. In general, the research activities shall be divided into four main parts: Conceptual development of the methodology, implementation of the framework, verification of the applicability of the framework and case study analysis.

1. CONCEPTUAL DEVELOPMENT OF THE METHODOLOGY

In this phase the coupling strategy which will be considered should be determined. To achieve this, the inputs and outputs of each of the main modules should be determined. Following from the research question and the literature review the main modules which shall be part of the framework are the hybrid-electric aircraft design, the integrated scheduling fleet assignment and aircraft routing module and finally the mission analysis module (which allows to play with altitude, speed and degree of hybridization at each flight step).

Furthermore, from the identification of the main design variables, it is important to understand how they are related to each other, and which simplifications and assumptions are necessary (especially for the propulsion system). Moreover, during this phase an assessment of the available data (e.g. airline data) shall be conducted as well as a study of the available hybrid-electric aircraft design frameworks. In addition to this, the key performance indicators which shall be used to quantify the performance of the framework shall be decided, as it is important to know them before starting to implement the framework.

Finally, the main output of this phase is a clear and explicit diagram of the framework to be developed. It should include inputs and outputs between the different modules as well as the coupling logic.

2. IMPLEMENTATION OF THE FRAMEWORK

This phase of the research activities should be that which is the longest. Here the three modules should be implemented and connected. The first module which will be considered is the integrated schedule, fleet assignment and aircraft routing module. Based on the framework developed by *Wang* [74], the framework should be extended to account for the inclusion of hybrid-electric aircraft. Furthermore, at this stage it will also be necessary to consider the demand data.

Following the former, the hybrid-electric aircraft design framework developed by *Sheers* [8], should be extended to account for the aero-propulsive benefits of propeller aircraft. Furthermore, special attention should be given to the propulsion system modelling and design as it will greatly affect the block emissions of the aircraft.

Subsequently, the mission analysis module should be constructed. It should, in an inexpensive way, choose the degree of hybridization at each flight step. This could perhaps be done apriori for each aircraft by running an energy-based mission analysis for different target ranges and by using an optimal control optimization method to choose the degree of hybridization at each flight step. Nevertheless, the feasibility of this approach shall be assessed during the conceptual development of the methodology.

The final step in the framework implementation shall be to couple the aforementioned modules based on the logic constructed during the conceptual development of the methodology.

3. VERIFICATION OF THE APPLICABILITY OF THE FRAMEWORK

During this phase of the research activities, the correctness of the framework implemented shall be verified. This phase runs in parallel with the implementation of the framework. Once each module is completed, it should be verified and the necessary adjustments should be implemented and the results should be documented.

4. CASE STUDY ANALYSIS

The case study selected during the conceptual phase should be used to demonstrate the applicability of the framework developed. Hybrid-electric aircraft design trends should be identified and the research questions should be answered.

III

SUPPORTING WORK

1

Integrated Fleet Assignment and Scheduling Module

1.1. Module Structure

The logic and flow of information within the *Fleet Assignment and Scheduling Module* can be visualized in Figure 1.1. The module makes use of demand data, aircraft data and airport data to determine the fleet composition and the weekly flight schedule for a certain airline.

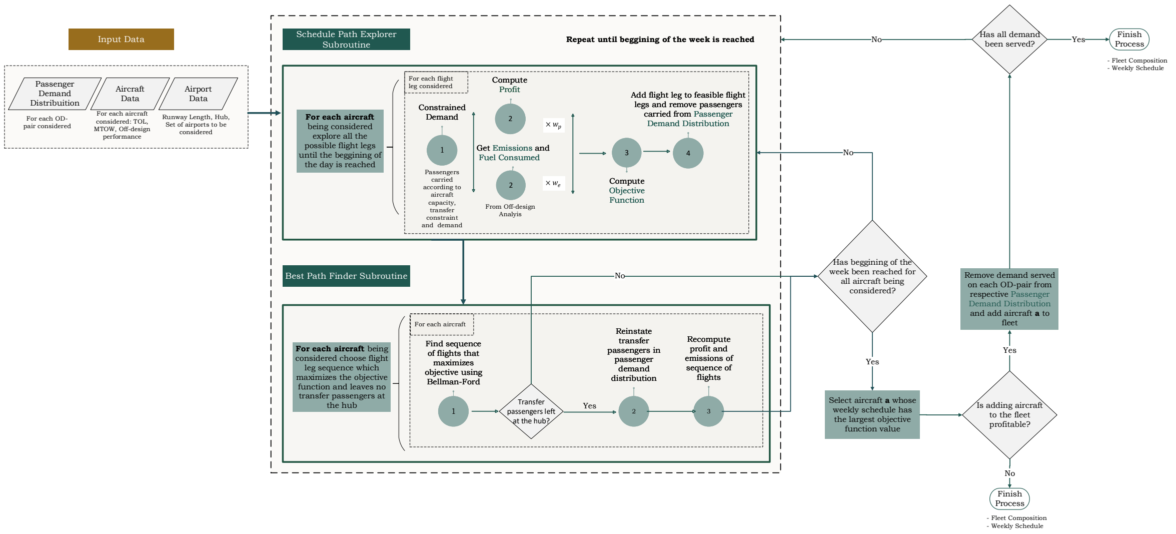

Figure 1.1: Fleet Assignment and Scheduling Module flowchart

1.2. Profit Estimation

Profit per flight leg was computed based on the revenue generated and the operating cost associated with that specific flight i. Revenue is assumed to depend on the number of passengers transported and the fare associated with each ticket. No distinction is made between classes nor between direct and transfer passengers. This is an oversimplification of the problem, however is adequate to the scope of the study. Furthermore, the estimation of the operating cost involves a larger level of detail. The components of the operating cost which were considered were the *crew costs*, *airport costs*, the *navigation fees*, the *fuel costs*, the *electricity production costs* and finally the *ownership costs*. In the following subsections, further details shall be given regarding how the crew costs, the airport costs and the navigation fees were taken into account.

1.2.1. CREW COSTS

The technique provided by *Roskam* [106] was used to estimate the crew costs. The captain, first officer, and cabin crew members were the three crew types considered. The number of captains and first officers are determined based on the flights block time. Given the fact that no flight longer than 10 hours was considered, it was always assumed there to be only one captain and one first officer. Furthermore, to determine the number of cabin crew memebers, the EASA standards were followed. These stipulate that there should be one cabin crew member for every 50 seats [107].

In addition, a yearly flight hour total (ah_{crew}), the flight's block velocity (V), an assumed annual salary (SAL), a travel expense factor TEF and a vacation pay factor (k_j) are used to determine the crew costs as per Equation 1.1. The parameters assumed to calculate the crew costs are summarised in Table 1.1.

$$C_{crew,i} = n_i \cdot \frac{1+k_j}{V} \cdot \frac{SAL_i}{ah_{crew}} + \frac{TEF}{V}, \quad i \in \text{[Captain, First Officer, Cabin Crew]} \tag{1.1}$$

Table 1.1: Assumed parameters for the calculation of the crew cost.

Variable	Value	Units
$SAL_{CabinAttendant}$	21700[1]	[USD]
$SAL_{FirstOfficer}$	38000[2]	[USD]
$SAL_{Captain}$	97900[2]	[USD]
k_j	0.26[a]	[-]
ah_{crew}	1000	[h]
TEF	7[a]	[USD/h]

[a] Retrieved from [106]

1.2.2. AIRPORT COSTS

Airport-specific taxes are not taken into account when estimating airport costs. Furthermore, the airport costs were estimated with the method used by *Wang* [74]. Hence, two different types of airport sub-costs were considered: landing and ground-handling fees. These were computed with Equation 1.2 and Equation 1.3, respectively. Moreover, the number of seats in the aircraft, and the maximum takeoff weight (MTOW) of the aircraft are the primary factors influencing these costs on a given flight.

$$\text{Landing fee} = 5.5 \cdot \frac{MTOW}{1000} \tag{1.2}$$

$$\text{Ground-handling fee} = 6 \cdot \text{Seats} \tag{1.3}$$

1.2.3. NAVIGATION FEES

As far as the navigation fees are concerned, these were considered to be dependent on the MTOW and the distance travelled (R) as per Equation 1.4. This is in accordance with the method detailed by *Wang* [74].

$$\text{Navigation fee} = \frac{R}{2} \cdot \sqrt{\frac{MTOW}{50000}} \tag{1.4}$$

1.3. PSEUDO-CODE FOR DEMAND MODELLING SUBROUTINES

At the core of the *Fleet Assignment and Scheduling Module* lies the way in which the demand data is treated and evaluated during the creation of the airline's fleet composition and schedule. The most important subroutines used are the **Constrained Demand Subroutine**, the **Update Demand Subroutine** and finally the **Transfer Passenger Check Subroutine**. The pseudo-codes for each of these can be found in subsection 1.3.1, subsection 1.3.2 and subsection 1.3.3, respectively.

[1] https://www.salaryexpert.com/salary/job/flight-attendant/spain [Accessed: 22/12/2023]
[2] https://worldaviationato.com/en/airplane-pilots-salary/ [Accessed: 22/12/2023]

1.3.1. CONSTRAINED DEMAND SUBROUTINE

The constrained demand subroutine evaluates the direct demand and the transfer demand for a certain flight between airport *i* and airport *j*. This demand is computed based on the passenger demand distribution function at a certain time *t* and the attraction band considered.

Algorithm 1 Constrained Demand

Input:
Passenger Demand Distribution F_t
Unconstrained Transfer Demand Dictionary $D_{UDemand,Transfer}$
Transfer Passengers at the Hub Dictionary $D_{Pax,hub}$
Destination airport *origin*
Origin airport *action*
OD-pair type *hub_spoke_boolean*
All OD-pairs Unconstrained Demand Matrix *demand_matrix*
Total Unconstrained Demand of OD-pair *total_demand*
Flight Departure Time *t*
Maximum Hours of Operation *max_block_time*
Check Transfer Passenger Function $F_{transfer,pax}$

transfer_demand, new_transfer, $D_{UDemand,Transfer} \leftarrow F_{transfer,pax}(D_{UDemand,Transfer}, D_{Pax,hub},$ *origin, action, hub_spoke_boolean, demand_matrix*)

if $hub\_spoke\_boolean == 1$ **then**
  direct_demand ← *total_demand* − *transfer_demand*
else
  if *transfer_demand* > 0 **then**
    direct_demand ← *total_demand* − sum of all unconstrained demand departing from airport *action*
  else
    direct_demand ← *total_demand*
  end if
end if
if *transfer_demand* ≠ 0 **then**
  if $hub\_spoke\_boolean == 1$ **then**
    leg_transfer_demand ← Unconstrained Transfer demand within the attraction band evaluated from (F_t, *transfer_demand, t, max_block_time*)
  else
    leg_transfer_demand ← *transfer_demand*
  end if
  if *leg_transfer_demand* < 1 **then**
    leg_transfer_demand ← 0
  end if
else
  leg_transfer_demand ← 0
end if

leg_direct_demand ← Unconstrained Direct demand within the attraction band evaluated from (F_t, *direct_demand, t, max_block_time*)
leg_demand ← *leg_transfer_demand* + *leg_direct_demand*

Output *leg_demand, leg_transfer_demand, leg_direct_demand, total_transfer_demand_dict, new_keys*

1.3.2. UPDATE DEMAND SUBROUTINE

The update demand subroutine is in charge of removing the demand that has been served at time *t*, on a specific OD-pair, from its passenger demand distribution.

Algorithm 2 Update Demand

```
Input:
   Passenger Demand Distribution F_t
   Flight Departure Time t
   Passengers pax
   Time Vector t⃗
   Total Unconstrained Demand in OD-Pair UDemand
   Time Step Step
   Maximum Hours of Operation max_block_time

delta_band ← step
delta_index ← 1
index ← i where t⃗ = t
sum ← pax
iterator ← 0

while sum ≠ 0 do
   lower_bound ← max(t⃗[index] − delta_band, 0)
   uper_bound ← min(t⃗[index] + delta_band, max_block_time),
   lower_bound_index ← b where t⃗[b] == lower_bound
   upper_bound_index ← b where t⃗[b] = uper_bound

   time_array ← np.arange(lower_bound, uper_bound + step/2, step)
   demand_series ← time_series_specific[lower_bound_index:upper_bound_index + delta_index]
   value ← integral(F_t[lower_bound_index : upper_bound_index])
   surplus ← pax − value

   if surplus > 0 then
      delta_band ← delta_band + step
      lower_bound_index_0 ← lower_bound_index
      upper_bound_index_0 ← upper_bound_index
      sum = surplus
   else if surplus < 0 then

      if iterator ≠ 0 then
         F_t[lower_bound_index_0:upper_bound_index_0 + delta_index] ← 0
      end if

      if t < max_block_time/2 then
         upper_demand ← F_t[upper_bound_index]
         remainder ← upper_demand + surplus
         idx ← upper_bound_index
         upper_bool ← True
      else if t ≥ max_block_time/2 then
         lower_demand ← F_t[lower_bound_index]
         remainder ← lower_demand + surplus
         idx ← lower_bound_index
         upper_bool ← False
      end if

      if remainder > 0 then
         F_t[idx] ← remainder
      else if remainder < 0 then
         if upper_bool then
            lower_demand ← F_t[lower_bound_index]
            remainder ← lower_demand + remainder
            F_t[lower_bound_index] ← remainder
```

end if
if not *upper_bool* **then**
$upper\_demand \leftarrow F_t[upper\_bound\_index]$
$remainder \leftarrow upper\_demand + remainder$
$F_t[upper\_bound\_index] \leftarrow remainder$
end if
end if

$sum \leftarrow 0$
else
$F_t[lower\_bound\_index{:}upper\_bound\_index + delta\_index] \leftarrow 0$
$sum \leftarrow 0$
end if
$iterator \leftarrow iterator + 1$

end while
Output Passenger Demand Distribution F_t

1.3.3. TRANSFER PASSENGER CHECK

The transfer passenger check subroutine is in charge of selecting for each aircraft the flight schedule for one day which minimizes the objective function and ensures that no transfer passengers are left at the hub.

Algorithm 3 Transfer Passenger Check

Input:
All feasible paths $\mathbf{P}_p$

for each path p in $\mathbf{P}_p$ **do**
Initialize an empty dictionary to store transfer passengers stuck at hub

for each edge (i, j) in p from the end to the beginning (excluding the first edge) **do**
Get relevant information from network, inputs, and results dataframes

if current edge is hub-to-spoke and there are transfer passengers at the hub **then**
Update edge weight considering the number of un-transported transfer passengers
Update results dataframe with new demand, fuel consumption, costs, etc. based on the number of un-transported transfer passengers
current edge is a spoke-to-hub route and there are transfer passengers on board
Check if the transfer passengers need to be removed based on hub-spoke data

if transfer passengers need to be removed **then**
Update number of passengers and weight considering removed transfer passengers
Update results dataframe with new demand, fuel consumption, costs, etc. based on the removed transfer passengers
end if
end if
Update total weight for the current path
end for
end if
end for
Select the path with the minimum weight (best objective)
best length, best schedule

2
VERIFICATION

2.1. POWERTRAIN OFF-DESIGN PERFORMANCE

The turboprop engine cycle analysis model used within the powertrain model has already been verified in the work developed by *Thijssen* [108]. However, it has not been evaluated if the powertrain model developed in the current work behaves as expected. The powertrain plays an especially central role when it comes to the evaluation of the performance of aircraft. Achieving sensible results when it comes to the fuel consumption of hybrid-electric aircraft for different flight conditions becomes vital for the credibility of the results of the current work.

As can be seen from Figure 2.1, the variation of the energy consumed by the battery (E_{bat}) and the fuel mass consumed (M_f) are plotted for the cruise and the climb phase. Note that E_{bat} and M_f are not the total battery energy and total fuel consumed to conduct the entire mission. Rather they are the battery energy and the fuel consumed during the phase of the mission being considered. The results associated with the cruise phase are in purple, while the results associated with the climb phase are in yellow. Moreover, for a hybrid-electric ATR 72-600 aircraft designed with a powersplit equal to 5% a design range equal to 1370 km a mission with a length equal to 400 km was considered. It was evaluated how the energy consumed and the fuel consumed change during the climb and the cruise phase if the powersplit ϕ during these phases is varied between zero and 15%. As expected, as the powersplit increases the fuel consumed decreases and the battery energy increases.

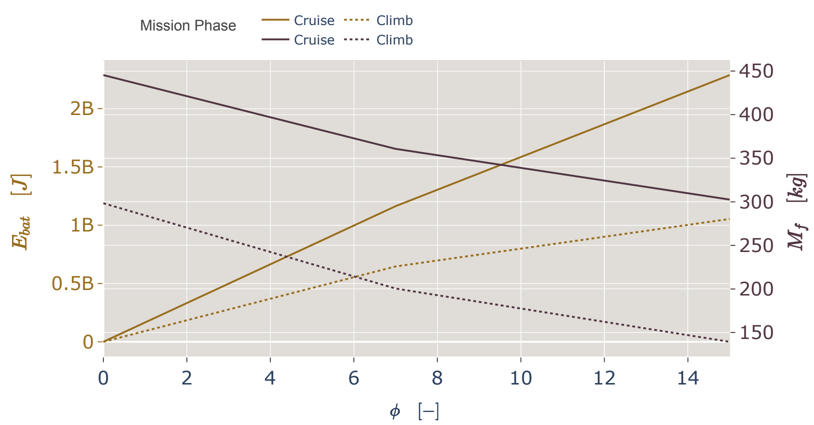

Figure 2.1: Variation of fuel consumed and battery energy consumed during cruise and climb with increasing powersplit for a 400km mission (Aircraft = ATR 72-600, ϕ = 0.05, R_{design} = 1370km)

3

Additional Framework Results

3.1. Computational Performance

The two most computationally expensive segments of the framework are the *Off-design Analysis Module* and the *Fleet Assignment and Scheduling Module*. The computational time of the former highly depends on the number of mission analysis evaluations. In general, the evaluation of one nominal mission analysis lasted between 40 s and 200s. The difference in time stems from whether or not the gas turbine was operating at extreme off-design conditions or not. For example, for the baseline HE aircraft short missions, when operating at extremely high cruise powersplits and low power demand (due to low weight), the gas turbine would be assumed to need to operate at extremely low power settings, which prolonged the time to compute the powertrain state. Furthermore, to converge on the conditions for a certain payload-range combination between 15-22 mission analysis evaluations were necessary. Given that, per off-design analysis 16 payload-range combinations were evaluated, it required on average 9.8 h to complete one off-design analysis. Reducing the computational time could only be attained by reducing the number of times the powertrain state is evaluated during the mission. Although, the former has already been adjusted per flight phase, reducing it even further, especially in the climb and descent phases, would require further insight as it can cause the climb profile and the descent profile to become unrealistic.

On another front, the computational performance analysis of the *Fleet Assignment and Scheduling Module* depends both on the number of iterations until the final fleet is selected and whether or not the cruise velocity is allowed to vary. For an initial fleet of 6 aircraft, and if it takes 10 iterations for the final fleet to be converged, if the velocity during cruise is kept constant it takes around 7h to construct the fleet's schedule. Moreover, if the velocity is allowed to vary this number triples.

Bibliography

[1] Boieng. *Commercial Market Outlook*. URL: https://www.boeing.com/commercial/market/commercial-market-outlook/index.page (visited on 05/04/2023).

[2] Airbus. *Global Market Forecast | Airbus*. en. June 2021. URL: https://www.airbus.com/en/products-services/commercial-aircraft/market/global-market-forecast (visited on 05/04/2023).

[3] United Nations. *The Paris Agreement*. en. URL: https://www.un.org/en/climatechange/paris-agreement (visited on 05/04/2023).

[4] NLR - Royal Netherlands Aerospace Centre and TU Delft. *Towards a Sustainable Air Transportation System*. White paper. 2021.

[5] R. de Vries. "Hybrid-Electric Aircraft with Over-the-Wing Distributed Propulsion: Aerodynamic Performance and Conceptual Design". Dissertation (TU Delft). 2022. DOI: 10.4233/uuid:ef87dc11-e7b2-4726-a41f-28588d64c58d.

[6] M. F. M. Hoogreef et al. "Scalability Assessment of Hybrid-Electric Technology Application to Various Aircraft Classes - an Overview of Opportunities and Challenges". In: *Aerospace Europe Conference 2023 – 10 EUCASS – 9 CEAS* (2023). Publisher: EUCASS. DOI: 10.13009/EUCASS2023-260.

[7] Vincent Bonnin and Maurice Hoogreef. *Deliverable D3.3 - Report on opportunities for cross-vehicle class and technology synergies*. Tech. rep. May 2023.

[8] Elise Scheers. "Coupled hybrid electric aircraft design and strategic airline planning". MA thesis. TU Delft, 2023.

[9] Noa Zuijderwijk. "Study to the adaptation of electrified aircraft by regional airlines: using strategic airline planning and aircraft design". MA thesis. TU Delft, 2022.

[10] EUROCONTROL. *EUROCONTROL Aviation Outlook 2050 released*. en. Apr. 2022. URL: https://www.eurocontrol.int/press-release/eurocontrol-2050-air-traffic-forecast-showing-aviation-pathway-net-zero (visited on 05/04/2023).

[11] ICAO. *The World of Air Transport in 2021*. URL: https://www.icao.int/sustainability/WorldofAirTransport/Pages/the-world-of-air-transport-in-2021.aspx (visited on 05/04/2023).

[12] Venkatasubramanian Viswanathan et al. "The challenges and opportunities of battery-powered flight". In: *Nature* 601.7894 (Jan. 2022), pp. 519–525. DOI: 10.1038/s41586-021-04139-1.

[13] Mohd Tariq et al. "Aircraft batteries: current trend towards more electric aircraft". en. In: *IET Electrical Systems in Transportation* 7.2 (2017). _eprint: https://onlinelibrary.wiley.com/doi/pdf/10.1049/iet-est.2016.0019, pp. 93–103. ISSN: 2042-9746. DOI: 10.1049/iet-est.2016.0019. URL: https://onlinelibrary.wiley.com/doi/abs/10.1049/iet-est.2016.0019 (visited on 05/08/2023).

[14] Shoichi Matsuda et al. "Criteria for evaluating lithium–air batteries in academia to correctly predict their practical performance in industry". en. In: *Materials Horizons* 9.3 (Mar. 2022). Publisher: The Royal Society of Chemistry, pp. 856–863. ISSN: 2051-6355. DOI: 10.1039/D1MH01546J. URL: https://pubs.rsc.org/en/content/articlelanding/2022/mh/d1mh01546j (visited on 05/08/2023).

[15] Giuseppe Palaia and Karim Abu Salem. "Mission Performance Analysis of Hybrid-Electric Regional Aircraft". In: *Aerospace* 10.3 (Mar. 2023), p. 246. DOI: 10.3390/aerospace10030246.

[16] Peter Belobaba, Amedeo Odoni, and Cynthia Barnhart. *The Global Airline Industry*. Hoboken, UNITED KINGDOM: John Wiley & Sons, Incorporated, 2009.

[17] Alejandro A. Rios Cruz et al. "Identification of the Actual Mission Profiles and Their Impact on the Integrated Aircraft and Airline Network Optimization". In: *AIAA AVIATION 2021 FORUM*. American Institute of Aeronautics and Astronautics.

[18] IEEE. "ISO/IEC/IEEE International Standard – Systems and software engineering – System of systems (SoS) considerations in life cycle stages of a system". In: *ISO/IEC/IEEE 21839:2019(E)* (July 2019). Conference Name: ISO/IEC/IEEE 21839:2019(E), pp. 1–40. DOI: 10.1109/IEEESTD.2019.8767116.

[19] Mark W. Maier. “Architecting principles for systems-of-systems”. In: *Systems Engineering* 1.4 (1998), pp. 267–284. DOI: 10.1002/(SICI)1520-6858(1998)1:4<267::AID-SYS3>3.0.CO;2-D.

[20] Geoffrey Bower and Ilan Kroo. “Multi-Objective Aircraft Optimization for Minimum Cost and Emissions over Specific Route Networks”. In: *The 26th Congress of ICAS and 8th AIAA ATIO*. Aviation Technology, Integration, and Operations (ATIO) Conferences. American Institute of Aeronautics and Astronautics, Sept. 2008. DOI: 10.2514/6.2008-8905. URL: https://arc.aiaa.org/doi/10.2514/6.2008-8905 (visited on 03/28/2023).

[21] A.T. Isikveren et al. “Pre-design strategies and sizing techniques for dual-energy aircraft”. In: *Aircraft Engineering and Aerospace Technology: An International Journal* 86.6 (Jan. 2014). Ed. by Riti Singh, pp. 525–542. DOI: 10.1108/AEAT-08-2014-0122.

[22] Benjamin J. Brelje and Joaquim R. R. A. Martins. “Electric, hybrid, and turboelectric fixed-wing aircraft: A review of concepts, models, and design approaches”. en. In: *Progress in Aerospace Sciences* 104 (Jan. 2019), pp. 1–19. ISSN: 0376-0421. DOI: 10.1016/j.paerosci.2018.06.004. URL: https://www.sciencedirect.com/science/article/pii/S0376042118300356 (visited on 03/28/2023).

[23] Ye Xie et al. “Review of hybrid electric powered aircraft, its conceptual design and energy management methodologies”. en. In: *Chinese Journal of Aeronautics* 34.4 (Apr. 2021), pp. 432–450. ISSN: 1000-9361. DOI: 10.1016/j.cja.2020.07.017. URL: https://www.sciencedirect.com/science/article/pii/S1000936120303368 (visited on 05/09/2023).

[24] Eviation. *Aircraft – Eviation*. en-US. URL: https://www.eviation.com/aircraft/ (visited on 05/10/2023).

[25] Jennifer Korn. *Alice, the first all-electric passenger airplane, takes flight | CNN Business*. en. Sept. 2022. URL: https://www.cnn.com/2022/09/27/tech/eviation-alice-first-flight/index.html (visited on 05/10/2023).

[26] Mirko Hornung et al. “Ce-Liner - Case Study for eMobility in Air Transportation”. In: *2013 Aviation Technology, Integration, and Operations Conference*. AIAA AVIATION Forum. Aug. 2013. DOI: 10.2514/6.2013-4302.

[27] *Commercial Aircraft Propulsion and Energy Systems Research: Reducing Global Carbon Emissions*. Washington, D.C.: National Academies Press, 2016. ISBN: 978-0-309-44096-7. DOI: 10.17226/23490. URL: http://www.nap.edu/catalog/23490 (visited on 05/10/2023).

[28] S. Stückl, J. Toor, and H. Lobentanzer. “Voltair - the all electric propulsion concept platform - a vision for atmospheric friendly flight”. In: 4 (Jan. 2012), pp. 2737–2747.

[29] Jason Welstead and James L. Felder. “Conceptual Design of a Single-Aisle Turboelectric Commercial Transport with Fuselage Boundary Layer Ingestion”. In: *54th AIAA Aerospace Sciences Meeting*. AIAA SciTech Forum. American Institute of Aeronautics and Astronautics, Jan. 2016. DOI: 10.2514/6.2016-1027. URL: https://arc.aiaa.org/doi/10.2514/6.2016-1027 (visited on 05/10/2023).

[30] Benjamin T. Schiltgen and Jeffrey Freeman. “Aeropropulsive Interaction and Thermal System Integration within the ECO-150: A Turboelectric Distributed Propulsion Airliner with Conventional Electric Machines”. en. In: *16th AIAA Aviation Technology, Integration, and Operations Conference*. Washington, D.C.: American Institute of Aeronautics and Astronautics, June 2016. DOI: 10.2514/6.2016-4064. URL: https://arc.aiaa.org/doi/10.2514/6.2016-4064 (visited on 05/11/2023).

[31] Hyun Dae Kim et al. “Turboelectric distributed propulsion benefits on the N3-X vehicle”. In: *Aircraft Engineering and Aerospace Technology: An International Journal* 86.6 (Jan. 2014). Ed. by Riti Singh. Publisher: Emerald Group Publishing Limited, pp. 558–561. ISSN: 0002-2667. DOI: 10.1108/AEAT-04-2014-0037. URL: https://doi.org/10.1108/AEAT-04-2014-0037 (visited on 05/10/2023).

[32] Airbus. *E-Fan X - Electric Flight - Airbus*. en. Section: Innovation. July 2021. URL: https://www.airbus.com/en/innovation/zero-emission/electric-flight/e-fan-x (visited on 05/10/2023).

[33] Zunum Aero. *Aircraft*. en-CA. URL: https://zunum.aero/aircraft/ (visited on 05/10/2023).

[34] C. Pornet and A. T. Isikveren. “Conceptual design of hybrid-electric transport aircraft”. In: *Progress in Aerospace Sciences* 79 (Nov. 2015), pp. 114–135. DOI: 10.1016/j.paerosci.2015.09.002.

[35] Marty K. Bradley and Christopher K. Droney. *Subsonic Ultra Green Aircraft Research: Phase 2*. Tech. rep. NF1676L-21005. NTRS Author Affiliations: Boeing Research and Technology NTRS Document ID: 20150017039 NTRS Research Center: Langley Research Center (LaRC). Apr. 2015. URL: https://ntrs.nasa.gov/citations/20150017039 (visited on 05/10/2023).

[36] Kevin R. Antcliff and Francisco M. Capristan. "Conceptual Design of the Parallel Electric-Gas Architecture with Synergistic Utilization Scheme (PEGASUS) Concept". In: NTRS Author Affiliations: Langley Research Center NTRS Document ID: 20210011499 NTRS Research Center: Langley Research Center (LaRC). Denver, CO, Mar. 2021. URL: https://ntrs.nasa.gov/citations/20210011499 (visited on 05/10/2023).

[37] Francisco M. Capristan and Nathaniel J. Blaesser. *Analysis of the Parallel Electric-Gas Architecture with Synergistic Utilization Scheme (PEGASUS) Concept*. Tech. rep. NF1676-33672. NTRS Author Affiliations: NASA Langley Research Center NTRS Document ID: 20190030874 NTRS Research Center: Langley Research Center (LaRC). Aug. 2019. URL: https://ntrs.nasa.gov/citations/20190030874 (visited on 05/10/2023).

[38] D. Felix Finger et al. "A Comparison of Hybrid-Electric Aircraft Sizing Methods". In: *AIAA Scitech 2020 Forum*. American Institute of Aeronautics and Astronautics, Jan. 2020. DOI: 10.2514/6.2020-1006. URL: https://arc.aiaa.org/doi/abs/10.2514/6.2020-1006 (visited on 03/29/2023).

[39] D. Felix Finger, Cees Bil, and Carsten Braun. "Initial Sizing Methodology for Hybrid-Electric General Aviation Aircraft". In: *Journal of Aircraft* 57.2 (Mar. 2020). Publisher: American Institute of Aeronautics and Astronautics, pp. 245–255. ISSN: 0021-8669. DOI: 10.2514/1.C035428. URL: https://arc.aiaa.org/doi/10.2514/1.C035428 (visited on 05/15/2023).

[40] Snorri Gudmundsson. *General Aviation Aircraft Design:Applied Methods and Procedures*. Oxford England UK: Butterworth-Heinemann, 2022.

[41] Daniel Raymer. *Aircraft Design: A Conceptual Approach, Sixth Edition*. Washington, DC: American Institute of Aeronautics and Astronautics, Inc., 2018.

[42] Jacopo Zamboni. "A method for the conceptual design of hybrid electric aircraft". en. PhD thesis. 2018. URL: https://repository.tudelft.nl/islandora/object/uuid%3A7b7dc56b-6647-4cc9-98f6-2ed5d488c759 (visited on 05/19/2023).

[43] F. Orefice et al. "Aircraft Conceptual Design Including Powertrain System Architecture and Distributed Propulsion". In: *2019 AIAA/IEEE Electric Aircraft Technologies Symposium (EATS)*. Aug. 2019, pp. 1–20. DOI: 10.2514/6.2019-4465.

[44] Benjamin Yan, Peter Jansen, and Ruben Perez. "Multidisciplinary Design Optimization of Airframe and Trajectory Considering Cost, Noise, and Fuel Burn". In: *12th AIAA Aviation Technology, Integration, and Operations (ATIO) Conference and 14th AIAA/ISSMO Multidisciplinary Analysis and Optimization Conference*. Aviation Technology, Integration, and Operations (ATIO) Conferences. American Institute of Aeronautics and Astronautics, Sept. 2012. DOI: 10.2514/6.2012-5494.

[45] R. de Vries, M. F. M. Hoogreef, and Roelof Vos. "Range equation for hybrid-electric aircraft with constant power split". In: *Journal of Aircraft: devoted to aeronautical science and technology* 57.3 (2020). DOI: 10.2514/1.C035734.

[46] M. Voskuijl, J. van Bogaert, and A. Gangoli Rao. "Analysis and design of hybrid electric regional turboprop aircraft". In: *CEAS Aeronautical Journal* (2017). DOI: 10.1007/s13272-017-0272-1.

[47] Francesco Orefice et al. "Aircraft Conceptual Design of Commuter Aircraft including Distributed Electric Propulsion". In: *AIAA AVIATION 2020 FORUM*. AIAA AVIATION Forum (June 2020). DOI: 10.2514/6.2020-2627.

[48] D. K. Hall et al. *Feasibility of Electrified Propulsion for Ultra-Efficient Commercial Aircraft Final Report*. Tech. rep. GRC-E-DAA-TN72076. Dec. 2019. URL: https://ntrs.nasa.gov/citations/20190033478 (visited on 03/28/2023).

[49] Timothy P. Dever et al. *Assessment of Technologies for Noncryogenic Hybrid Electric Propulsion*. Jan. 2015.

[50] Bruno Scrosati and Jürgen Garche. "Lithium batteries: Status, prospects and future". In: *Journal of Power Sources* 195.9 (May 2010), pp. 2419–2430. DOI: 10.1016/j.jpowsour.2009.11.048.

[51] Ashkan Barzkar and Mona Ghassemi. "Components of Electrical Power Systems in More and All-Electric Aircraft: A Review". In: *IEEE Transactions on Transportation Electrification* 8.4 (Dec. 2022). Conference Name: IEEE Transactions on Transportation Electrification, pp. 4037–4053. ISSN: 2332-7782. DOI: 10.1109/TTE.2022.3174362.

[52] Michel Armand et al. "Lithium-ion batteries – Current state of the art and anticipated developments". In: *Journal of Power Sources* 479 (Dec. 2020), p. 228708. DOI: 10.1016/j.jpowsour.2020.228708.

[53] Reynard de Vries, Malcom T. Brown, and Roelof Vos. "A Preliminary Sizing Method for Hybrid-Electric Aircraft Including Aero-Propulsive Interaction Effects". In: *2018 Aviation Technology, Integration, and Operations Conference*. AIAA AVIATION Forum. American Institute of Aeronautics and Astronautics, June 2018. DOI: 10.2514/6.2018-4228. URL: https://arc.aiaa.org/doi/10.2514/6.2018-4228 (visited on 05/27/2023).

[54] Michael D. Patterson, Matthew J. Daskilewicz, and Brian German. "Simplified Aerodynamics Models to Predict the Effects of Upstream Propellers on Wing Lift". In: *53rd AIAA Aerospace Sciences Meeting*. AIAA SciTech Forum. American Institute of Aeronautics and Astronautics, Jan. 2015. DOI: 10.2514/6.2015-1673. URL: https://arc.aiaa.org/doi/10.2514/6.2015-1673 (visited on 05/27/2023).

[55] Michael Dobson Patterson. "Conceptual Design of High-Lift Propeller Systems for Small Electric Aircraft". en_US. Publisher: Georgia Institute of Technology. PhD thesis. May 2016. URL: http://hdl.handle.net/1853/55569 (visited on 05/27/2023).

[56] Bruno dos Santos. *Lecture 1: Introduction, planning framework and demand analysis*. 2021.

[57] Christopher A. Hane et al. "The fleet assignment problem: Solving a large-scale integer program". In: *Mathematical Programming* 70.1 (Oct. 1995), pp. 211–232. DOI: 10.1007/BF01585938.

[58] Mark S. Daskin and Nicholaos D. Panayotopoulos. "A Lagrangian Relaxation Approach to Assigning Aircraft to Routes in Hub and Spoke Networks". In: *Transportation Science* 23.2 (May 1989). Publisher: INFORMS, pp. 91–99. ISSN: 0041-1655. DOI: 10.1287/trsc.23.2.91. URL: https://pubsonline.informs.org/doi/abs/10.1287/trsc.23.2.91 (visited on 05/24/2023).

[59] George Bernard Dantzig and Allen R. Ferguson. *The Problem of Routing Aircraft–A Mathematical Solution*. en. Tech. rep. RAND Corporation, Jan. 1954. URL: https://www.rand.org/pubs/papers/P561.html (visited on 05/22/2023).

[60] Stuart E. Dreyfus. *A Comparison of Linear Programming and Dynamic Programming*. en. Tech. rep. RAND Corporation, Jan. 1956. URL: https://www.rand.org/pubs/papers/P885.html (visited on 05/22/2023).

[61] George B. Dantzig. "Origins of the simplex method". In: *A history of scientific computing*. New York, NY, USA: Association for Computing Machinery, June 1990, pp. 141–151. URL: https://doi.org/10.1145/87252.88081 (visited on 05/22/2023).

[62] A. H. Land and A. G. Doig. "An Automatic Method of Solving Discrete Programming Problems". In: *Econometrica* 28.3 (1960). Publisher: [Wiley, Econometric Society], pp. 497–520. ISSN: 0012-9682. DOI: 10.2307/1910129. URL: https://www.jstor.org/stable/1910129 (visited on 05/22/2023).

[63] Richard Ernest Bellman. *The Theory of Dynamic Programming*. Tech. rep. RAND Corporation, Jan. 1954.

[64] Warren B. Powell. *Approximate dynamic programming: solving the curses of dimensionality*. English. 2nd ed. Hoboken, N.J.: Wiley, 2011. ISBN: 978-1-118-02917-6 978-0-470-60445-8 978-1-118-02915-2 978-1-118-02916-9. URL: http://www.books24x7.com/marc.asp?bookid=44302 (visited on 05/22/2023).

[65] Jeph Abara. "Applying Integer Linear Programming to the Fleet Assignment Problem". In: *Interfaces* 19.4 (1989). Publisher: INFORMS, pp. 20–28. ISSN: 0092-2102. URL: https://www.jstor.org/stable/25061245 (visited on 05/24/2023).

[66] Cynthia Barnhart, Timothy Kniker, and Manoj Lohatepanont. "Itinerary-Based Airline Fleet Assignment". In: *Transportation Science* 36 (May 2002), pp. 199–217. DOI: 10.1287/trsc.36.2.199.566.

[67] Manoj Lohatepanont and Cynthia Barnhart. "Airline Schedule Planning: Integrated Models and Algorithms for Schedule Design and Fleet Assignment". In: *Transportation Science* 38.1 (Feb. 2004), pp. 19–32. DOI: 10.1287/trsc.1030.0026.

[68] Cedric Y. Justin, Alexia P. Payan, and Dimitri N. Mavris. "Integrated fleet assignment and scheduling for environmentally friendly electrified regional air mobility". en. In: *Transportation Research Part C: Emerging Technologies* 138 (May 2022), p. 103567. ISSN: 0968-090X. DOI: 10.1016/j.trc.2022.103567. URL: https://www.sciencedirect.com/science/article/pii/S0968090X22000158 (visited on 03/31/2023).

[69] Cynthia Barnhart et al. "Flight String Models for Aircraft Fleeting and Routing". In: *Transportation Science* 32.3 (Aug. 1998), pp. 208–220. DOI: 10.1287/trsc.32.3.208.

[70] Yusuf Ziya Unal et al. "A new approach to fleet assignment and aircraft routing problems". In: *Transportation Research Procedia* 59 (Jan. 2021), pp. 67–75. DOI: 10.1016/j.trpro.2021.11.098.

[71] Thijs Woudenberg. "Air Freighter Schedule Planning: A Dynamic Programming Optimisation Approach". MA thesis. 2019.

[72] Warren Hyman and Larry Gordon. "Commercial airline scheduling technique". In: *Transportation Research* 2.1 (Mar. 1968), pp. 23–29. DOI: 10.1016/0041-1647(68)90005-1.

[73] Marvin Hersh. "Airline scheduling: a heurisitic approach". In: *Transportation Planning and Technology* 2.4 (Jan. 1974), pp. 277–285. DOI: 10.1080/03081067408717082.

[74] Xueying Wang. "Development of a dynamic operations optimization modelling framework". MA thesis. Delft, The Netherlands: TU Delft, 2016.

[75] P. Rubbrecht. *Development of an Airline Systems Simulation Program*. Tech. rep. Delft, The Netherlands: TU Delft, 1989.

[76] Maria Seoane Álvarez. "Assessment of the Climate Impact Mitigation Potential of Intermediate Stop Operations: A Dynamic Programming Approach". MA thesis. Delft, The Netherlands: TU Delft, 2021.

[77] Mahdi Noorafza et al. "Airline network planning considering climate impact: assessing new operational improvements". In: (2023).

[78] Hooi Ling Khoo and Lay Eng Teoh. "A bi-objective dynamic programming approach for airline green fleet planning". In: *Transportation Research Part D: Transport and Environment* 33 (Dec. 2014), pp. 166–185. DOI: 10.1016/j.trd.2014.06.003.

[79] Tanya E. Kannon et al. "The aircraft routing problem with refueling". en. In: *Optimization Letters* 9.8 (Dec. 2015), pp. 1609–1624. ISSN: 1862-4480. DOI: 10.1007/s11590-015-0849-8. URL: https://doi.org/10.1007/s11590-015-0849-8 (visited on 05/24/2023).

[80] Jinning Zhang, Ioannis Roumeliotis, and Argyrios Zolotas. "Model-based fully coupled propulsion-aerodynamics optimization for hybrid electric aircraft energy management strategy". English. In: *Energy* 245 (Apr. 2022), p. 123239. ISSN: 0360-5442. DOI: 10.1016/j.energy.2022.123239. URL: https://linkinghub.elsevier.com/retrieve/pii/S0360544222001426 (visited on 04/12/2023).

[81] D. S. Lee et al. "The contribution of global aviation to anthropogenic climate forcing for 2000 to 2018". en. In: *Atmospheric Environment* 244 (Jan. 2021), p. 117834. ISSN: 1352-2310. DOI: 10.1016/j.atmosenv.2020.117834. URL: https://www.sciencedirect.com/science/article/pii/S1352231020305689 (visited on 06/07/2023).

[82] J. Hansen et al. "Efficacy of climate forcings". In: *Journal of Geophysical Research: Atmospheres* 110.D18 (2005). DOI: 10.1029/2005JD005776.

[83] Henning Rodhe. "A Comparison of the Contribution of Various Gases to the Greenhouse Effect". In: *Science* 248.4960 (June 1990), pp. 1217–1219. DOI: 10.1126/science.248.4960.1217.

[84] Liam Megill. "Analysis of Climate Metrics for Aviation". en. MA thesis. Delft, The Netherlands: TU Delft, 2022. URL: https://repository.tudelft.nl/islandora/object/uuid%3A9e84ee4d-af69-4550-8938-2ccf4caccb8c (visited on 06/07/2023).

[85] Myles R. Allen et al. "New use of global warming potentials to compare cumulative and short-lived climate pollutants". In: *Nature Climate Change* 6.8 (Aug. 2016), pp. 773–776. DOI: 10.1038/nclimate2998.

[86] Keith P. Shine et al. "Alternatives to the Global Warming Potential for Comparing Climate Impacts of Emissions of Greenhouse Gases". In: *Climatic Change* 68.3 (Feb. 2005), pp. 281–302.

[87] Emily Dallara and Ilan Kroo. "Aircraft Design for Reduced Climate Impact". en. In: *49th AIAA Aerospace Sciences Meeting including the New Horizons Forum and Aerospace Exposition*. Orlando, Florida: American Institute of Aeronautics and Astronautics, Jan. 2011. ISBN: 978-1-60086-950-1. DOI: 10.2514/6.2011-265. URL: https://arc.aiaa.org/doi/10.2514/6.2011-265 (visited on 06/07/2023).

[88] Kamil Çaugatay Bayindir, Mehmet Ali Gözüküçük, and Ahmet Teke. "A comprehensive overview of hybrid electric vehicle: Powertrain configurations, powertrain control techniques and electronic control units". en. In: *Energy Conversion and Management* 52.2 (Feb. 2011), pp. 1305–1313. ISSN: 0196-8904. DOI: 10.1016/j.enconman.2010.09.028. URL: https://www.sciencedirect.com/science/article/pii/S0196890410004309 (visited on 05/17/2023).

[89] HyunKi Lee et al. "A Method for Simultaneous Optimization of Power Split and Flight Path Trajectories for Hybrid Electric Aircraft". en. In: *AIAA Scitech 2021 Forum*. VIRTUAL EVENT: American Institute of Aeronautics and Astronautics, Jan. 2021. ISBN: 978-1-62410-609-5. DOI: 10.2514/6.2021-1010. URL: https://arc.aiaa.org/doi/10.2514/6.2021-1010 (visited on 04/11/2023).

[90] David Trawick et al. "A Method for Determining Optimal Power Management Schedules for Hybrid Electric Airplanes". en. In: *AIAA Propulsion and Energy 2019 Forum*. Indianapolis, IN: American Institute of Aeronautics and Astronautics, Aug. 2019. ISBN: 978-1-62410-590-6. DOI: 10.2514/6.2019-4500. URL: https://arc.aiaa.org/doi/10.2514/6.2019-4500 (visited on 04/11/2023).

[91] Viorel Badescu. "The Maximum Principle (Pontryagin)". en. In: *Optimal Control in Thermal Engineering*. Ed. by Viorel Badescu. Studies in Systems, Decision and Control. Cham: Springer International Publishing, 2017, pp. 89–109. ISBN: 978-3-319-52968-4. DOI: 10.1007/978-3-319-52968-4_5. URL: https://doi.org/10.1007/978-3-319-52968-4_5 (visited on 05/17/2023).

[92] Namwook Kim, Sukwon Cha, and Huei Peng. "Optimal Control of Hybrid Electric Vehicles Based on Pontryagin's Minimum Principle". In: *IEEE Transactions on Control Systems Technology* 19.5 (Sept. 2011). Conference Name: IEEE Transactions on Control Systems Technology, pp. 1279–1287. ISSN: 1558-0865. DOI: 10.1109/TCST.2010.2061232.

[93] Kilian Swannet. "Optimal Control And Energy Management For Hybrid Aircraft". en. MA thesis. Delft, The Netherlands: TU Delft, 2022. URL: https://repository.tudelft.nl/islandora/object/uuid%3A511989dc-0e95-414c-839b-7af0ff5ad7a0 (visited on 06/13/2023).

[94] J. P. Soares Pinto Leite and M. Voskuijl. "Optimal energy management for hybrid-electric aircraft". en. In: *Aircraft Engineering and Aerospace Technology: an international journal* 92.6 (2020). ISSN: 1748-8842. DOI: 10.1108/AEAT-03-2019-0046. URL: https://repository.tudelft.nl/islandora/object/uuid%3Acdb277e8-e9de-4bdb-a3cd-82faecf7aae3 (visited on 05/29/2023).

[95] R. Mori. "Fuel-Saving Climb Procedure by Reduced Thrust near Top of Climb". In: *Journal of Aircraft* 57.5 (Sept. 2020). Publisher: American Institute of Aeronautics and Astronautics, pp. 800–806. ISSN: 0021-8669. DOI: 10.2514/1.C035200. URL: https://arc.aiaa.org/doi/10.2514/1.C035200 (visited on 04/13/2023).

[96] Katrin Dahlmann et al. "Climate-Compatible Air Transport System—Climate Impact Mitigation Potential for Actual and Future Aircraft". en. In: *Aerospace* 3.4 (Dec. 2016). Number: 4 Publisher: Multidisciplinary Digital Publishing Institute, p. 38. ISSN: 2226-4310. DOI: 10.3390/aerospace3040038. URL: https://www.mdpi.com/2226-4310/3/4/38 (visited on 04/13/2023).

[97] Peter W. Jansen and Ruben E. Perez. "Coupled Optimization of Aircraft Design and Fleet Allocation with Uncertain Passenger Demand". In: *2013 Aviation Technology, Integration, and Operations Conference*. Los Angeles, CA: American Institute of Aeronautics and Astronautics, Aug. 2013. DOI: 10.2514/6.2013-4392.

[98] Satadru Roy et al. "A Mixed Integer Efficient Global Optimization Algorithm for the Simultaneous Aircraft Allocation-Mission-Design Problem". In: *58th AIAA/ASCE/AHS/ASC Structures, Structural Dynamics, and Materials Conference*. American Institute of Aeronautics and Astronautics, Jan. 2017. DOI: 10.2514/6.2017-1305.

[99] Christine Taylor and Olivier de Weck. "Coupled Vehicle Design and Network Flow Optimization for Air Transportation Systems". In: *7th AIAA ATIO Conf, 2nd CEIAT Int'l Conf on Innov and Integr in Aero Sciences*. American Institute of Aeronautics and Astronautics, Sept. 2007.

[100] Alexander Koch. "Climate Impact Mitigation Potential given by Flight Profile and Aircraft Optimization". PhD thesis. Nov. 2013. DOI: 10.13140/RG.2.1.4896.9047.

[101] Nicolas E. Antoine and Ilan M. Kroo. "Framework for Aircraft Conceptual Design and Environmental Performance Studies". In: *AIAA Journal* 43.10 (Oct. 2005), pp. 2100–2109. DOI: 10.2514/1.13017.

[102] John Hwang and Joaquim R. R. A. Martins. "Allocation-mission-design optimization of next-generation aircraft using a parallel computational framework". In: *57th AIAA/ASCE/AHS/ASC Structures, Structural Dynamics, and Materials Conference*. AIAA SciTech Forum. American Institute of Aeronautics and Astronautics, Jan. 2016. DOI: 10.2514/6.2016-1662. URL: https://arc.aiaa.org/doi/10.2514/6.2016-1662 (visited on 03/30/2023).

[103] John T. Hwang, John P. Jasa, and Joaquim R. R. A. Martins. "High-Fidelity Design-Allocation Optimization of a Commercial Aircraft Maximizing Airline Profit". In: *Journal of Aircraft* 56.3 (May 2019), pp. 1164–1178. DOI: 10.2514/1.C035082. URL: https://arc-aiaa-org.tudelft.idm.oclc.org/doi/10.2514/1.C035082 (visited on 04/05/2023).

[104] Satadru Roy et al. "Monolithic Approach for Next-Generation Aircraft Design Considering Airline Operations and Economics". In: *Journal of Aircraft* 56.4 (2019), pp. 1565–1576. DOI: 10.2514/1.C035312.

[105] P. Govindaraju and W.A. Crossley. "Concurrent aircraft design and trip assignment under both design parameter and demand uncertainty". English. In: 2015. ISBN: 978-1-62410-369-8. DOI: 10.2514/6.2015-2545.

[106] Jan Roskam. *Airplane design. Pt. 8. Airplane cost estimation: design, development, manufacturing and operating*. English. Ottawa, Kansas: Roskam Aviation and Engineering, 1990.

[107] . *Commission Regulation (EU) No 965/2012*. Mattingly. Legislative Body: COM. Oct. 2012.

[108] Roel Thijssen. "Propeller Aircraft Design Optimization for Reduced Climate Impact". MA thesis. 2022.